Synthesis and Testing of Novel Polypeptides for Biological Applications

by

Amanda Catherine Engler

B.S. Chemical Engineering and Chemistry, University of Wisconsin, Madison, 2005
M.S. Chemical Engineering Practice, Massachusetts Institute of Technology, 2007

Doctor of Philosophy in Chemical Engineering

at the

MASSACHUSETTS INSTITUTE OF TECHNOLOGY

February 2011

Author:_____
Department of Chemical Engineering
September, 2010

Certified by:_____
Paula T. Hammond, Professor
Thesis Supervisor

Accepted by:_____
Professor William M. Deen
Professor of Chemical Engineering
Chairman, Departmental Committee on Graduate Students

Synthesis and Testing of Novel Polypeptides for Biological Applications

by

Amanda Catherine Engler

Submitted to the Department of Chemical Engineering on November 15, 2010 in partial fulfillment of the requirements for the degree of

Doctor of Philosophy in Chemical Engineering

Abstract

Natural systems produce macromolecules that assemble into complex, highly ordered structures. In particular, proteins and peptides derived from the 20 naturally occurring amino acids are sequenced macromolecules that can fold into secondary and tertiary structures and can self assemble into quaternary structures. Through weak interactions, these ordered systems produce high-strength materials, provide physical cues to induce cell functions and morphologies, efficiently harvest energy, and transport materials. One of the key challenges in the field of polymer chemistry is the ability to generate synthetic systems that can demonstrate the highly ordered structure, self-assembly, and responsive behavior of these macromolecules.

Synthetic polypeptides have received attention because of their unique structural properties and biocompatibility. Like their naturally occurring analogs, these molecules have a poly(amino acid) backbone and posses the ability to fold into secondary structures. Synthetic homo polypeptides are synthesized by the ring opening polymerization of N-carboxyanhydrides formed from naturally occurring amino acids. Although these macromolecules' secondary structure can be controlled to some extent, we are limited by the given side chain, which dictates polymer function, structure, and responsive behavior to temperature or pH among many other properties. We have developed a new approach to the manipulation of synthetic polypeptide composition and function through the introduction of a new NCA polymer, poly(γ-propargyl-L-glutamate) (PPLG) which contains a pendant alkyne group that can be reacted with an azide by the 1,3 cycloaddition "click" reaction. With this system, we can incorporate functional groups that are ordinarily difficult to introduce because of cross-reactions or exhaustive protection-deprotection steps. In addition, we can more directly mimic the adaptive function and responsive behavior of naturally occurring polypeptides.

This thesis focuses on the development of the PPLG system and the use of the system for synthetic biomimics, drug delivery, and gene delivery. For synthetic biomimics, as an initial example, densely grafted polymers were synthesized to demonstrate the utility of this synthetic approach. In addition, synthetic antimicrobial polypeptides were synthesized to mimic naturally occurring antimicrobial peptides. For drug and gene delivery, a library of pH responsive peptides were synthesized and characterized.

Thesis Supervisor:	Paula T. Hammond
Title:	Executive Officer, Chemical Engineering
	Bayer Professor of Chemical Engineering

Acknowledgements

I could not have completed this thesis without the generosity and support of many. It has been an amazing journey and there are many people that I would like to thank...

There are many faculty that have helped contribute to my success at MIT. First, I would like to thank my thesis advisor Prof. Paula Hammond for being a wonderful mentor and role model. Without your endless support and encouragement, this thesis would not have been possible. My thesis committee, Prof. Linda Griffith, Prof. J. Christopher Love, and Prof. Darrell Irvine have been incredibly helpful. Thank you for your time, patience, and invaluable advice on both my research and professional development. I would like to give a special thanks to Prof. Daniel Blankschtein. Thank you for your encouragement and mentorship in the early years of my research and during my time as a 10.40 TA. You always believed in me even when I did not think I would make it through. To Prof. Bob Fischer and Prof. Claude Lupis, thank you for being wonderful mentors and for all the helpful advice throughout my time away at practice school and here at MIT.

During my time here at MIT I have had the opportunity to work with so many talented post docs, graduate students, and undergraduates. First, I would like to thank those who took me under their wings and introduced me to chemistry. Prof. Hyung-il Lee, your energy and excitement for polymer chemistry was truly inspirational. Thank you for sharing your knowledge with me and providing countless hours mentoring me both in and out of the lab. Dr. Ryan Moslin, thank you for answering all my chemistry questions, helping me trouble shoot my failed reactions, and providing me with hours of conversation as I rotovapped my time away. Thank you Dr. Phoung Nguyen for showing me the ways of NCA polymerization and providing mentorship early in my PhD. To the members of the Hammond lab, both past and present, thank you for all of your support and encouragement throughout my time in the lab. I would like to specially thank the linear dendritic/polymer synthesis team (Shujun Chen, Zhiyong Poon, Hyung-il Lee, Dan Bonner, Michael Petr, Steven Elliott, Abby Oelker, Megan O'Grady, Dong Sook Chang, Xiaoyong Zhao, Jong Bum Lee, and an honorary member Caroline Chopko). Thank you for all your helpful discussions and great advice. Thank you Anita Shukla and Dan Bonner for being the best collaborators anyone could possibly have. To the Swager lab (especially Ryan Moslin, Jason Cox, and Stefanie Sydlik), thank you for answering all my crazy chemistry questions, providing helpful discussion, and letting me borrow equipment. I would also like to thank the Blankschtein group for all of the encouragement early in my thesis work. Hilda Buss and Eva Cheung have been wonderful UROPS. Thank you for all your time and enthusiasm.

The support staff at MIT has been incredible! I would like to extend a thank you to the ISN staff (Amy Tatem-Bannister, Donna Johnson, Bill DiNatale, Steve Kooi, and Marlisha McDaniels) for keeping the ISN in top shape and making sure all the equipment ran properly. The administrative staff, including Linda Mousseau and Christine Preston was always willing to help me out. Thank you to the support staff at the BIF (Debby Pheasant) and the DCIF (Anne Gorham, Jeff Simpson, and Li Li). Thank you for keeping the instruments up and running.

A special thank you to my friends, from all phases of life! Thank you for your support through both the good times and the bad. The ISN breakfast club (organized by Zhiyong and Nisarg) turned the ISN offices into a great place to hang out. To the Whale Wars and Spizzles crew (Joe, Wally, EA, Beez, Kevin), thanks for all the encouragement, great advice, and laughter. To the

MIT women's water polo team (especially Blair, Analiese, Charlotte, and Carrie), thank you for introducing me to a wonderful sport and providing me with hours of entertainment. To the ladies of 15E and my dinner crew friends (especially Claire, Jess, Rachel, and Jon), thanks for all of the wonderful times in Tang and the many great meals among friends. To Next 3W, thank you for all of the memories and for letting Curtis and I be a part of your college experience. To Melissa and Becky, thanks for always being just a short phone call away. Although I have not mentioned everyone here, you have not been forgotten.

Last but most important, I would like to thank my family (Mom, Dad, Mary, Nathan, Marian, Melissa, Steve, Alexander, Michael, and Curtis). Thank you Mom and Dad for being incredibly supportive and telling me I could do anything I wanted to do. My siblings (Mary, Melissa, and Michael) have been incredibly supportive and have reminded me that there is life outside of graduate school. A special thanks to Mary for all her chemistry advice! To my husband Curtis, thank you for providing me with the gifts of love and laughter.

Table of Contents

List of Figures

List of Tables

List of Schemes

1 Introduction and Background

1.1 Motivation

Natural systems produce macromolecules that assemble into complex, highly ordered structures.[1] In particular, proteins and peptides derived from the 20 naturally occurring amino acids, are sequenced macromolecules that can fold into secondary and tertiary structures and can self assemble into quaternary structures (Figure 1-1). Through weak interactions, these ordered systems produce high-strength materials, provide physical cues to induce cell functions and morphologies, efficiently harvest energy, and transport materials.[2, 3] One of the key challenges in the field of polymer chemistry is the ability to generate synthetic systems that can demonstrate the highly ordered structure, self-assembly, and responsive behavior of these macromolecules.[4-8] In essence, can we mimic nature?

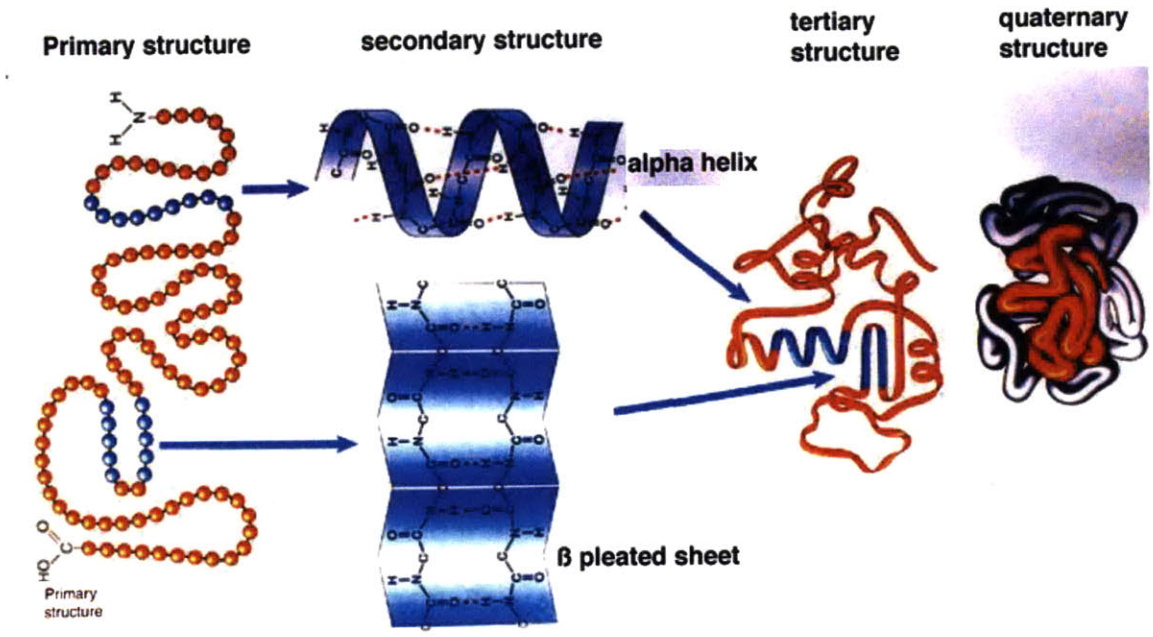

Figure 1-1. Schematic of protein structure. Image adapted from: http://academic.brooklyn.cuny.edu/biology/bio4fv/page/3d_prot.htm

1.2 Synthetic polypeptides

Sequenced peptides can be accurately synthesized using a solid state peptide synthetic approach; yet these molecules are limited to relatively short peptide sequences (< 30 residues) and small quantities. This approach has low yields, requires time consuming processing steps, has costly purifications, and is overall very expensive.[4] While approaches that use genetic engineering or synthetic biology are quite promising,[5, 9, 10] these systems require significant development of biological platforms and the purification can be challenging. Many synthetic polymers can be produced that have controlled chain length but do not have the ability to adopt a secondary structure, such as beta sheets or helices. These highly ordered structures are imperative because they allow proteins and peptides to optimally display surface moieties that dictate cell signaling and molecular docking as well as supramolecular shape and programmable function.[1, 7, 11-13] Synthetic polypeptides, although simpler than proteins, introduce a powerful capability to generate macromolecular species that have an amino acid backbone and thus possess the ability to fold into stable secondary structures. Furthermore, these polymers have low toxicity, have long-term biodegradability, and can be inexpensively produced on the large scale. These properties give synthetic polypeptides an advantage over sequenced peptides prepared by either solid state synthesis, genetic engineering, or other biosynthetic methods.

1.3 Limitations of synthetic polypeptides generated from N-carboxyanhydrides

Synthetic polypeptides are synthesized by a well-studied ring-opening polymerization (ROP) of N-carboxyanhydrides (NCA), shown in Figure 1-1. The polymerization can be initiated by a variety of initiators; here the polymerization is initiated with a primary amine, which is the method of initiation utilized in this body of work. There are a number of additional initiation methods for controlling the polymerization and formation of homopolymers and block

copolymers.[1, 12-16] The NCA monomer is typically formed from amino acids containing alkyl end groups or protected functional groups. The functional groups, in particular, the carboxylic acid moiety (e.g. glutamate and aspartate) and amino (e.g. lysine) moiety, have been used to add chemical complexities, such as pharmaceutical drugs and molecules that dictate hydrophobicity or pH responsiveness.[17-19] When creating polypeptides with functional groups, a three step process is often required: (1) polymerization with the protected functional group, (2) the deprotection of the functional group, and (3) the functionalization. If a high degree of functionalization is required, the added chemical moieties are limited to small molecules and low molecular-weight oligomers. There is a pressing need to create a more readily adaptable platform to attach a broad range of groups at the amino acid backbone with ease and control.

Scheme 1-1. Ring opening polymerization of N-carboxyanhydrides initiated by a primary amine

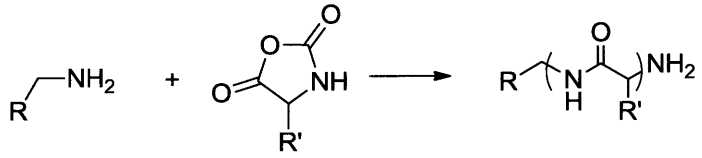

1.4 Click chemistry and polymers

Highly quantitative functionalization chemistries have been developed and evolved for use with polymers over the past several years. Click reactions, which were first described by Sharpless et al., [20] refer to a series of highly efficient reactions that include the adapted Huisgen 1,3-dipolar cycloaddition reaction between an alkyne and an azide to form a triazole (Scheme 1-2).[20] These reactions have received a significant amount of attention because of their high reaction efficiency (near 100%), mild reaction conditions, functional group tolerance, and few byproducts.[20] In recent years, click chemistry has been used in a wide variety of polymer applications including functionalization of polymers with small molecules, formation of diblock

polymers, formation of new dendrimers, formation of macromonomers, crosslinking of micelles, polymer attachment to surfaces, and the "grafting onto" method for the formation of molecular brushes.[21-30]

Scheme 1-2. 1,3-dipolar cycloaddition reaction between an alkyne and an azide to form a triazole[20]

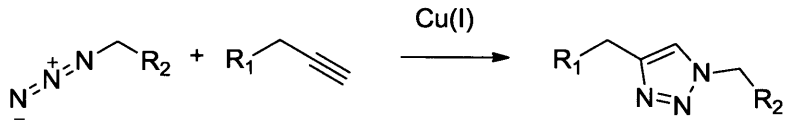

1.5 A library or polypeptides based on PPLG

To broaden the range of capabilities possible with the NCA chemistry platform, we have synthesized a new NCA polymer, poly(γ-propargyl-L-glutamate) (PPLG), which incorporates an alkyne group that can be easily reacted with an azide using click chemistry.[31] Ease of synthesis of both small molecule and macromolecule side groups that exhibit a broad range of polarity and charge provide a key platform for the generation of families of synthetic polypeptides. With this system, we can incorporate functional groups that are ordinarily difficult to introduce because of cross-reactions or exhaustive protection-deprotection steps. In addition, we can more directly mimic the adaptive function and responsive behavior of naturally occurring polypeptides. In Scheme 1-1, PPLG and a library of reactive click groups synthesized for this thesis are shown. This library is just a small subset of a much larger library of polypeptides that can be synthesized utilizing this approach.

Scheme 1-3. PPLG and a library of reactive click groups synthesized for this thesis

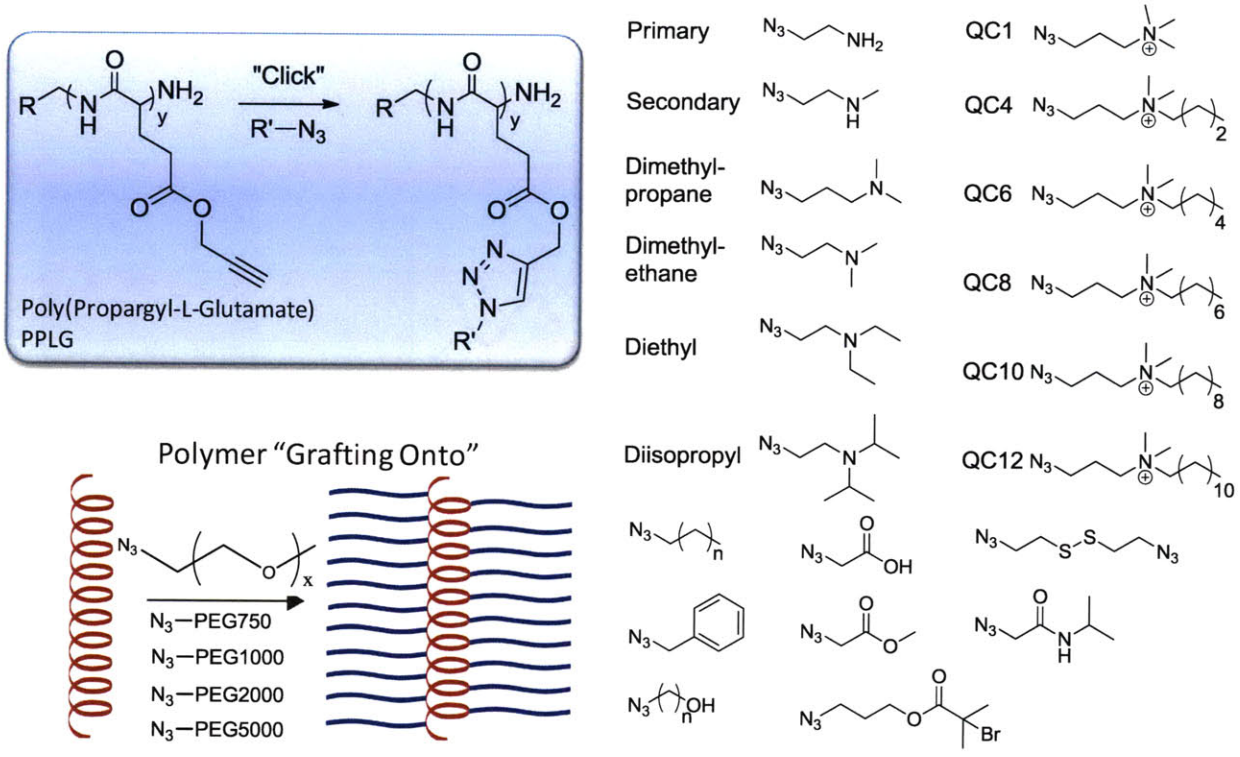

There are many potential applications for this system, several of which are illustrated in Figure 1-2. From left to right, these applications are pH responsive polymers that interact reversibly with biological cell membranes or liposomal structures, polyelectrolytes for layer by layer deposition, reversible colloid formation for drug and gene delivery, highly grafted polypeptides designed to exhibit biophysical properties appropriate to mimic the intracellular microenvironment, and responsive hydrogels for tissue engineering. This thesis focuses on the development of the PPLG system and the use of the system for synthetic biomimics, drug delivery, and gene delivery. For synthetic biomimics, as an initial example, densely grafted polymers were synthesized to demonstrate the utility of this synthetic approach. In addition, synthetic antimicrobial polypeptides were synthesized to mimic naturally occurring antimicrobial peptides. For drug and gene delivery, a library of pH responsive peptides were synthesized and

characterized. A brief introduction of each area of research and the role of PPLG in each area is provided below.

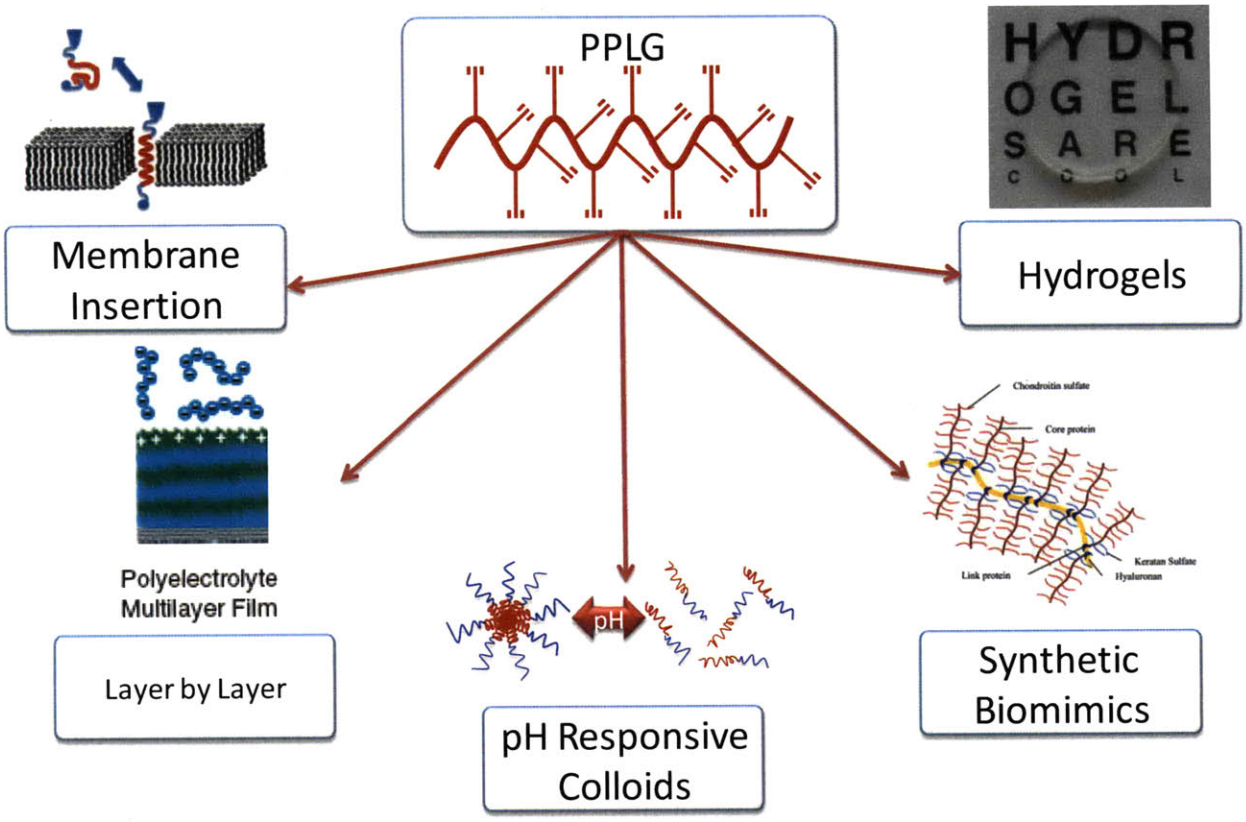

Figure 1-2. Schematic illustrating application of the clickable synthetic polypeptides. The LBL image is from Hammond PT. Advanced Materials. 2004;16(15):1271-93.[32], The synthetic biomimics image is from K. Lienkamp et. al., Macromolecules 2007, 40, 2486.[33], and the hydrogel image was provided by Abigail Oelker (PhD).

1.6 Synthetic biomimics

1.6.1 Proteoglycans and glycoproteins

A cell's extracellular matrix consists of macromolecules, such as glycoproteins, proteoglycans, and collagen, that control both the mechanical structure and the microenvironment.[2] These properties provide physical cues that are necessary to induce various

cell functions and morphologies. An important goal of tissue engineering is to mimic the environment of the extracellular matrix on several levels, mechanically, chemically, and architecturally.[34] Glycoproteins are loosely grafted brush polymers that contain short oligosaccharide side chains that can contain 1-60 wt% carbohydrates. Proteoglycans contain polypeptides that are heavily grafted with unbranched glycosaminoglycan chains, typically 80 sugars long and contain as much as 95 wt% carbohydrates.[35] These macromolecules, in particular, have the ability to absorb a large amount of water and form gels which give elasticity and structural integrity to many tissues including blood vessels, skin, and cartilage.[33] These large macromolecules are difficult to isolate and therefore the development of synthetic mimics would aid in providing a fundamental understanding as to the role of these macromolecules in the extracellular environment. With these macromolecules in mind, the synthetic approach for highly efficient grafting onto a peptide backbone was developed for the PPLG system.

1.6.2 Antimicrobial peptides

The overuse of systemic antibiotics has led to a rise in multidrug resistant bacteria.[36] Compounded by a lack of discovery and approval of new classes of antibiotics, there is a pressing need for the development of novel antimicrobial agents.[36, 37] Antimicrobial peptides (AmPs) are a promising alternative to traditional small molecule antibiotics. These peptides are components of the natural immune system and show broad spectrum activity against bacteria, fungi, and some viruses. Unlike traditional antibiotics, these macromolecules have a low propensity to induce pathogen resistance. These short peptide sequences (20-50 residues) adopt amphiphilic topologies in which the hydrophobic and positively charged hydrophilic segments segregate. The positive charge interacts with the negatively charged bacteria phospholipid membrane and the hydrophobic portion can penetrate into the membrane resulting in disruption

of the membrane and in some cases bacteria death.[38] Despite the advantages over traditional antibiotics, there are several limitations which hinder the use of AmPs. AmPs are subject to proteolytic degradation, can be toxic to mammalian cells, and are expensive to produce. [38, 39] Polymeric synthetic mimics of AmPs could provide a promising alternative to naturally occurring AmPs. With the PPLG system, we have a great deal of control over polymer functionality as well as secondary structure, making this synthetic strategy useful for developing AmP mimics.

1.7 Drug and Gene Delivery

Polymer therapeutics and drug carriers show great promise for applications such as drug and gene delivery. They have many features of biological macromolecular drugs with the added benefit of synthetic versatility.[40] There are many types of polymer therapeutics, as shown in Figure 1-3; however the focus of this thesis is on the design of polymeric micellar drug and gene delivery carriers.

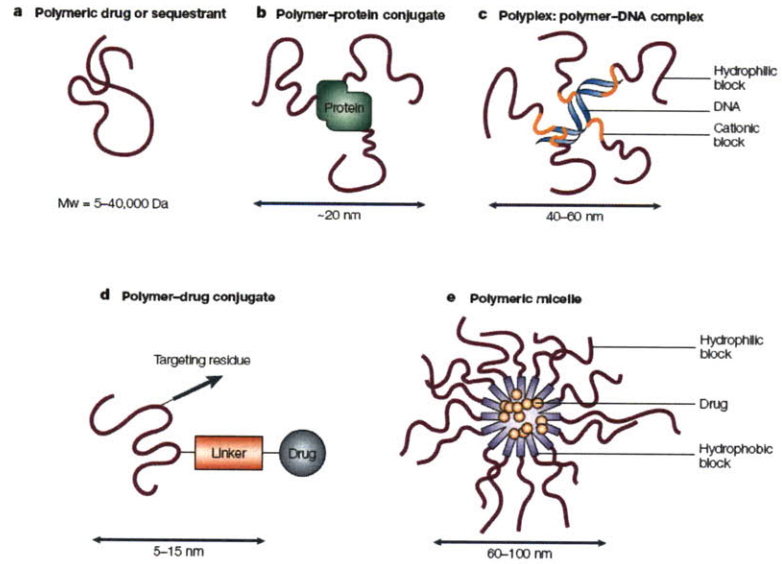

Figure 1 | **Schematic representation of polymer therapeutics now in, or progressing towards, clinical development.** The nano-sized and frequently multicomponent nature of these structures is visible. Mw, molecular weight.

Figure 1-3: Polymer therapeutics[40]

1.7.1 Delivery Barriers

For the effective intravenous delivery of drug carriers through the blood stream to desired tissue (e.g. organ or tumor), there are four main barriers that must be overcome:[17]

1. The carriers must have a long blood circulation time. Small molecule drugs are rapidly cleared from plasma by the kidneys. This obstacle can be avoided by designing a system with a high molecular weight.
2. The carrier must be small enough to be taken up from the blood into target tissue.
3. Carriers must be taken up by cells and undergo endocytosis. Targeting may be necessary for systems that have low permeability through cellular membranes or when specific tissue is targeted.
4. Intracellular trafficking is important such that the gene or drug reaches the desired target inside the cell.

In addition to overcoming the systemic barrier to delivery, the delivery vehicles must be designed to successfully encapsulate the desired cargo, whether it is a drug or genetic material, and release the cargo at the desired location.

1.7.2 A modular delivery system

To overcome the barriers of systemic delivery, modular delivery systems are being designed with multiple functional domains. We have selected a simple block copolymer system with a poly(ethylene glycol) (PEG) block and a PPLG block that can be easily functionalized with small molecules to optimize either pH responsive drug delivery or gene delivery. The PEG block can also have an attached target moiety. A schematic of the design is show in Figure 1-4.

The rational design of this system is explained below. Each polymer of the diblock system was selected to overcome different barriers of systemic delivery.

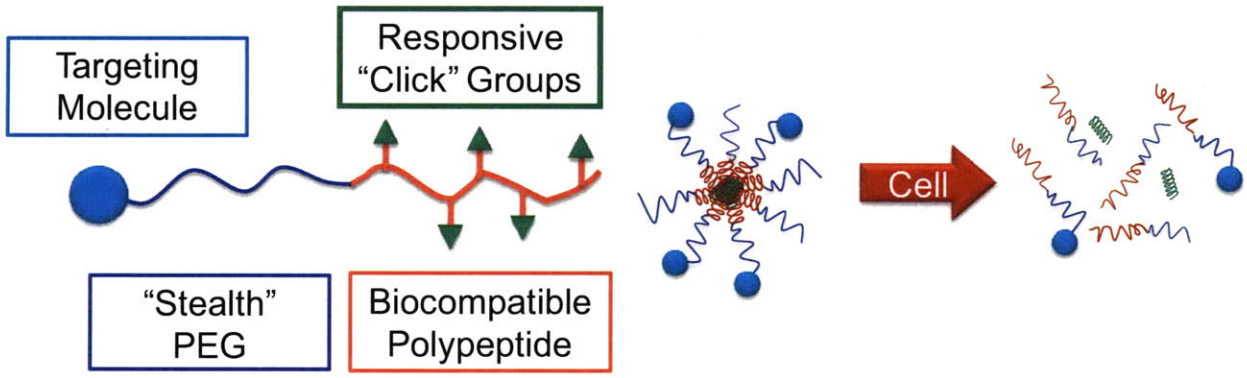

Figure 1-4. Schematic of drug or gene delivery vehicle

1.7.3 Designing micelles: overcoming the delivery barriers

Micelle delivery systems have shown great promise in the area of both drug and gene delivery. When designing these particles, controlling size and surface properties is of utmost importance. For both active and passive targeting systems, the longer the micelle system circulates in the body the better chance it has of reaching its desired target. For example, passive drug delivery to cancerous tumors takes advantage of the enhanced permeation and retention effect (EPR).[41] Because of the increased circulation time of these colloids, they are able to extravasate into the leaky vasculature of tumor tissue. Since the lymphatic drainage system for tumor tissues are poorly developed, the end result is the accumulation of the colloidal nanoparticles in tumors. In the literature, there are numerous examples of diblock copolymer systems that take advantage of EPR effect. [17, 19, 42-44]

To increase circulation time in the blood stream, particle size is very important. Particles must have a diameter smaller than 150 nm in order to avoid the reticuloendothelial system (RES)

but larger than 2-3 nanometers to avoid being filtered out by the kidneys.[45] The size of the particles is also important in determining the rate of endocytosis of the particles; endocytosis in non-phogocytic cells will not occur for particles larger than 150 nm.[46] Overall, an intermediate particle size is desired.

The RES is also aided by the adsorption of proteins onto the nanoparticle surface, which would promote phagocytosis.[47] The design of surface properties such that proteins do not adsorb is very important in increasing circulation time. Neutrally charged surfaces have a lower tendency to be cleared by the RES than charged surfaces. Cationic particles stick to negatively charged cell membranes and are then quickly removed from circulation.[48] Furthermore, some cationic polymers can cause hemolysis and are cytotoxic.[49, 50] Anionic particles are recognized by receptors found on macrophages and are therefore rapidly cleared from the body.[51]

The most common surface coverage for particles is the neutral polymer, poly(ethylene glycol) (PEG). This water soluble polymer has stealth-like properties when delivered systemically. PEG decreases the toxicity of the nanoparticle by decreasing the interaction with the body and is used to reduce the rate of uptake by the RES, therefore increasing circulation half-life.[52] When PEG is in the blood stream, water molecules form a sheath around the PEG. This neutral coating prevents the adsorption of opsonins to the particle surface and significantly reduces the interaction of the particle with the physiological environment.[50, 53] Due to these properties, PEG is often selected as the hydrophilic, exterior block of diblock micelle drug and gene carriers, including PEG-b-poly(amino-acids).[17, 19, 44, 54-58] For our system, PEG has been selected as the exterior polymer because of its stealth properties and diblock polymers created with an exterior PEG block can be tuned to the proper size for systemic delivery.

To provide cargo protection and overcome the intracellular barriers, we focused on designing the interior block using the biocompatible PPLG polymers with varied side groups. For drug delivery, the goal is to develop a block that is pH responsive, such that in the blood stream (pH 7.00-7.45)[59] the interior block is hydrophobic to solublize a hydrophobic drug and in the endosome (early endosome pH 5.5-6.3 and late endosome pH < 5.5)[60-62] or the hypoxic region of tumors (pH approaching 6.0),[59] the interior block becomes hydrophilic, thus destabilizing the micelle to release the drug.

For gene delivery, the amine groups have two different roles. The first is to complex the positively charged polymer with the negatively charged siRNA or DNA. Cationic polymers with primary or in some cases secondary amines are typically selected for this role. A secondary role of many cationic polymers is to assist the polyplexes in endosomal escape through the "proton sponge" effect. The "proton sponge" effect is the use of cationic functional groups with pKa values that lie near the range of 5-6 so that when the polyplexes are inside the acidic endosome, the amines become protonated. To maintain an acidic environment, the endosome generates more acidic protons, resulting in more chloride ions and water entering the endosome. As a result, the osmotic pressure increases, and the endosomal membrane destabilizes and ruptures, releasing the polyplex into the cytoplasm.[63]

1.8 Thesis Overview

The remainder of this thesis is divided into 5 additional chapters. Chapter 2 contains detailed experimental protocols for all of the remaining Chapters. This chapter also provides additional protocols for materials that were synthesized but are not reported in later chapters. This information is provided to aid future researchers working with the PPLG and other clickable polypeptide systems.

In Chapter 3, the PPLG system is initially described. A model PPLG-g-PEG system is used to show the capabilities of this synthetic approach. The kinetics of the PPLG click reaction, the efficiency of the grafting onto reaction, and backbone integrity during the reaction were examined. The goal of this brush polymer system is to mimic naturally occurring biomacromolecules on the molecular level.

Chapter 4 explores the use of the PPLG system to create an entire library of pH responsive polypeptides. These polymers include both poly(γ-propargyl L-glutamate) (PPLG) based homopolymers and poly(ethylene glycol-b-γ-propargyl L-glutamate) (PEG-b-PPLG) block copolymers substituted with various amine moieties that range in pKa and hydrophobicity, providing the basis for a library of new synthetic structures that can be tuned for specific interactions and responsive behaviors. These properties are of interest for a number of applications; preliminary experiments were performed that demonstrate that these polymers are strong candidates for drug and gene delivery.

In Chapter 5, the PPLG system was utilized to synthesize an entire library of antimicrobial polypeptides that mimic naturally occurring AmPs. The effect of the side chain functionality and the polypeptide length was evaluated using a modified microdilution assay to determine the minimum inhibitory concentration (MIC), or the lowest point at which visible bacteria growth is inhibited, against both gram-negative and gram-positive bacteria. A bacteria attachment assay was also carried out on polypeptide coatings to evaluate their potential efficacy for use as antimicrobial surface coatings. To determine their level of biocompatibility, red blood cell (RBC) lysis was monitored in the presence of these polypeptides.

Chapter 6 includes the overall conclusion for this thesis as well as suggestions of future applications and extensions of the clickable polypeptide system.

1.9 References

1. Deming, T. J., Synthetic polypeptides for biomedical applications. *Prog. Polym. Sci.* **2007,** *32* (8-9), 858-875.

2. Griffith, L. G.; Swartz, M. A., Capturing complex 3D tissue physiology in vitro. *Nat. Rev. Mol. Cell Biol.* **2006,** *7* (3), 211-224.

3. Ober, C. K.; Zheng, S. Z. D.; Hammond, P. T.; Muthukumar, M.; Reichmanis, E.; Wooley, K. L.; Lodge, T. P., Research in Macromolecular Science: Challenges and Opportunities for the Next Decade. *Macromolecules* **2009,** *42* (2), 465-471.

4. Badi, N.; Lutz, J. F., Sequence control in polymer synthesis. *Chemical Society Reviews* **2009,** *38* (12), 3383-3390.

5. Connor, R. E.; Tirrell, D. A., Non-canonical amino acids in protein polymer design. *Polymer Reviews* **2007,** *47* (1), 9-28.

6. Langer, R.; Tirrell, D. A., Designing materials for biology and medicine. *Nature* **2004,** *428* (6982), 487-492.

7. Patterson, J.; Martino, M. M.; Hubbell, J. A., Biomimetic materials in tissue engineering. *Materials Today* **2010,** *13* (1-2), 14-22.

8. Tomalia, D. A.; Wang, Z. G.; Tirrell, M., Experimental self-assembly: the many facets of self-assembly. *Current Opinion in Colloid & Interface Science* **1999,** *4* (1), 3-5.

9. Montclare, J. K.; Tirrell, D. A., Evolving proteins of novel composition. *Angewandte Chemie-International Edition* **2006,** *45* (27), 4518-4521.

10. Wang, A.; Nairn, N. W.; Johnson, R. S.; Tirrell, D. A.; Grabstein, K., Processing of N-terminal unnatural amino acids in recombinant human interferon-beta in Escherichia coli. *ChemBioChem* **2008,** *9* (2), 324-330.

11. Bromley, E. H. C.; Channon, K.; Moutevelis, E.; Woolfson, D. N., Peptide and Protein Building Blocks for Synthetic Biology: From Programming Biomolecules to Self-Organized Biomolecular Systems. *ACS Chemical Biology* **2008,** *3* (1), 38-50.

12. Deming, T. J., Methodologies for preparation of synthetic block copolypeptides: materials with future promise in drug delivery. *Advanced Drug Delivery Reviews* **2002,** *54* (8), 1145-1155.

13. Deming, T. J., Polypeptide and polypeptide hybrid copolymer synthesis via NCA polymerization. *Peptide Hybrid Polymers* **2006,** *202*, 1-18.

14. Aliferis, T.; Iatrou, H.; Hadjichristidis, N., Living polypeptides. *Biomacromolecules* **2004,** *5* (5), 1653-1656.

15. Gibson, M. I.; Cameron, N. R., Experimentally Facile Controlled Polymerization of N-Carboxyan hydrides (NCAs), Including O-Benzyl-L-threonine NCA. *J. Polym. Sci. Pol. Chem.* **2009,** *47* (11), 2882-2891.

16. Lu, H.; Cheng, J. J., Hexamethyldisilazane-mediated controlled polymerization of alpha-Amino acid N-carboxyanhydrides. *J. Am. Chem. Soc.* **2007,** *129* (46), 14114-14115.

17. Osada, K.; Kataoka, K., Drug and gene delivery based on supramolecular assembly of PEG-polypeptide hybrid block copolymers. In *Peptide Hybrid Polymers*, Springer-Verlag Berlin: Berlin, 2006; Vol. 202, pp 113-153.

18. Yokoyama, M.; Kwon, G. S.; Okano, T.; Sakurai, Y.; Seto, T.; Kataoka, K., Preparation of micelle-forming polymer-drug conjugates. *Bioconjugate Chem.* **1992,** *3* (4), 295-301.

19. Lavasanifar, A.; Samuel, J.; Kwon, G. S., Poly(ethylene oxide)-block-poly(L-amino acid) micelles for drug delivery. *Advanced Drug Delivery Reviews* **2002,** *54* (2), 169-190.

20. Kolb, H. C.; Finn, M. G.; Sharpless, K. B., Click chemistry: Diverse chemical function from a few good reactions. *Angewandte Chemie-International Edition* **2001,** *40* (11), 2004-2021.

21. Hawker, C. J.; Wooley, K. L., The convergence of synthetic organic and polymer chemistries. *Science* **2005,** *309* (5738), 1200-1205.

22. Joralemon, M. J.; O'Reilly, R. K.; Hawker, C. J.; Wooley, K. L., Shell Click-crosslinked (SCC) nanoparticles: A new methodology for synthesis and orthogonal functionalization. *J. Am. Chem. Soc.* **2005,** *127* (48), 16892-16899.

23. Helms, B.; Mynar, J. L.; Hawker, C. J.; Frechet, J. M. J., Dendronized linear polymers via "click chemistry". *J. Am. Chem. Soc.* **2004,** *126* (46), 15020-15021.

24. Wu, P.; Feldman, A. K.; Nugent, A. K.; Hawker, C. J.; Scheel, A.; Voit, B.; Pyun, J.; Frechet, J. M. J.; Sharpless, K. B.; Fokin, V. V., Efficiency and fidelity in a click-chemistry route to triazole dendrimers by the copper(I)-catalyzed ligation of azides and alkynes. *Angewandte Chemie-International Edition* **2004,** *43* (30), 3928-3932.

25. Gondi, S. R.; Vogt, A. P.; Sumerlin, B. S., Versatile Pathway to Functional Telechelics via RAFT Polymerization and Click Chemistry. *Macromolecules* **2007,** *40* (3), 474-481.

26. Vogt, A. P.; Sumerlin, B. S., An Efficient Route to Macromonomers via ATRP and Click Chemistry. *Macromolecules* **2006,** *39* (16), 5286-5292.

27. Sumerlin, B. S.; Tsarevsky, N. V.; Louche, G.; Lee, R. Y.; Matyjaszewski, K., Highly Efficient "Click" Functionalization of Poly(3-azidopropyl methacrylate) Prepared by ATRP. *Macromolecules* **2005,** *38* (18), 7540-7545.

28. Riva, R.; Schmeits, S.; Jerome, C.; Jerome, R.; Lecomte, P., Combination of Ring-Opening Polymerization and "Click Chemistry"; Toward Functionalization and Grafting of Poly(ε-caprolactone). *Macromolecules* **2007,** *40* (4), 796-803.

29. Constable, E. C.; Housecroft, C. E.; Neuburger, M.; Rosel, P., Clicking hard-core sugar balls. *Chem. Commun.* **2010,** *46* (10), 1628-1630.

30. Wu, P.; Malkoch, M.; Hunt, J. N.; Vestberg, R.; Kaltgrad, E.; Finn, M. G.; Fokin, V. V.; Sharpless, K. B.; Hawker, C. J., Multivalent, bifunctional dendrimers prepared by click chemistry. *Chem. Commun.* **2005,** (46), 5775-5777.

31. Engler, A. C.; Lee, H. I.; Hammond, P. T., Highly Efficient "Grafting onto" a Polypeptide Backbone Using Click Chemistry. *Angewandte Chemie-International Edition* **2009,** *48* (49), 9334-9338.

32. Hammond, P. T., Form and function in multilayer assembly: New applications at the nanoscale. *Advanced Materials* **2004,** *16* (15), 1271-1293.

33. Lienkamp, K.; Noe, L.; Breniaux, M.-H.; Lieberwirth, I.; Groehn, F.; Wegner, G., Synthesis and Characterization of End-Functionalized Cylindrical Polyelectrolyte Brushes from Poly(styrene sulfonate). *Macromolecules* **2007,** *40* (7), 2486-2502.

34. Benoit, D. S. W.; Schwartz, M. P.; Durney, A. R.; Anseth, K. S., Small functional groups for controlled differentiation of hydrogel-encapsulated human mesenchymal stem cells. *Nat. Mater.* **2008,** *7* (10), 816-823.

35. Alberts, B., Johnson, A., Lewis, J., Raff, R., Roberst, K., Walter, P., *Molecular Biology of the Cell.* Garland Science: New York, NY, 2002.

36. Taubes, G., The Bacteria Fight Back. *Science* **2008,** *321* (5887), 356-361.

37. Gabriel, G. J.; Som, A.; Madkour, A. E.; Eren, T.; Tew, G. N., Infectious disease: Connecting innate immunity to biocidal polymers. *Materials Science and Engineering: R: Reports* **2007,** *57* (1-6), 28-64.

38. Choi, S.; Isaacs, A.; Clements, D.; Liu, D. H.; Kim, H.; Scott, R. W.; Winkler, J. D.; DeGrado, W. F., De novo design and in vivo activity of conformationally restrained antimicrobial arylamide foldamers. *Proceedings of the National Academy of Sciences of the United States of America* **2009,** *106* (17), 6968-6973.

39. Zhou, C.; Qi, X.; Li, P.; Chen, W. N.; Mouad, L.; Chang, M. W.; Leong, S. S. J.; Chan-Park, M. B., High Potency and Broad-Spectrum Antimicrobial Peptides Synthesized via Ring-Opening Polymerization of γ-Aminoacid-N-carboxyanhydrides. *Biomacromolecules* **2009,** *11* (1), 60-67.

40. Duncan, R., The dawning era of polymer therapeutics. *Nat. Rev. Drug Discov.* **2003,** *2* (5), 347-360.

41. Iyer, A. K.; Khaled, G.; Fang, J.; Maeda, H., Exploiting the enhanced permeability and retention effect for tumor targeting. *Drug Discovery Today* **2006,** *11* (17-18), 812-818.

42. Tian, L.; Yam, L.; Wang, J. Z.; Tat, H.; Uhrich, K. E., Core crosslinkable polymeric micelles from PEG-lipid amphiphiles as drug carriers. *Journal of Materials Chemistry* **2004,** *14* (14), 2317-2324.

43. Nguyen, P. M.; Hammond, P. T., Amphiphilic linear-dendritic triblock copolymers composed of poly(amidoamine) and poly(propylene oxide) and their micellar-phase and encapsulation properties. *Langmuir* **2006,** *22* (18), 7825-7832.

44. Kwon, G.; Naito, M.; Yokoyama, M.; Okano, T.; Sakurai, Y.; Kataoka, K., Micelles Based on Ab Block Copolymers of Poly(Ethylene Oxide) and Poly(Beta-Benzyl L-Aspartate). *Langmuir* **1993,** *9* (4), 945-949.

45. Kumar, N.; Ravikumar, M. N. V.; Domb, A. J., Biodegradable block copolymers. *Advanced Drug Delivery Reviews* **2001,** *53* (1), 23-44.

46. Reddy, J. A.; Low, P. S., Folate-mediated targeting of therapeutic and imaging agents to cancers. *Critical Reviews in Therapeutic Drug Carrier Systems* **1998,** *15*, 578-627.

47. Patel, H. M., Serum Opsonins and Liposomes - Their Interaction and Opsonophagocytosis. *Critical Reviews in Therapeutic Drug Carrier Systems* **1992,** *9* (1), 39-90.

48. De Jesus, O. L. P.; Ihre, H. R.; Gagne, L.; Frechet, J. M. J.; Szoka, F. C., Polyester dendritic systems for drug delivery applications: In vitro and in vivo evaluation. *Bioconjugate Chem.* **2002,** *13* (3), 453-461.

49. Beezer, A. E.; King, A. S. H.; Martin, I. K.; Mitchell, J. C.; Twyman, L. J.; Wain, C. F., Dendrimers as potential drug carriers; encapsulation of acidic hydrophobes within water soluble PAMAM derivatives. *Tetrahedron* **2003,** *59* (22), 3873-3880.

50. Kojima, C.; Kono, K.; Maruyama, K.; Takagishi, T., Synthesis of polyamidoamine dendrimers having poly(ethylene glycol) grafts and their ability to encapsulate anticancer drugs. *Bioconjugate Chem.* **2000,** *11* (6), 910-917.

51. Allen, T. M.; Hansen, C.; Martin, F.; Redemann, C.; Yauyoung, A., Liposomes Containing Synthetic Lipid Derivatives of Poly(Ethylene Glycol) Show Prolonged Circulation Half-Lives Invivo. *Biochimica Et Biophysica Acta* **1991,** *1066* (1), 29-36.

52. Kataoka, K.; Harada, A.; Nagasaki, Y., Block copolymer micelles for drug delivery: design, characterization and biological significance. *Advanced Drug Delivery Reviews* **2001,** *47* (1), 113-131.

53. Li, Y. P.; Pei, Y. Y.; Zhang, X. Y.; Gu, Z. H.; Zhou, Z. H.; Yuan, W. F.; Zhou, J. J.; Zhu, J. H.; Gao, X. J., PEGylated PLGA nanoparticles as protein carriers: synthesis, preparation and biodistribution in rats. *Journal of Controlled Release* **2001,** *71* (2), 203-211.

54. Adams, M. L.; Lavasanifar, A.; Kwon, G. S., Amphiphilic block copolymers for drug delivery. *Journal of Pharmaceutical Sciences* **2003,** *92* (7), 1343-1355.

55. Harada, A.; Cammas, S.; Kataoka, K., Stabilized alpha-helix structure of poly(L-lysine)-block-poly(ethylene glycol) in aqueous medium through supramolecular assembly. *Macromolecules* **1996,** *29* (19), 6183-6188.

56. Katayose, S.; Kataoka, K., PEG-poly(lysine) block copolymer as a novel type of synthetic gene vector with supramolecular structure. *Advanced Biomaterials in Biomedical Engineering and Drug Delivery Systems* **1996**, 319-320.

57. Itaka, K.; Ishii, T.; Hasegawa, Y.; Kataoka, K., Biodegradable polyamino acid-based polycations as safe and effective gene carrier minimizing cumulative toxicity. *Biomaterials* **2010,** *31* (13), 3707-3714.

58. Masago, K.; Itaka, K.; Nishiyama, N.; Chung, U. I.; Kataoka, K., Gene delivery with biocompatible cationic polymer: Pharmacogenomic analysis on cell bioactivity. *Biomaterials* **2007,** *28* (34), 5169-5175.

59. Vaupel, P.; Kallinowski, F.; Okunieff, P., Blood-Flow, Oxygen and Nutrient Supply, and Metabolic Microenvironment of Human-Tumors - a Review. *Cancer Research* **1989,** *49* (23), 6449-6465.

60. Mellman, I., The Importance of Being Acid-The Role of Acidification in Intracellular Membrane Traffic. *J. Exp. Biol.* **1992,** *172*, 39-45.

61. Sonawane, N. D.; Szoka, F. C.; Verkman, A. S., Chloride accumulation and swelling in endosomes enhances DNA transfer by polyamine-DNA polyplexes. *Journal of Biological Chemistry* **2003,** *278* (45), 44826-44831.

62. Boeckle, S.; von Gersdorff, K.; van der Piepen, S.; Culmsee, C.; Wagner, E.; Ogris, M., Purification of polyethylenimine polyplexes highlights the role of free polycations in gene transfer. *Journal of Gene Medicine* **2004,** *6* (10), 1102-1111.

63. Boussif, O.; Lezoualch, F.; Zanta, M. A.; Mergny, M. D.; Scherman, D.; Demeneix, B.; Behr, J. P., A Versatile Vector for Gene and Oligonucleotide Transfer into Cells in Culture and in-Vivo - Polyethylenimine. *Proceedings of the National Academy of Sciences of the United States of America* **1995,** *92* (16), 7297-7301.

2 Detailed Synthetic and Experimental Protocols

A full description of the chemical structures and synthetic routes can be found in Chapters 3-5. The detailed synthetic protocols for the monomer, polymers, and side chain "click" groups can be found below. ^{1}H-NMR analysis is included with each protocol. ^{1}H-NMR spectrum for each functionalized polymer is included for completeness in Sections 2.8.2 and 2.8.3. For polymer backbones, GPC analysis of the sample polymer is included with the protocol and GPC traces are included in Sections 2.9.1 and 2.9.2. Many of the "click" groups synthesized are not mentioned in later chapters but are included here to provide a record for future researchers using the PPLG polymer system. Azide safety is also discussed here because organic azides can be *explosive*. The safe handling and storage of these materials is very important. General experimental protocols are also included in this chapter to avoid repetition throughout this thesis. For some protocols, additional notes are included to explain why certain experimental conditions were selected.

2.1 Materials for synthesis of PPLG and PEG-b-PPLG

L-(+)-glutamic acid, 99% minimum was purchased from EMD Chemicals. Do not use the L-glutamic acid purchased from Sigma-Aldrich. It contains an impurity (unidentified) that interferes with the formation of γ-propargyl L-glutamate hydrochloride. Anhydrous 99.8% dimethylformamide (DMF), purchased from Sigma Aldrich was used for polymerization. New bottles or bottles open less than month old were used for polymerizations to ensure the highest purity DMF, free of residual amines. PEG-NH_2 was purchase from NOF Corporation. All chemicals were used as received.

2.2 Monomer synthesis

Synthesis of γ-propargyl L-glutamate hydrochloride. γ-propargyl L-glutamate hydrochloride was synthesized following the procedure presented by Belshaw et al.[1] L-glutamic acid (15 g, 102 mmol) was suspended in propargyl alcohol (550 mL) under argon. Chlorotrimethylsilane (28.5 mL, 224 mmol) was added dropwise to the suspension over 1 hour. The resulting solution was stirred at room temperature for two days until there was no undissolved L-glutamic acid. The final reaction solution looked like a dark tea. The reaction solution was filtered to ensure any residual L-glutamic acid was removed and precipitated into diethyl ether giving a white solid. The crude product was removed by filtration, dissolved in boiling isopropanol, and precipitated into diethyl ether. The product was filtered, washed with diethyl ether, and dried under vacuum to yield 19.13 g (84.5%). ^{1}H-NMR (400MHz, D_2O) δ (ppm) = 4.69 (d, 2H, CH_2CO), 4.05 (t, 1H, CH), 2.86 (t, 1H, C≡CH), 2.63 (dt, 2H, CH-CO), 2.20 (m, 2H, CH_2).

Synthesis of N-carboxyanhydride of γ-propargyl L-glutamate (PLG-NCA). The N-carboxyanhydride of γ-propargyl L-glutamate was synthesized following the procedure presented by Poche et al.[2] γ-propargyl L-glutamate hydrochloride (6 g, 27 mmol) was suspended in dry ethyl acetate (190 mL). The solution was heated to reflux and triphosgene (2.67 g, 9 mmol) was added. The reaction solution was refluxed for 6 hours under nitrogen. The reaction solution was cooled to room temperature and any unreacted γ-propargyl L-glutamate hydrochloride was removed by filtration. The reaction solution was then cooled to 5°C and washed with 190 mL of water, 190 mL of saturated sodium bicarbonate, and 190 mL of brine all at 5°C. The solution was then dried with magnesium sulfate, filtered, and concentrated down to viscous oil (4.53 g, 79.2% yield). ^{1}H-NMR (400MHz, $CDCl_3$) δ (ppm) = 6.5 (s, 1H, NH), 4.68

(d, 2H, CH_2CO), 4.39 (t, 1H, CH), 2.58 (t, 2H, CH-CO), 2.49 (t, 1H, C≡CH), 2.20 (dm, 2H, CH_2). HRMS m/z (ESI, M + NA^+) calculated 212.0553, found 212.0563.

2.3 Homopolymer (PPLG) and Diblock copolymer (PEG-b-PPLG) synthesis

Synthesis of Poly(γ-propargyl L-glutamate) initiated by heptylamine. A typical procedure for the polymerization is as follows. To a flame dried Schlenk flask, heptylamine (14.5 μL, 0.0980 mmol) and DMF (8 mL) were combined under Ar. In a separate vial, PLG-NCA (1.552 g, 7.35 mmol) was dissolved in DMF (8 mL) and added to the reaction flask. The reaction mixture was stirred for three days at room temperature. The polymer was precipitated into diethyl ether and removed by centrifugation (0.823 g, 67.0% recovered, by ^{1}H-NMR n=75, by DMF GPC with PMMA standards M_w=14,100, PDI=1.09).^{1}H-NMR (400MHz, DMF-d_7) δ (ppm) = 8.5 (m, 1H, NH), 4.76 (m, 2H, CH_2CO), 4.09 (m, 1H, CH), 3.38 (m, 1H, C≡CH), 2.55 (dm, 2H, CH-CO), 2.28 (dm, 2H, CH_2). The integration here is per polymer repeat unit (RU).

Synthesis of Poly(ethylene glycol)-b-Poly(γ-propargyl L-glutamate). A typical procedure for the polymerization is as follows. A round bottom flask was rinsed with acetone and oven dried. In a glove box, PEG-NH_2 (0.900 g, 0.180 mmol) was dissolved in DMF (9 mL) in a round bottom flask. PLG-NCA (0.950 g, 4.50 mmol) was dissolved in dry DMF (9 mL) added to the reaction flask. The reaction mixture was stirred for three days at room temperature. The reaction solution was rotovaped and dried under high vacuum to remove the DMF. To remove and residual PLG-NCA and DMF, the polymer was redissolved in dichloromethane precipitated into diethyl ether and removed by centrifugation (1.45 g, 87.9% recovered, by ^{1}H-NMR n = 23, by GPC $M_{wPEG\text{-}NH2}$ = 11500, PDI = 1.14, $M_{wPEG\text{-}b\text{-}PPLG}$ = 15800, PDI = 1.08).

^{1}H-NMR (400MHz, [D_6] DMF) δ (ppm) = 8.5 (m, 1H, PPLG RU, NH), 4.76 (m, 2H, PPLG RU, CH_2CO), 4.09 (m, 1H, PPLG RU, CH), 3.59 (s, 4H, PEG RU, CH_2CH_2O), 3.38 (m, 1H, PPLG RU, C≡CH), 2.55 (dm, 2H, PPLG RU, CH-CO), 2.28 (dm, 2H, PPLG, CH_2).

2.4 "Click" group synthesis

2.4.1 Azide Safety: AZIDES CAN BE EXPLOSIVE[3]

Organic azides can be EXPLOSIVE! There are several things to consider when making and storing these compounds. Sodium azide itself is relatively safe; however it can be acidified to HN_3, a volatile and highly TOXIC gas. In general, when working with azides, keep in mind the "rule of six." Six carbons to every azide (N_3) provide enough dilution to render the compound relatively safe. Decomposition of organic azides can be catalyzed by certain transition metals, strong acids, and heat. Azides are very sensitive to heat. When heating azides, a bulk solution should not be heated above 50°C (personal experience, the solution will start to boil and a large amount of heat is generated, resulting in a violent reaction) and a dilute solution should not be heated above 80°C. Do NOT distill azides. If you absolutely need to distill an azide, use vacuum distillation and carefully watch temperature. If leaving a reaction solution overnight, please label everything as explosive and leave detailed instructions as to how to handle your reaction if there is an emergency in the laboratory (fire, power loss, etc). If running a reaction in bulk rather than in solution, use small volumes to prevent injury or serious damage if there is a violent reaction. You can store azides in bulk but please use common sense. I store my azides in 20 mL vials in a fridge rated to hold organics. Please keep in mind that some azide containing compounds are volatile.

2.4.2 Synthesis of azido-terminated PEG (PEG-N_3)

PEG-N_3 was synthesized following the protocol present by Gao and Matyjaszewski.[4] Briefly, PEG-OH with $M_n \sim 750$ g/mol (13.7 g, 18.3 mmol) was dissolved in 100 mL dichloromethane (dried with $MgSO_4$) and placed in a clean, dry round bottom flask. The solution was cooled in an ice bath and triethylamine (12.5 mL, 91.3 mmol) and methane sulfonyl chloride (7 mL, 91.3 mmol) were added sequentially. The reaction was allowed to stir at room temperature for two days. The solution turned a slight yellow color and white precipitant formed (triethylamine salt). The precipitant was filtered and the reaction solution was washed sequentially with 300 mL 1M HCl, 300 mL 1M NaOH, and 300 mL brine (saturated NaCl solution). The organic layer was dried over $MgSO_4$ and the product was isolated by removing the solvent by rotovap and high vacuum, yielding a yellow viscous liquid (PEG 750, 8.7839 g, 64% recovered) (for low MW PEG) or a yellow/white solid (for high MW PEG). ^{13}C-NMR (400MHz, $CDCl_3$) δ (ppm) = 70.4 (s, CH_2CH_2O), 58.9 (s, CH_3O), 37.6 (s, OSO_2CH3). The PEG-OSO_2CH_3 (8.7839 g, 10.6 mmol) was dissolved in 40 mL DMF and heated to 50° C in a round bottom flask. Sodium azide (1.4818 g, 21.2 mmol) and tetrabutyl ammonium iodide (0.16 g) were added sequentially. The reaction mixture was stirred at 50° C for 24 hours. The DMF was removed by rotovap and the remaining solid was dissolved in dichloromethane. The cloudy organic solution was washed with water twice and then dried over $MgSO_4$. The dichloromethane was removed by rotovap and the remaining solid was dried under high vacuum yielding PEG-N_3 (5 g, 63% recovered). The structure was verified by ^{13}C-NMR (400MHz, $CDCl_3$) δ (ppm) = 70.4 (s, CH_2CH_2O), 58.9 (s, CH_3O), 50 (s, CH_2N_3). PEG-N_3 with M_w = 1000, 2000, 5000 g/mol were synthesized following the same protocol.

2.4.3 Synthesis of amino azides

Synthesis of 2-bromo-N-methylethanamine hydrobromide (precursor to 2-azido-N-methylethanamine). 2-bromo-N-methylethanamine hydrobromide was synthesized following the protocol presented by Shutte et al.[5] Briefly, in a round bottom flask, 48% w/w HBr (30mL) was cooled in an ice bath to 4°C and 2-(methylamino)ethanol (10 mL, 125 mmol) was added dropwise. H_2O and HBr were distilled off and the crude product solution was cooled to 60°C. The solution was slowly added to a solution of cold acetone, where it precipitated out to form a white solid. The precipitant was removed, washed with cold acetone, and dried under high vacuum (16.46 g, 60.4% yield). ^{1}H-NMR (400MHz, D_2O) δ (ppm) = 3.69 (t, 2H), 3.50 (t, 2H), 2.75 (s, 3H).

General synthesis of amino azides (1°, 2°, 3°). Amino azides were synthesized using the protocol presented by Carboni et al.[6] A representative example, 3-dimethylamino-1-propylchloride hydrochloride (10 g, 63 mmol) and sodium azide (8.22 g, 126 mmol) were dissolved in water (1 mL/mmol) and heated at 75°C for 15 h. The reaction mixture was cooled in an ice bath and NaOH (4 g) was added. The solution phase separated and the organic phase was removed. The aqueous phase was extracted with diethyl ether twice. The organic layers were combined, dried with $MgSO_4$, and concentrated down to an oil using a rotovap. Residual diethyl ether was removed by allowing the ether to evaporate off in the hood, leaving a pure product (6.60 g, 80.8% yield). Some of the amino azides are volatile so do not dry them under high vacuum. Dimethylpropanamine (3-azido-N,N-dimethylpropan-1-amine) ^{1}H-NMR (400MHz, $CDCl_3$) δ (ppm) = 3.30 (t, 2H, $N_3CH_2CH_2CH_2N(CH_3)_2$), 2.30 (t, 2H, $N_3CH_2CH_2CH_2N(CH_3)_2$), 2.17 (s, 6H, $N_3CH_2CH_2CH_2N(CH_3)_2$), 1.71 (m, 2H, $N_3CH_2CH_2CH_2N(CH_3)_2$). Primary amine (2-azidoethanamine) ^{1}H-NMR (400MHz, $CDCl_3$) δ

(ppm) = 3.32 (t, 2H, $N_3CH_2CH_2NH_2$), 2.83 (t, 2H, $N_3CH_2CH_2NH_2$), 1.45 (s, 2H, $N_3CH_2CH_2NH_2$). Secondary amine (2-azido-N-methylethanamine) ^{1}H-NMR (400MHz, $CDCl_3$) δ (ppm) = 3.45 (t, 2H, $N_3CH_2CH_2NHCH_3$), 2.72 (t, 2H, $N_3CH_2CH_2NHCH_3$), 2.39 (s, 3H, $N_3CH_2CH_2NHCH_3$), 1.28 (s, 1H, $N_3CH_2CH_2NHCH_3$). Dimethylethanamine (2-azido-N,N-dimethylethanamine) ^{1}H-NMR (400MHz, $CDCl_3$) δ (ppm) = 3.32 (t, 2H, $N_3CH_2CH_2N(CH_3)_2$), 2.47 (t, 2H, $N_3CH_2CH_2N(CH_3)_2$), 2.24 (s, 6H, $N_3CH_2CH_2N(CH_3)_2$). Diethylamine (2-azido-N,N-diethylethanamine) ^{1}H-NMR (400MHz, $CDCl_3$) δ (ppm) = 3.25 (t, 2H, $N_3CH_2CH_2N(CH_2CH_3)_2$), 2.62 (t, 2H, $N_3CH_2CH_2N(CH_2CH_3)_2$), 2.52 (q, 2.54, $N_3CH_2CH_2N(CH_2CH_3)_2$), 1.00 (s, 6H, $N_3CH_2CH_2N(CH_2CH_3)_2$). Diisopropylamine (N-(2-azidoethyl)-N-isopropylpropan-2-amine) ^{1}H-NMR (400MHz, $CDCl_3$) δ (ppm) = 3.01 (t, 2H, $N_3CH_2CH_2N(CH_2(CH_3)_2)_2$), 2.98 (m, 2H, $N_3CH_2CH_2N(CH_2(CH_3)_2)_2$), 2.62 (t, 2.54, $N_3CH_2CH_2N(CH_2(CH_3)_2)_2$), 0.99 (d, 12H, $N_3CH_2CH_2N(CH_2(CH_3)_2)_2$).

General synthesis of amino azides (4°). The quaternary amines were prepared following the protocol presented by Vial et al.[7] Briefly, in a typical experiment, 3-azido-N,N-dimethylpropan-1-amine (0.5 g, 3.9 mmol) was dissolved in methanol (5 mL) and added to the haloalkane (bromododecane 0.88 g, 3.54 g) dissolved in methanol (5 mL). The reaction mixture was refluxed for 20 hours and then cooled to room temperature. The methanol and any unreacted 3-azido-N, N-dimethylpropan-1-amine was removed under high vacuum. QC12 ^{1}H-NMR (400MHz, $CDCl_3$) δ (ppm) = 3.71 (m, 2H, CH_2N), 3.56 (t, 2H, N_3CH_2), 3.46 (m, 2H, NCH_2), 3.40 (s, 6H, CH_3), 2.04 (m, 2H, CH_2), 1.70 (m, 2H, CH_2), 1.33 (m, 2H, CH_2), 1.23 (m, 18H, $(CH_2)_9$), 0.85 (t, 3H, CH_3). QC10 ^{1}H-NMR (400MHz, $CDCl_3$) δ (ppm) = 3.64 (m, 2H, CH_2N), 3.53 (t, 2H, N_3CH_2), 3.46 (m, 2H, NCH_2), 3.34 (s, 6H, CH_3), 1.99 (m, 2H, CH_2), 1.66 (m, 2H, CH_2), 1.28 (m, 4H, $(CH_2)_2$, 1.18 (m, 10H, $(CH_2)_5$), 0.80 (t, 3H, CH_3). QC8 ^{1}H-NMR (400MHz,

$CDCl_3$) δ (ppm) =3.66 (m, 2H, CH_2N), 3.54 (t, 2H, N_3CH_2), 3.43 (m, 2H, NCH_2), 3.36 (s, 6H, CH_3), 2.01 (m, 2H, CH_2), 1.68 (m, 2H, CH_2), 1.31 (m, 4H, CH_2CH_2), 1.23 (m, 6H, $(CH_2)_3$), 0.82 (m, 3H, CH_3). QC6 ^{1}H-NMR (400MHz, $CDCl_3$) δ (ppm) =3.62 (m, 2H, CH_2N), 3.52 (t, 2H, N_3CH_2), 3.45 (m, 2H, NCH_2), 3.42 (s, 6H, CH_3), 1.97 (m, 2H, CH_2), 1.65 (m, 2H, CH_2), 1.23 (m, 6H, $(CH_2)_3$), 0.79 (m, 3H, CH_3). QC4 ^{1}H-NMR δ (ppm) =3.66 (m, 2H, CH_2N), 3.55 (t, 2H, N_3CH_2), 3.49 (m, 2H, NCH_2), 3.33 (s, 6H, CH_3), 2.01 (m, 2H, CH_2), 1.66 (m, 2H, CH_2), 1.37 (m, 2H, CH_2), 0.94 (m, 3H, CH_3) (400MHz, $CDCl_3$). QC1 ^{1}H-NMR (400MHz, D_2O) δ=3.50 (t, 2H, N_3CH_2), 3.45 (m, 2H, NCH_2), 3.15 (s, 9H, CH_3), 2.10 (m, 2H, CH_2).

2.4.4 Synthesis of alkyl azides

Alkyl azides were synthesized using the protocol presented by Boyer and Hamer.[8] A representative example, dodecylbromide (10 g, 40 mmol), sodium azide (2.9 g, 45 mmol), and methanol (80 mL) were combined in a round bottom flask. The solution was refluxed overnight. The methanol was removed by rotovap and dichloromethane was added. A white precipitant was formed which was removed by filtration. The dichloromethane was removed by rotovap, yielding the final product as an oil. 1-azidododecane ^{1}H-NMR (400MHz, $CDCl_3$) δ (ppm) = 3.23 (t, 2H, N_3CH_2), 1.55 (m, 2H, $N_3CH_2CH_2$), 1.22 (m, 18H, CH_2), 0.85 (t, 3H, CH_3). 1-azidobutane ^{1}H-NMR (400MHz, $CDCl_3$) δ (ppm) = 3.23, 1.55 (m, 2H, $N_3CH_2CH_2$), 1.33 (m, 2H, CH_2), 0.90 (t, 3H, CH_3). (Azidomethyl) benzene ^{1}H-NMR (400MHz, $CDCl_3$) δ = 7.30 (m, 5H, C_6H_5), 4.48 (s, 2H, CH_2).

2.4.5 Synthesis of azido alcohols

A representative example, 2-bromoethanol (10 mL, 141 mmol), sodium azide (22.9 g, 352 mmol), tetrabutyl ammonium hydrogen sulfate (0.48 g, 1.4 mmol), and water (40 mL) were

combined in a round bottom flask and heated at 30°C for 1 hour. The reaction solution temperature was raised to 75°C and let react for 2 or 3 days (checked crude by NMR). The reaction solution was cooled to room temperature and extracted with dichloromethane or diethyl ether four times. The combined organic phase was dried with $MgSO_4$ and rotovaped to an oil. 2-azidoethanol ^{1}H-NMR (400MHz, $CDCl_3$) δ (ppm) = 3.75 (t, 2H, CH_2OH), 3.41 (t, 2H, CH_2N_3). 3-azidopropan-1-ol ^{1}H-NMR (400MHz, $CDCl_3$) δ (ppm) = 3.72 (t, 2H, CH_2OH), 3.42 (t, 2H, CH_2N_3), 1.80 (m, 2H, CH_2).

2.4.6 Synthesis of carboxylic acid, ester, and amide click groups

Synthesis of azidoacetic acid.[9] Sodium azide (1.979 g, 30.5 mmol) was dissolved in DMSO (20 mL). Bromoacetic acid (2 g, 14.5 mmol) was dissolved in (20 mL) and added dropwise to the sodium azide solution. After 12 hours, the reaction solution was diluted with water (30 mL) and acidified with HCl to protonate the carboxylic acid. The solution was extracted with ethyl acetate three times. The organic layers were combined, washed with brine, dried with $MgSO_4$, and concentrated to an oil. ^{1}H-NMR (400MHz, $CDCl_3$) δ (ppm) = 3.9 (s, 2H, CH_2).

Synthesis of methyl azidoacetate.[10] Methylbromoacetate (8 mL, 84.5 mmol), sodium azide (5.85g, 89.6 mmol), and DMF (20 mL) were stirred in a round bottom flask for 2.5 hours and a white solid formed. Water (20 mL) was added and the mixture was extracted with diethyl ether three times. The organic layer was washed six times with water and then dried with $MgSO_4$. The solvent was removed by rotovap yielding an oil. ^{1}H-NMR (400MHz, $CDCl_3$) δ (ppm) = 3.85 (s, 2H, CH_2), 3.76 (s, 3H, CH_3).

Synthesis of azido isopropylacetamide. N-isopropyl-2-chloroacetamide (2 g, 14.7 mmol) and sodium azide (1.92 g, 29.5 mmol) were dissolved in DMSO (10 mL). The reaction solution was heated at 75°C for 18 hours. The reaction solution was diluted with water and the product was

extracted with diethyl ether three times. The organic phases were combined, dried with $MgSO_4$, and rotovaped down to an oil. ^{1}H-NMR (400MHz, $CDCl_3$) δ (ppm) = 6.18 (s, 1H, NH), 4.04 (m, 1H, CH), 3.87 (s, 2H, CH_2), 1.1 (s, 6H, CH_3).

2.4.7 Preparation of azido disulfide

Synthesis of tosylated bis(hydroxyethyl)disulfide. The bisalcohol (4 g, 25.9 mmol) and pyridine (10 mL) were combined and cooled in an ice bath. 4-toluene sulfonyl chloride (10.9 g, 57.0 mmol) and pyridine (10 mL) and was added dropwise to bisalcohol solution. The reaction was left for 2 hours and then diluted with water. The reaction mixture was extracted three times with dichloromethane. The organic layers were combined, washed three times with 2 M HCl and one time with brine, dried with $MgSO_4$, and rotovaped down to a solid. The solid was dried overnight under high vacuum. ^{1}H-NMR (400MHz, $CDCl_3$) δ (ppm) = 7.77 (d, 4H, (-$SCH_2CH_2SO_2$*Ph*$CH_3)_2$), 7.23 (d, 4H, (-$SCH_2CH_2SO_2$*Ph*$CH_3)_2$), 4.19 (t, 4H, (-SCH_2*CH*$_2$SO-$_2$Ph$CH_3)_2$), 2.81 (t, 4H, (-S*CH*$_2CH_2SO_2PhCH_3)_2$), 2.43 (s, 6H, (-$SCH_2CH_2SO_2$Ph*CH*$_3)_2$).

Synthesis of Bis-(azidoethyl) disulfide. Tosylated bis(hydroxyethyl)disulfide (2.13 g, 4.61 mmol), sodium azide (1.20 g, 18.4 mmol), and tetrabutyl ammonium iodide (0.035 g, 0.095 mmol) were dissolved in dioxane (20 mL). The reaction mixture was stirred at 75 °C overnight. Most of the dioxane was removed by rotovap and the reaction solution was redissolved in dichloromethane. The organic solution was washed twice with water, followed by sodium bicarbonate and brine. The organic phase was dried with $MgSO_4$ and concentrated down by rotovap to an oil. ^{1}H-NMR (400MHz, $CDCl_3$) δ (ppm) = 3.57 (d, 4H, (-SCH_2*CH*$_2N_3)_2$) and 2.84 (d, 4H, (-S*CH*$_2CH_2N_3)_2$).

2.5 Functionalization of PPLG and PEG-b-PPLG

Synthesis of PEG functionalized PPLG. A typical procedure started with a feed ratio of alkyne/azide/CuBr/N,N,N',N',N''-pentamethyldiethylenetriamine (PMDETA) equal to 1/2/0.33/0.33 unless otherwise directly stated. PPLG, PEG-N_3, and PMDETA were all dissolved in DMF (3 mL, the minimum amount for adequate degassing) and placed in a Schlenk tube (25 mL). After the solution was degassed with Ar, the CuBr catalyst (0.0043 g, 0.0299 mmol) was added and the reaction solution was stirred at room temperature. Once the reaction was complete, the reaction solution was passed through a short aluminum oxide column and purified by dialysis against water for days to remove excess side chain. The dialysis solution was freeze dried, yielding a white solid. The polymer structure was verified by ^{1}H-NMR and the molecular weight increase was verified by GPC. See Section 3.2.3 for ^{1}H-NMR spectra of representative PEG functionalized polymers.

Synthesis of amino functionalized PPLG and PEG-b-PPLG. A typical procedure started with a feed ratio of alkyne/azide/CuBr/PMDETA equal to 1/1.2/0.1/0.1 for primary, secondary, tertiary, and QC1 amines and a feed ratio of 1/1.1/0.1/0.1 for QC4-QC12. PPLG (0.050, 0.299 mmol alkyne repeat units), amino azide (0.124 g, 0.329 mmol QC12 azide), and PMDETA (6.25 μL, 0.0299 mmol) were all dissolved in DMF (3 mL). After the solution was degassed, the CuBr catalyst (0.0043 g, 0.0299 mmol) was added and the reaction solution was stirred at room temperature. Once the reaction was complete, the reaction solution was purified by dialysis against water acidified by HCl (pH < 4) for 2-3 days to remove excess amino azide and copper catalyst and freeze dried, yielding a white powder. The polymer structure was verified by ^{1}H-NMR. See Section 2.8.2 and 2.8.3 for ^{1}H-NMR spectra of representative amine functionalized polymers.

Synthesis of functionalized PPLG and PEG-b-PPLG with other click groups. A typical procedure started with a feed ratio of alkyne/azide/CuBr/PMDETA equal to 1/1.1-1.5/0.1/0.1. PPLG, azide, and PMDETA were all dissolved in DMF (at least 3 mL). After the solution was degassed, the CuBr catalyst was added and the reaction solution was stirred at room temperature. Purification varied depending on the water solubility of the polymer. If the polymer was completely water soluble, the product was purified by dialysis against acidified water and freeze dried, yielding a white powder. If the polymer was not soluble, the reaction solution was passed through an aluminum oxide column to remove the copper catalyst and then precipitated into diethyl ether. Polymer structures were verified by ^{1}H-NMR.

Synthesis of functionalized PPLG and PEG-b-PPLG with multiple click groups. A typical procedure started with a feed ratio of alkyne/azide 1/CuBr/PMDETA equal to 1/desired substitution/0.1/0.1. PPLG, azide 1, and PMDETA were all dissolved in DMF (at least 3 mL) and the reaction solution was degassed in a Schlenk tube. A separate vial with 1 mL DMF and azide 2, at a ratio making the Azide/Alkyne total ratio 1.2-1.5/1, was degassed. CuBr was added to the Schlenk tube and the reaction solution was reacted for several hours before the azide 2 solution was added. Once the reaction was complete, the product was purified by dialysis against acidified water and freeze dried, yielding a white solid. Polymer structures were verified by ^{1}H-NMR (see Section 2.8.2).

2.6 Polymer Characterization Methods

Outlined below are the experimental methods for polymer characterization. The facility where each piece of equipment is located is also mentioned to aid future researchers.

2.6.1 Nuclear magnetic resonance (NMR)

^{1}H-NMR and ^{13}C NMR were recorded on Bruker 400 MHz spectrometers. COSY NMR was recorded on a Varian 500 MHz spectrometer by Dr. Jeff Simpson at the Department of Chemistry Instrumentation Facility.

Facility: Department of Chemistry Instrumentation Facility

2.6.2 Fourier transform infrared (FTIR)

FTIR spectra were recorded on a Thermo Nicolet NEXUS 870 series spectrophotometer. For liquid phase FTIR, PPLG was dissolved in DMF (52 mg/mL) and placed in a zinc selenide cell with a pathlength of 0.015 mm. For monitoring the polymerization and determining solvent cast polymer secondary structure, the solution was solvent cast onto a KBr plate. For obtaining backbone conformation, samples were solvent cast onto KBr or solvents were examined in their bulk state using ATR-FTIR.

Facility: Center for Materials Science and Engineering and Institute for Soldier Nanotechnology

2.6.3 Gel permeation chromatograph (GPC).

GPC measurements were carried out using a Water Breeze 1525 HPLC system equipped with two Polypore columns operated at 75°C, series 2414 refractive index detector, series 1525 binary HPLC pump, and 717 plus autosampler. Waters' Breeze Chromatography Software Version 3.30 was used for data collection as well as data processing. DMF with 0.01 M LiBr was used as eluent for analysis and as solvent for sample preparation. The average molecular weight of the sample was calibrated against narrow molecular weight poly(methyl methacrylate) standards.

Facility: Institute for Soldier Nanotechnologies

2.6.4 Circular dichroism (CD)

Circular dichroism (CD) spectroscopy of polymer solution was carried out by using an Aviv model 202 CD spectrometer. Measurements were performed at 25 ± 0.1°C, sampling every 1 nm with a 3-5 s averaging time over the range of 190–260 nm (bandwidth = 1.0 nm). The averaging time was extended to reduce measurement noise if the curves were not smooth. Measurements were taken using a cell with a 1 mm path length.

Facility: Biophysical Instrumentation Facility

2.6.5 Discussion of determination of sample concentration for CD

To determine the correct sample concentration for CD, different concentrations of PPLG-g-PEG750 were prepared, as shown in Figure 2-1. If the sample concentration was too high, the CD dynode increased significantly causing the readings to be unreliable in the region between 190 nm and 215 nm, as indicated by the large error bars. When sample concentration was too high, the α-helix minimum at 208 nm did not show up and the sample reading merged to zero. When the concentration was decreased from 10 mg/mL to 2.5 mg/mL, stable CD spectra were obtained and both minima were observed.

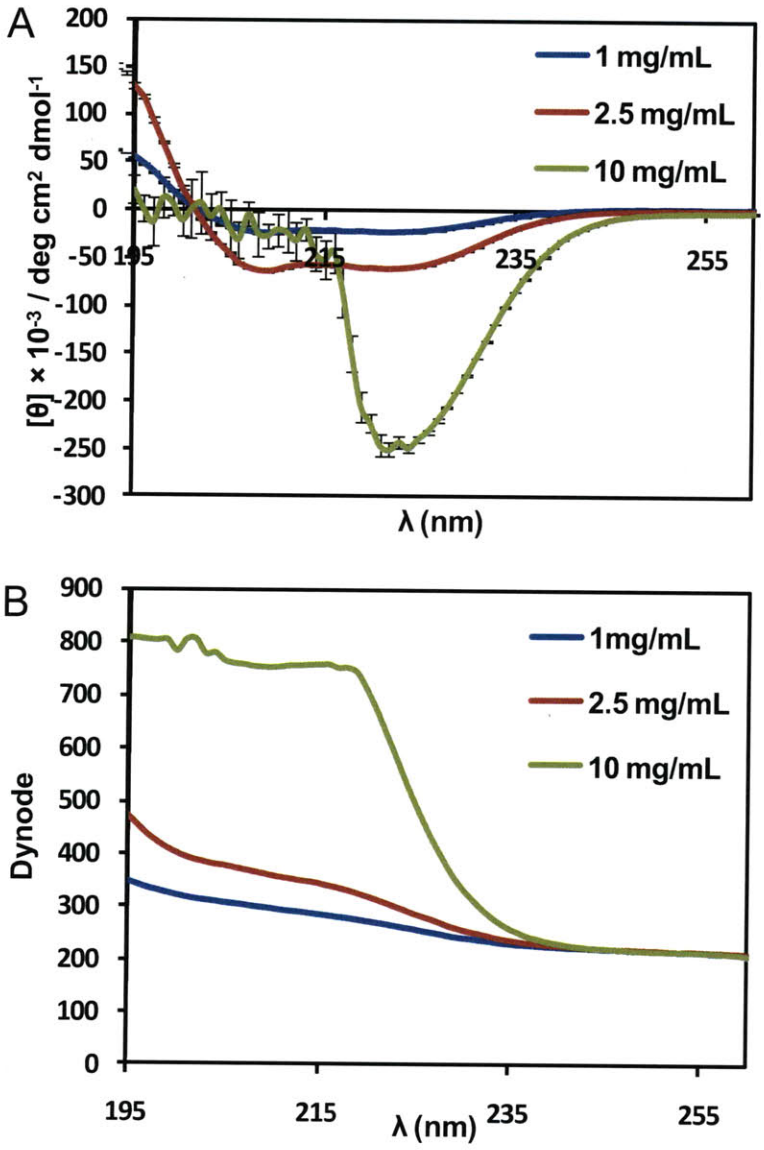

Figure 2-1. A) CD of PPLG-g-PEG at varied concentrations B) Dynode from CD for each concentration

2.6.6 Discussion of absorbance of triazole ring for CD studies

UV/Vis was also performed on the 2.5 mg/mL to determine if the triazole ring was UV active in the region of interest for CD. As shown in Figure 2-2, there are no absorbance peaks caused by the triazole ring in the region of interest. The absorbance does increase at lower

wavelengths but does not interfere with the CD measurement. The absorbance is relatively constant in the region where the α-helix minimums occur.

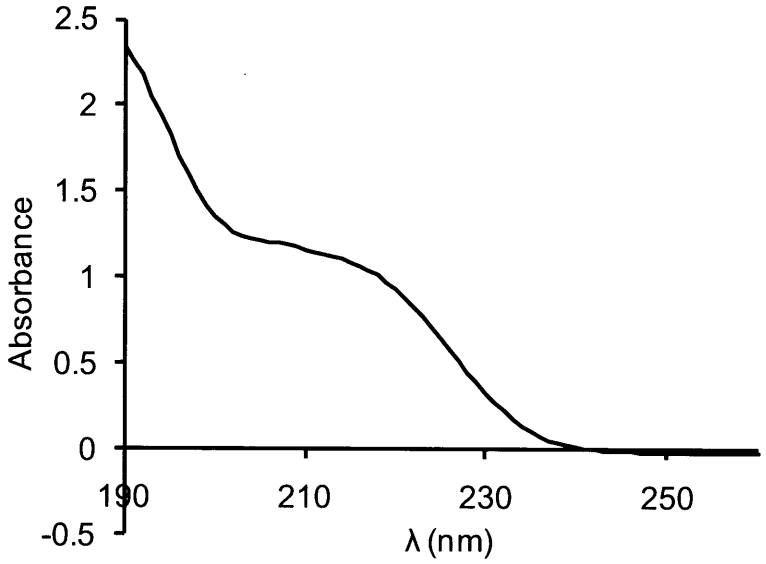

Figure 2-2. UV/Vis of PPLG-g-PEG in water at 2.5 mg/mL

2.6.7 Atomic force microscopy (AFM)

Tapping-mode atomic force microscopy measurements were conducted in air with a Dimension 3100 system (Digital Instruments, Santa Barbara, CA) operated under ambient conditions. The samples were prepared for AFM analysis by spin coating a silicon wafer with a polymer solution at a concentration of 1 mg/mL in Milli-Q water with the pH adjusted using 0.1M NaOH.

Facility: Institute for Soldier Nanotechnologies

2.6.8 Critical micelle concentration (CMC) measurements

Critical micelle concentration measurements of the diblock polymers in aqueous solutions at different pH values were performed by fluorescence spectroscopy using a pyrene

probe. Pyrene undergoes a shift in excitation from 373 to 393 nm in the emissions spectrum when the polarity of its microenvironment is changed. Pyrene is sparingly soluble in water and preferentially partitions into the hydrophobic micelle core when micelles are present. Fluorescence peak intensity emissions ratios (*373* nm/ *393* nm) were plotted against the logarithm of polymer concentrations to determine CMC as the onset of micellization. Fluorescence spectroscopy was carried out on a Horiba FluoroLog®-3 spectrofluorometer at 25°C. A stock solution of pyrene at 5.00×10^{-7} M in water was prepared. Polymer samples were dissolved in the stock pyrene solution and diluted to specific concentrations.

Facility: Institute for Soldier Nanotechnologies

2.6.9 UV/Visible Spectrophotometry

UV/Visible measurements were carried out on an Agilent Technologies G3172A spectrometer. UV/Vis was used to determine the UV activity of the triazole ring and to monitor solution turbidity.

Facility: Institute for Soldier Nanotechnologies

2.6.10 Acid-base titrations on amine functionalized PPLG

Acid-base titrations were performed on all amine functionalized PPLG. 3 mL of 10 mM amine in 125 mM NaCl was adjusted to a pH of 3 using 1 M HCl. The solution was titrated with 10 μL aliquots of 0.1 M NaOH, measuring the pH with each addition. For polymers where precipitation was observed, UV/Vis measurements were obtained at 550 nm to monitor the solution turbidity.

2.6.11 Ester hydrolysis on amine functionalized PPLG

Ester hydrolysis samples were prepared by dissolving polymer in a stock solution at 10 mg/mL for homopolymer and 20 mg/mL for diblock copolymer. The stock solutions were then diluted with pH buffer to a concentration of 0.5 mg/mL for homopolymer and 1 mg/mL for diblock copolymer. At various time points, samples were analyzed by CD. Samples were also freeze dried, reconcentrated to 2.5 mg/mL for homopolymers and 3.75 mg/mL for diblock copolymers, acidified to stop hydrolysis, and analyzed by ^{1}H-NMR.

2.7 Biological Characterization Methods

2.7.1 Materials

siRNA was purchased from Dharmacon RNAi Technologies and QuantiT Ribogreen RNA Reagent was purchased from Invitrogen. Dual-Glo Luciferase Assay System was purchased from Promega. *Staphylococcus aureus 25923* (*S. aureus*) and *Escherichia coli K-12* (*E. coli*) was obtained from ATCC (Manassas, VA) and the *E. coli* Genetic Stock Center (New Haven, CT), respectively. Cation-adjusted Mueller Hinton Broth (CaMHB), LB-Miller Broth (LB), Bacto agar, and trypticase soy agar plates (w/ 5% sheep blood) were obtained from BD Biosciences (San Jose, CA). Bovine RBCs were obtained from Innovative Research (Novi, MI). Trizma hydrochloride buffer and ultrapure distilled water were obtained from Sigma-Aldrich (St. Louis, MO) and Invitrogen (Carlsbad, CA), respectively. Triton-X 100 was purchased from Electron Microscopy Sciences (Hatfield, PA).

2.7.2 Ribogreen assay to determine siRNA complexation efficiency

Ribogreen assays (QuantiT Ribogreen RNA Quantification Reagent, Invitrogen) were performed to determine the complexation efficiency of the polymers with siRNA. 25 μL of

siRNA at 0.006 μg/mL was aliquoted into wells of a 96 well plate and the appropriate amount of polymer was added to attain the desired polymer:siRNA ratio (w/w) in a total volume of 50 μL. After allowing 10 minutes for complexation, 20 μL of the complex solution was added to a black, flat-bottomed, polypropylene 96-well plate containing 100 μL of Ribogreen (diluted 1:200 μL per manufacturer instructions). The fluorescence of each well was measured on a Perkin Elmer Plate 1420 Multilabel Counter plate reader and the fraction of uncomplexed siRNA was determined by comparing the fluorescence of the polymer complexes with the fluorescence of an siRNA control. For the heparin destabilization titrations, heparin (167 IU/mg) was dissolved in a stock solution at 0.5 IU/mL and added to polyplex/picogreen solutions.

2.7.3 Cell transfection studies

Transfection studies were performed in quadruplicate. HeLa cells were grown in 96-well plates at an initial seeding density of 2000 cells/well with cell growth media comprised of Dulbecco's Modified Eagle Media (DMEM) supplemented with 10% fetal bovine serum (FBS) and 1% Penicillin-Streptomycin. Cells were allowed to attach and proliferate for 24 hours in a humidified incubator at 37°C and 5% CO_2. 25 μL of siRNA at 6 μg/mL in 25mM sodium acetate buffer was aliquoted into wells of a 96 well plate and the appropriate amount of polymer was added to attain the desired polymer:siRNA ratio (w/w) in a total volume of 50 μL/well. After mixing the polymer/siRNA solutions, the polyplexes were allowed to sit 10 minutes for complexation. 30 μL aliquots of the polyplex solution was then added to each well of a 96-well plate containing 200 μL/well Opti-Mem and the solution was mixed. Growth media was removed from the cells and 150 μL/well of complex/Opti-Mem solution was added. Lipofectamine at a 4:1 ratio was used as a positive control. Naked siRNA was used as a negative control and as an internal standard. In all cases, the each well contained 50 ng siRNA. The cells

were incubated for 4 hours, the media was removed and replaced with 10% serum-containing growth medium. A Luciferase assay was performed as using the Dual-Glo Luciferase Assay System (Promega, Madison, WI).

2.7.4 Cell viability assay

HeLa cells were seeded in a 96-well clear, flat-bottomed plate and transfected according to the above protocol. After 24 hrs, cell metabolic activity was assayed using the MTT cell proliferation assay (ATCC, Manassas, VA).

2.7.5 Polyplex uptake studies

Block copolymers and PEI were labeled with fluorescein isothiocyante (FITC) at a molar ratio of 4:1 (dye:polymer). Using the labeled polymers, polyplexes were formed and cells treated as described in the above section. At the time indicated, cells were removed from the incubator and analyzed using flow cytometery. Flow cytometry was performed in U-bottom 96-well plates using a HTS LSR II Flow cytometer (Becton-Dickinson, Mountain View, CA). To prepare samples, media was removed from cells and replaced with 25 μL trypsin for 5 minutes. 50 μL of PBS supplemented with 2% FBS was then added to each well, mixed, and the entire 75 μL cell suspension transferred into a U-bottom 96-well plate.

2.7.6 High-throughput endosomal escape

Complexes were assembled and transfection was conducted as described above, except that 25 mM Calcein was added to the Opti-MEM and cells were seeded in black, clear-bottom 96-well plates. 4 hours after transfection, 5 μL of a solution of Hoechst 33342 diluted to 1:30 in PBS was added. After 20 min of staining, complexes and free dye were removed, and the cells were washed 3 times with PBS. 150 μL of phenol-free Opti-MEM with 10% serum was added to

each well before the plate was covered with an opaque sticker, foiled, and analyzed. Imaging was done using a Cellomics ArrayScan VTI HCS Reader (Thermo Fisher, Waltham, MA) and analysis was done using the included software.

2.7.7 Confocal images

8-well Lab-Tek chamber slides (Thermo Fisher, Waltham, MA) were treated for 20 min with human fibronectin in PBS at 0.1 mg/mL. The fibronectin was removed and HeLa cells were trypsinized and seeded in each well at a concentration at 1000 cells/well 24 h before transfection. Polymers were fluorescently labeled with azide-modified FITC. Polyplexes between labeled siRNA (siGLO) and labeled polymers were formed in NaAc buffer as described earlier. 40 μL of complexes were added to 160 uL phenol-free Opti-MEM and added to each well. Complexes were removed after 4 h and replaced with growth media. At 1h or 24 h, cells were fixed with 3.7% formaldehyde in PBS, stained with Hoechst 33342, and were washed 3 times with PBS. Imaging was done on a PerkinElmer Ultraview spinning disc confocal (PerkinElmer, Waltham, MA).

2.7.8 Bacterial growth inhibition

Bacterial growth inhibition was examined to determine MIC values for the polypeptides. Bacterial growth inhibition for primary, secondary, tertiary, and QC1 polypeptides was monitored using a modified microdilution assay, as previously reported.[11] To summarize, polypeptide samples were serially diluted in a 96 well clear bottom plate in DI-water upon sterile filtration (20 μm pore size); the range of concentrations tested spanned from 70 – 4500 μg/mL. QCn ($n \geq 4$) polypeptides were dissolved and diluted in methanol. The methanol was allowed to evaporate, leaving a polymer coating on the surface; the range of concentrations tested spanned

from 20 – 2500 μg/mL (corresponding to a surface density of average mass of polymer per unit area of 6.1 – 780 μg/cm^2). This method of sample preparation was selected to mirror the attachment assay sample preparation outlined below. Bacteria (*S. aureus* or *E. coli*) were added to these wells in their exponential growth phase at a final concentration of 10^5 CFU/mL. Positive controls with no polypeptide and only bacteria treatment and negative controls with no bacteria (containing only CaMHB or LB) were included on each plate. Plates were incubated at 37 °C for 16-18 hours with constant shaking. Following incubation, the absorbance of each well was read at 600 nm for *S. aureus* and 540 nm for *E. coli*. Normalized bacteria density was calculated as follows:

$$Normalized\ Bacteria\ Density = \frac{(Sample\ Abs - Negative\ Control\ Abs)}{(Positive\ Control\ Abs - Negative\ Control\ Abs)}$$

2.7.9 Bacterial attachment inhibition

Inhibition of bacterial attachment to QCn ($n \geq 4$) polypeptide coatings was assessed as previously described.[11] Briefly, solvent cast polypeptide substrates were prepared by dissolving these polymers in methanol and evenly coating round glass cover slips (VWR, West Chester, PA) at a final polypeptide coverage of 330 μg/cm^2. These samples were incubated at 37°C in either *S. aureus* or *E. coli* suspensions at a concentration of 10^6 CFU/mL for 2 hours. Controls of uncoated substrates were also incubated in these bacteria suspensions. Following incubation, substrates and controls were removed and rinsed briefly in three separate sterile water baths and placed immediately on trypticase soy agar plates (w/ 5% sheep blood). These agar plates were incubated at 37°C for 16-18 hours. The presence of colonies upon incubation was monitored via digital imaging.

2.7.10 Polymer biocompatibility

Bovine RBC hemolysis was monitored as a measure of polypeptide biocompatibility adapted from previously reported protocols.[12, 13] Polypeptide samples were prepared for testing by dissolving in tris buffer (10 mM tris hydrochloride, 150 mM sodium chloride) for primary, secondary, tertiary, and QC1 polymers and methanol for QCn ($n \geq 4$) polymers. Samples were added in triplicate to a 96 well clear bottom plate and serial diluted (100 μL final volume in each well), with a concentration range of 39 to 5000 μg/mL. For methanol soluble polymers, solutions were allowed to evaporate, leaving a thin polymer coating on each well with surface coverage ranging from 12.2 - 1560 $\mu g/cm^2$. Negative controls of untreated wells and positive controls of 1% triton-X solution were added to control wells in each plate. Upon evaporation of methanol for QCn ($n \geq 4$) polypeptides, tris buffer (100 μL) was added to each well. Bovine RBCs (5% in tris buffer) were added to each sample and control wells (100 μL). These plates were subsequently incubated with agitation at 37°C. Following incubation, plates were centrifuged at 1000 RPM for 5 minutes. Samples (75 μL) were transferred to a fresh 96 well clear bottom plate and the absorbance of each well at 540 nm was determined. Final normalized hemolysis was calculated as follows:

$$Normalized\ Hemolysis = \frac{(Sample\ Abs_{540} - Negative\ Control\ Abs_{540})}{(Positive\ Control\ Abs_{540} - Negative\ Control\ Abs_{540})}.$$

2.8 Sample ^{1}H-NMRs

2.8.1 Monomer analysis

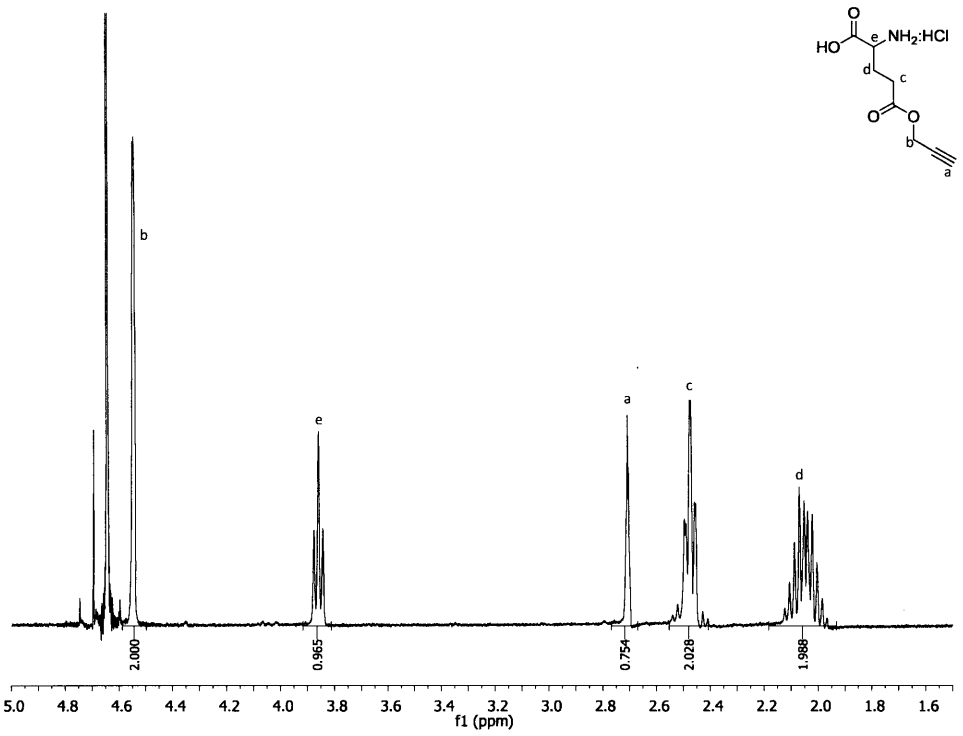

Figure 2-3. ^{1}H-NMR of γ-propargyl L-glutamate hydrochloride in D2O

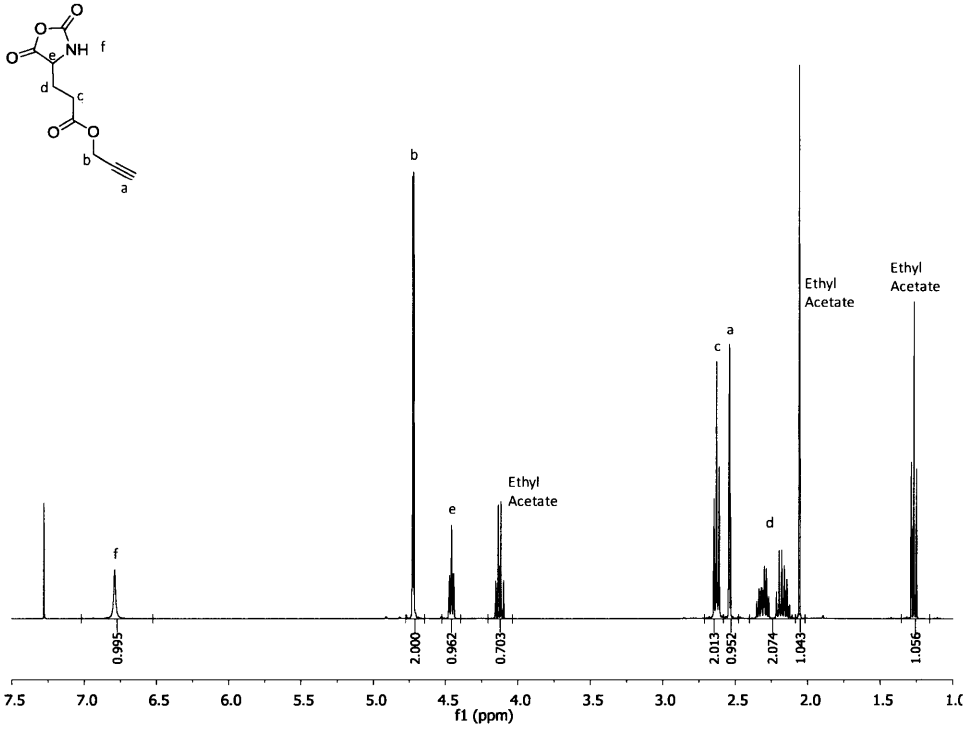

Figure 2-4. ^{1}H-NMR of γ-propargyl L-glutamate NCA in $CDCl_3$

2.8.2 PPLG and functionalized PPLG ^{1}H-NMR analysis

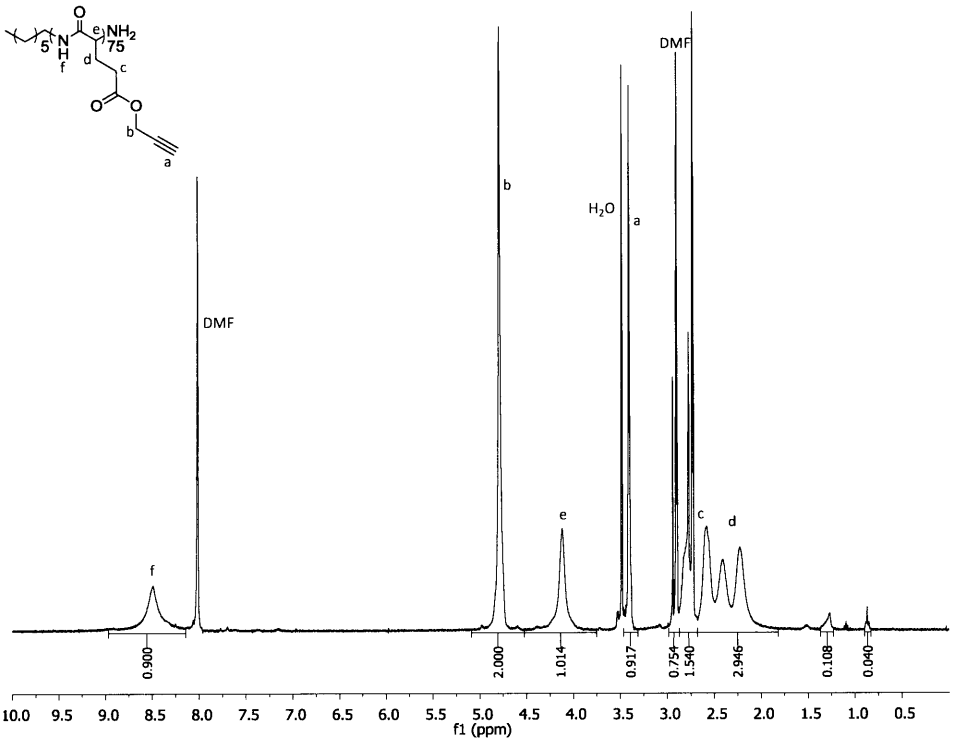

Figure 2-5. ^{1}H-NMR of $PPLG_{75}$ in DMF-d_7

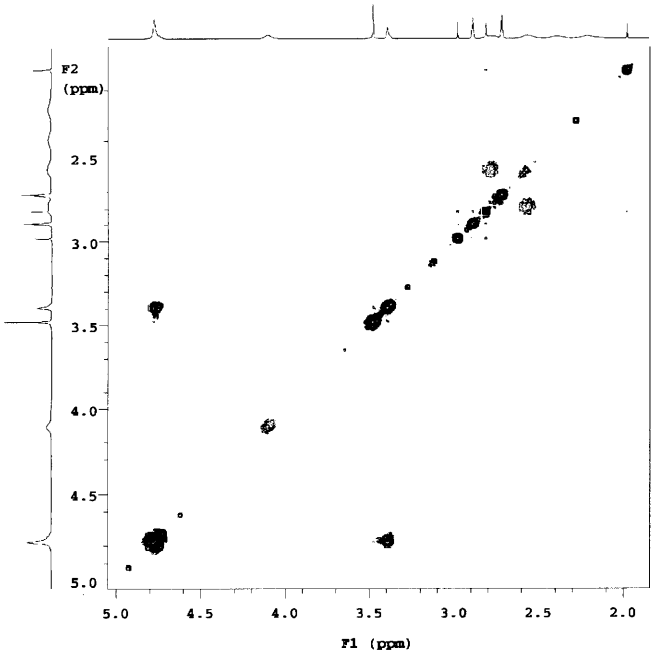

Figure 2-6. COSY ^{1}H-NMR of PPLG in DMF-d_7

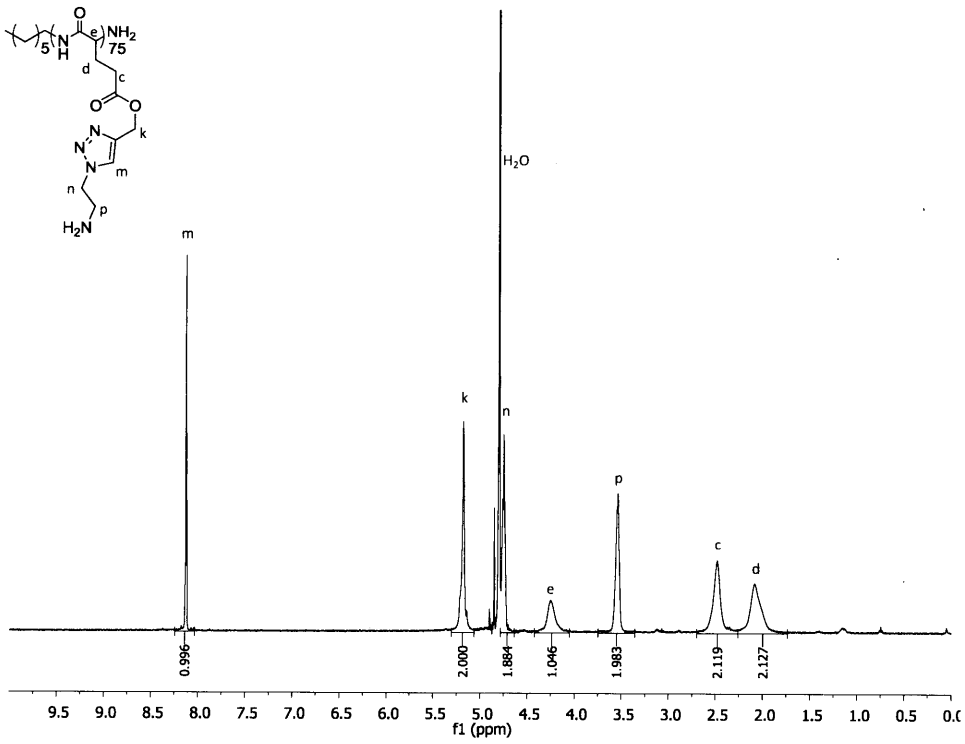

Figure 2-7. ^{1}H-NMR of $PPLG_{75}$ functionalized with primary amine (2-azidoethanamine) in D_2O

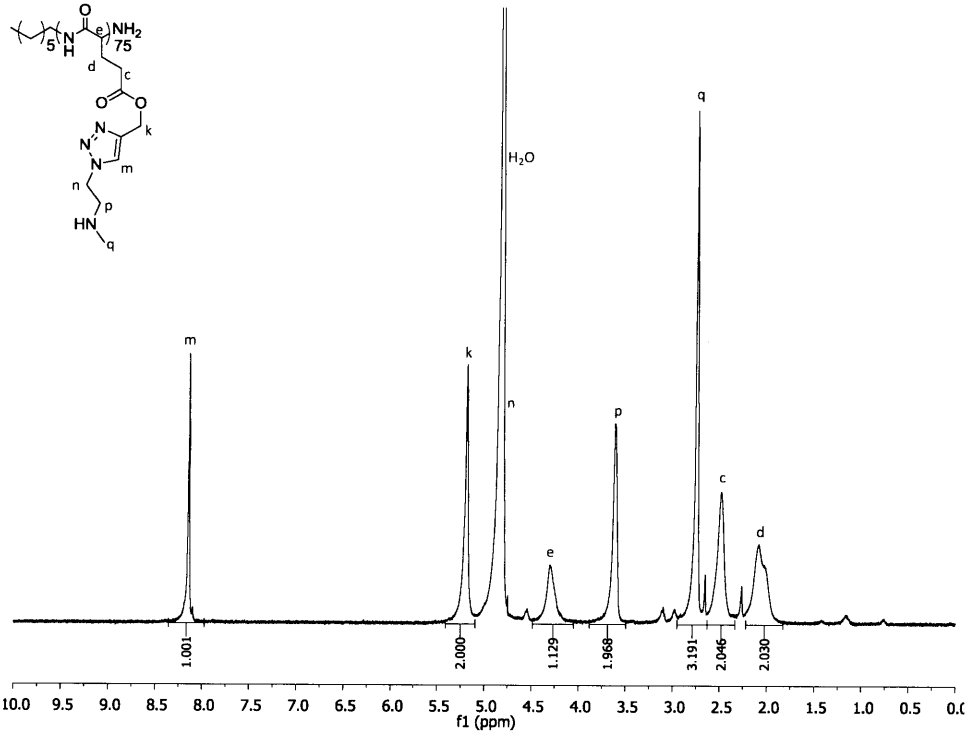

Figure 2-8. ^{1}H-NMR of $PPLG_{75}$ functionalized with secondary amine (2-azido-N-methylethanamine) in D_2O

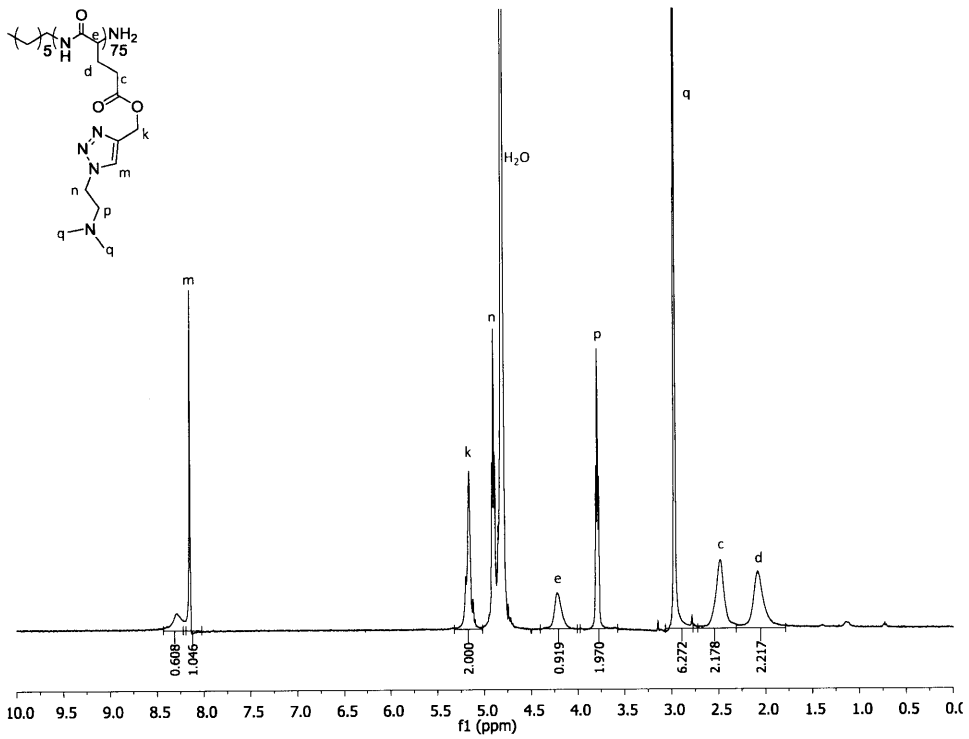

Figure 2-9. ^{1}H-NMR of $PPLG_{75}$ functionalized with dimethylethanamine (2-azido-N,N-dimethylethanamine) in D_2O

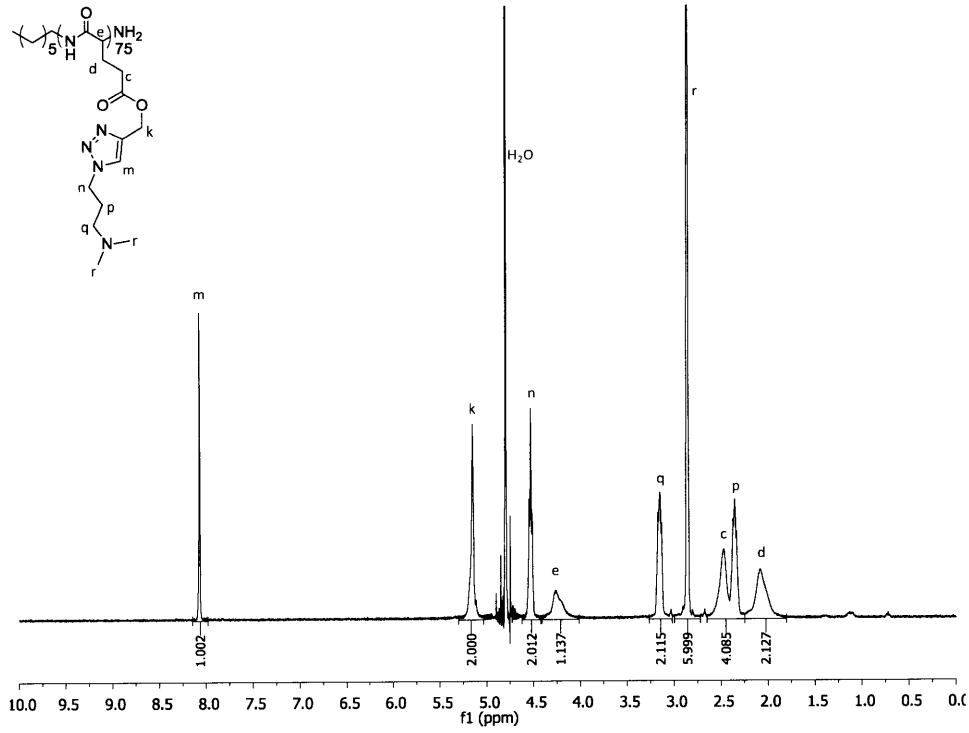

Figure 2-10. ^{1}H-NMR of $PPLG_{75}$ functionalized with dimethylpropanamine (2-azido-N,N-dimethylpropanamine) in D_2O

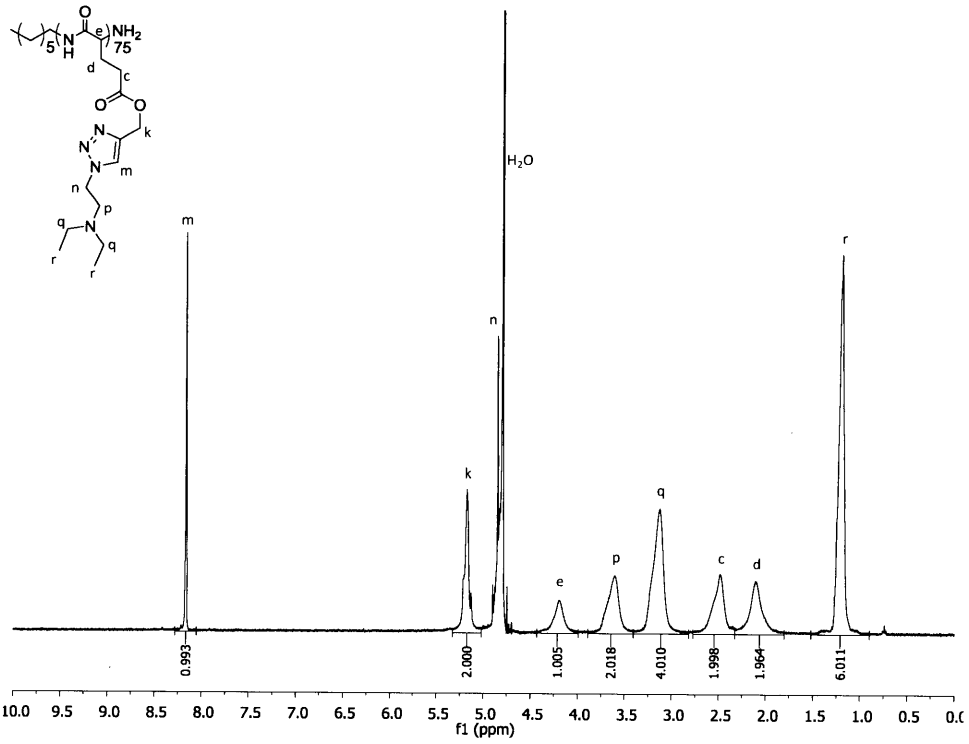

Figure 2-11. ^{1}H-NMR of $PPLG_{75}$ functionalized with diethylamine (2-azido-N,N-diethylethanamine) in D_2O

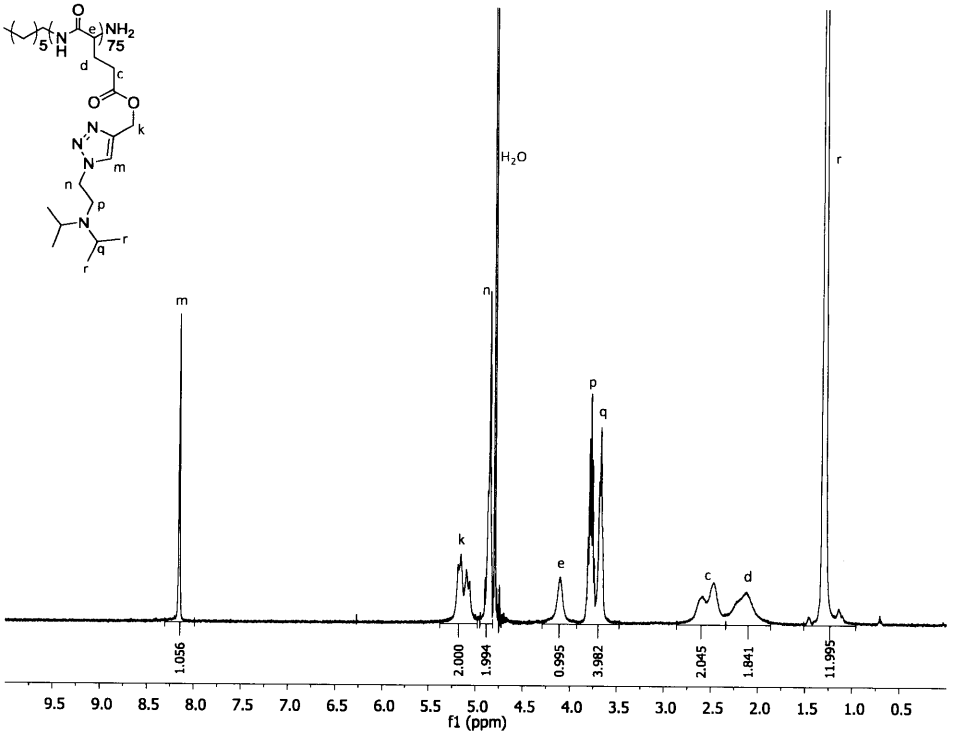

Figure 2-12. ^{1}H-NMR of $PPLG_{75}$ functionalized with diisopropylamine (N-(2-azidoethyl)-N-isopropylpropan-2-amine) in D_2O

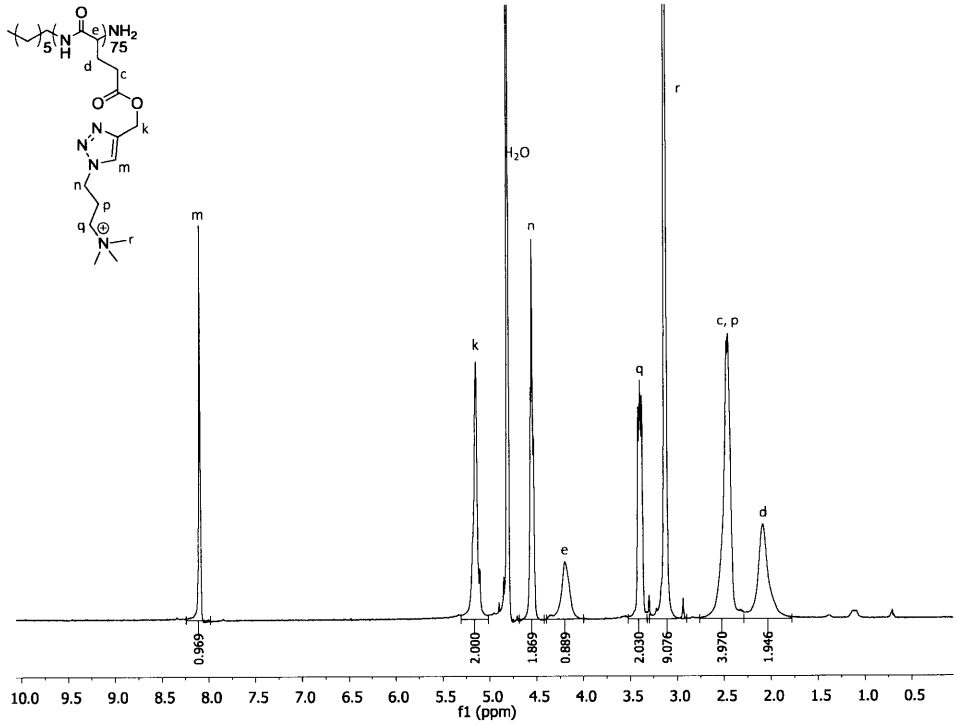

Figure 2-13. ^{1}H-NMR of $PPLG_{75}$ functionalized with QC1 (3-azido-N,N,N-trimethylpropan-1-aminium chloride) in D_2O

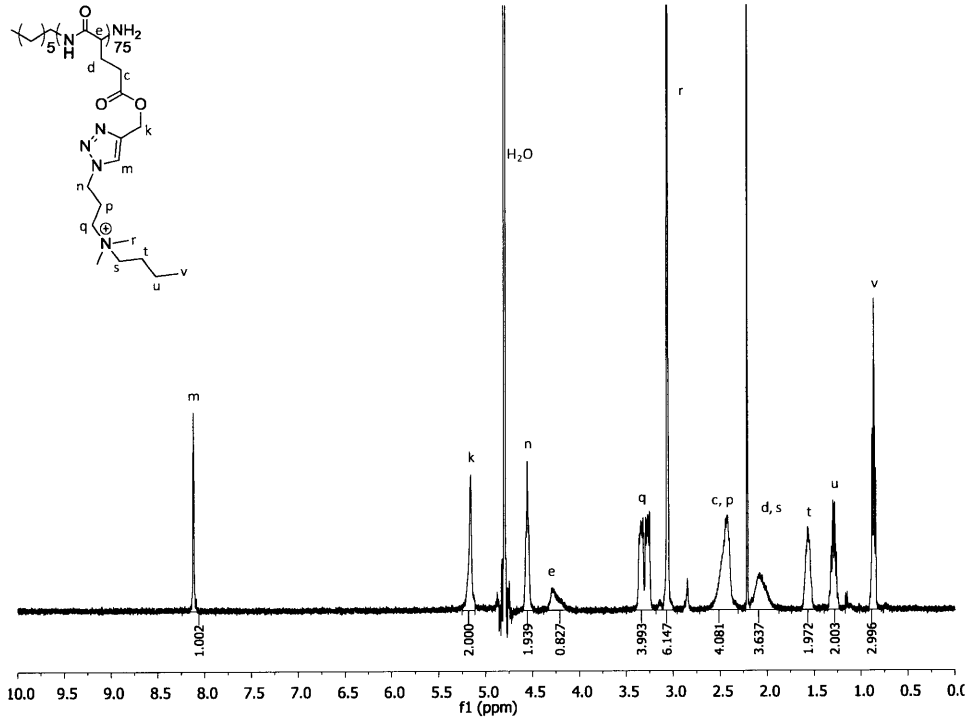

Figure 2-14. ^{1}H-NMR of $PPLG_{75}$ functionalized with QC4 (N-(3-azidopropyl)-N,N-dimethylbutan-1-aminium chloride) in D_2O

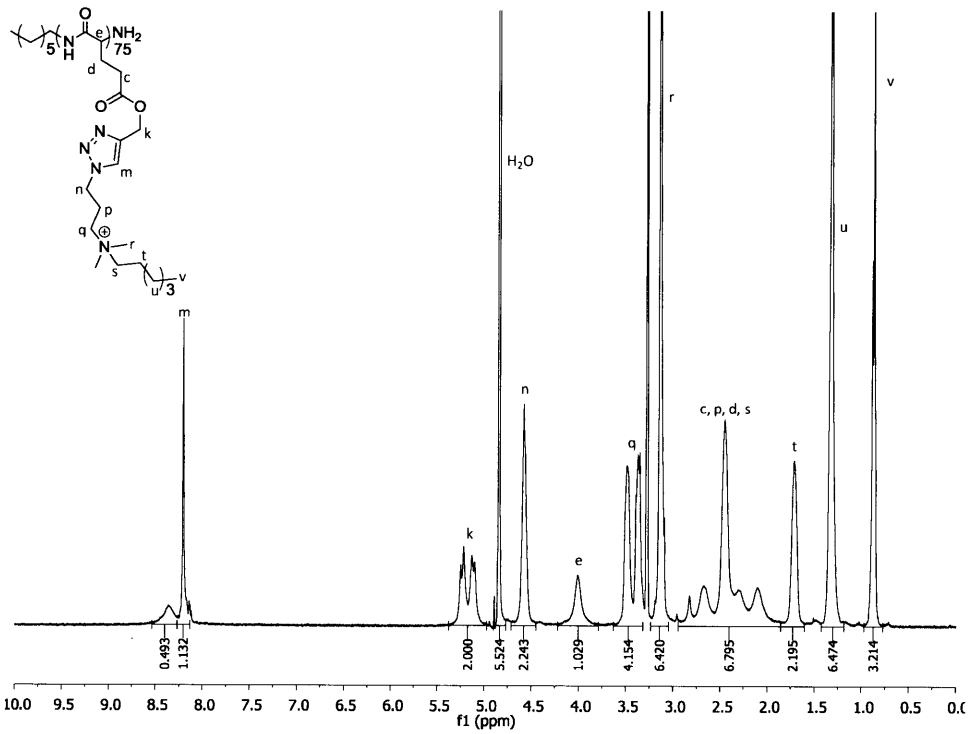

Figure 2-15. ^{1}H-NMR of $PPLG_{75}$ functionalized with QC6 (N-(3-azidopropyl)-N,N-dimethylhexan-1-aminium chloride) in MeOD

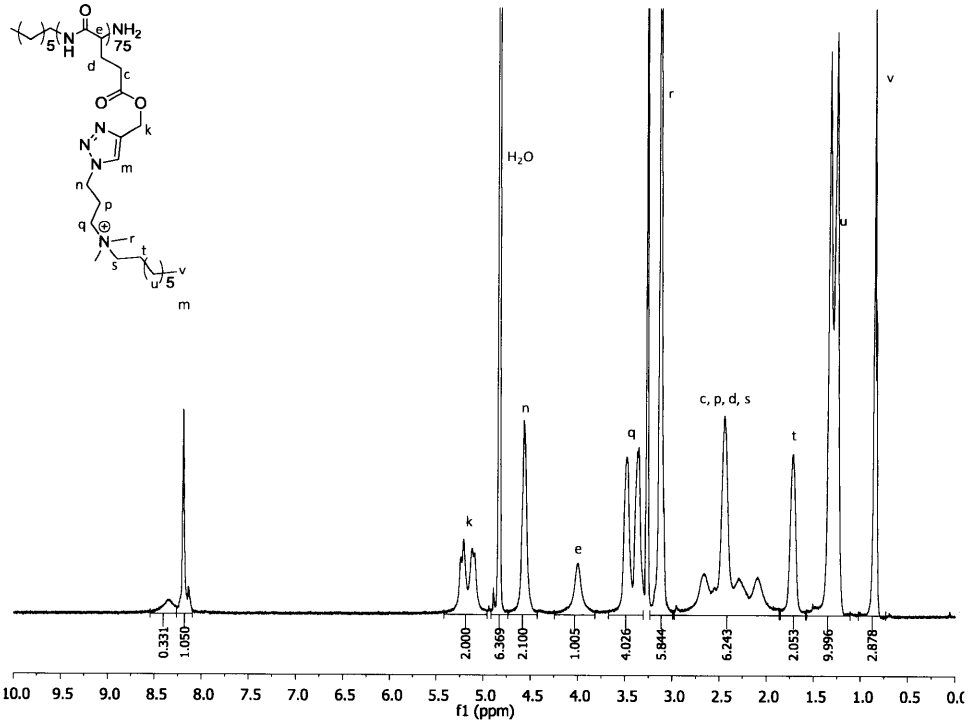

Figure 2-16. ^{1}H-NMR of $PPLG_{75}$ functionalized with QC8 (N-(3-azidopropyl)-N,N-dimethyloctan-1-aminium chloride) in MeOD

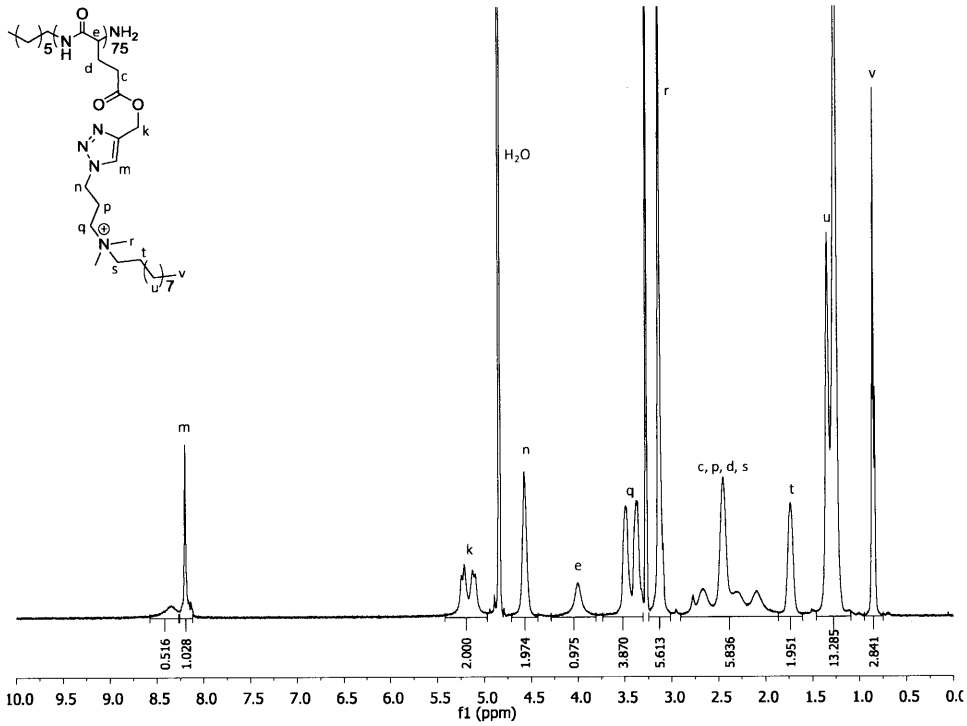

Figure 2-17. ^{1}H-NMR of $PPLG_{75}$ functionalized with QC10 (N-(3-azidopropyl)-N,N-dimethyldecan-1-aminium chloride) in MeOD

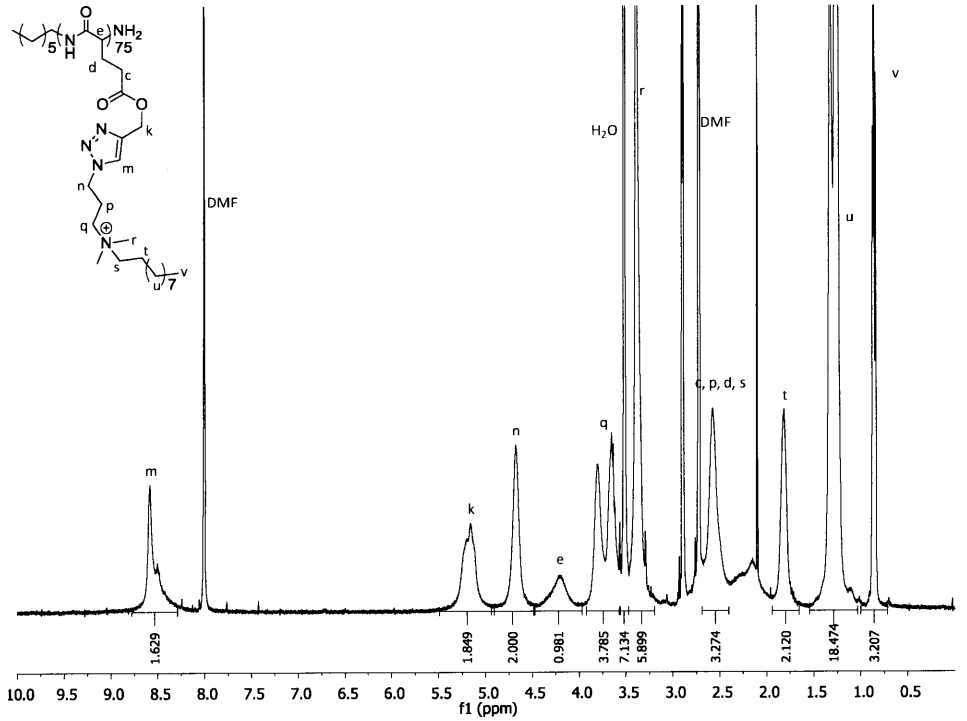

Figure 2-18. ^{1}H-NMR of $PPLG_{75}$ functionalized with QC12 (N-(3-azidopropyl)-N,N-dimethyldodecan-1-aminium chloride) in DMF-d_7. DMF is not the best solvent for QC12.

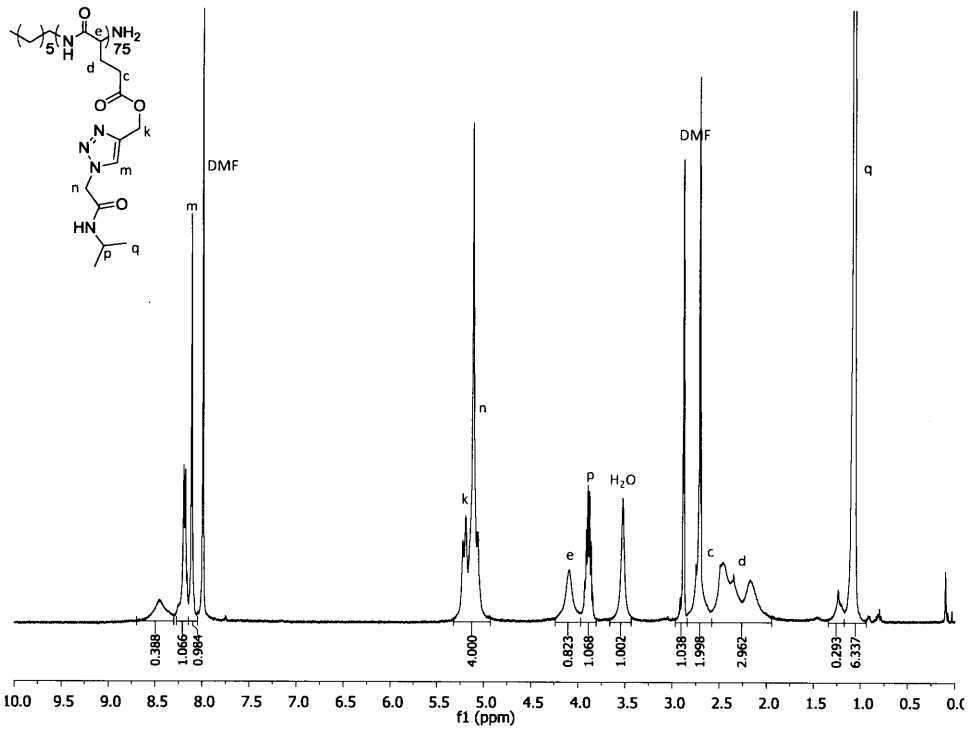

Figure 2-19. ^{1}H-NMR of $PPLG_{75}$ functionalized with 2-azido-N-isopropylacetamide in $CDCl_3$

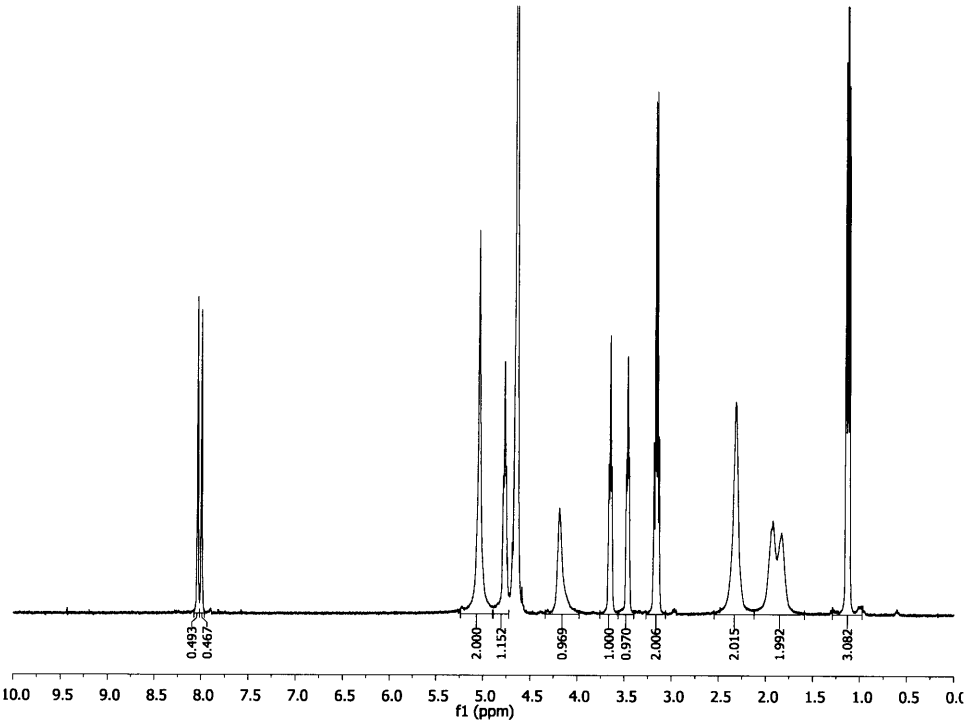

Figure 2-20. ^{1}H-NMR of $PPLG_{140}$ functionalized with a 1:1 ratio of primary amine (2-azidoethanamine) and diethylamine (2-azido-N,N-diethylethanamine)in D_2O. A 1:1 primary:diisopropyl ratio was planned and obtained as can be seen by comparing the two peaks at 3.5 and 3.7 or by looking at the two distinct triazole peaks.

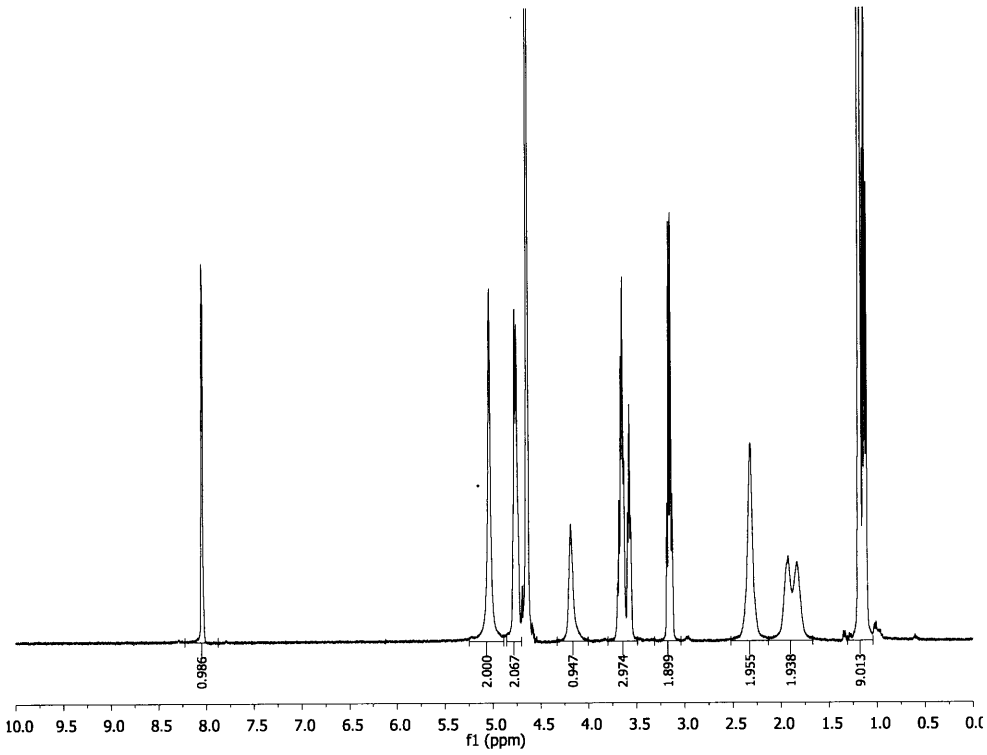

Figure 2-21. ^{1}H-NMR of $PPLG_{140}$ functionalized with a 1:1 ratio of diethylamine (2-azido-N,N-diethylethanamine) and (N-(2-azidoethyl)-N-isopropylpropan-2-amine) in D_2O. A 1:1 primary:diisopropyl ratio was planned and can be determined by the peak integration at 1.15 ppm. If there is a 1:1 ratio, one would expect three contributing protons from the diethyl group and 6 contributing protons from the diispropyl group making a total of 9 contributing protons as observed in the ^{1}H-NMR.

2.8.3 PEG-b-PPLG and functionalized PEG-b-PPLG polymers ^{1}H-NMR analysis

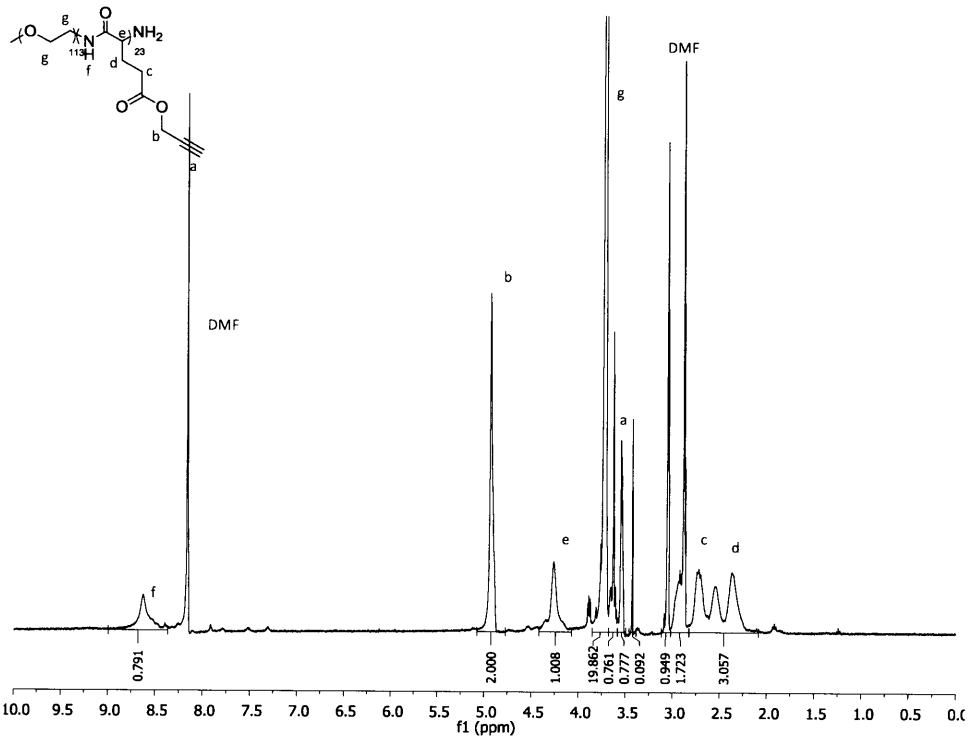

Figure 2-22. ^{1}H-NMR of PEG-b-PPLG in DMF-d_7

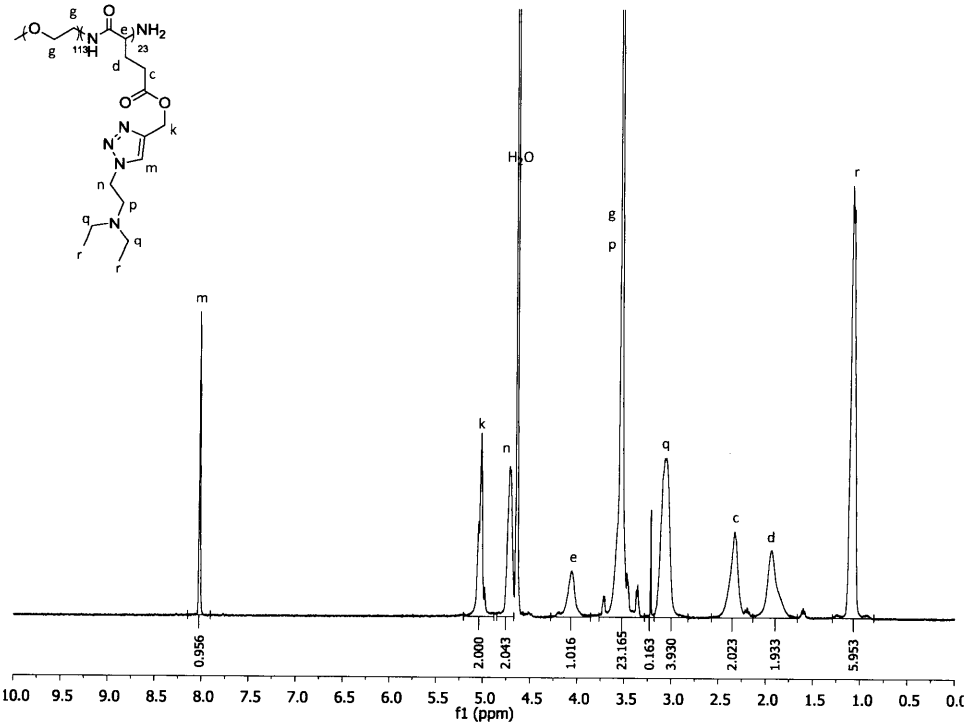

Figure 2-23. ^{1}H-NMR of PEG-b-PPLG functionalized with diethylamine (2-azido-N,N-diethylethanamine) in D_2O

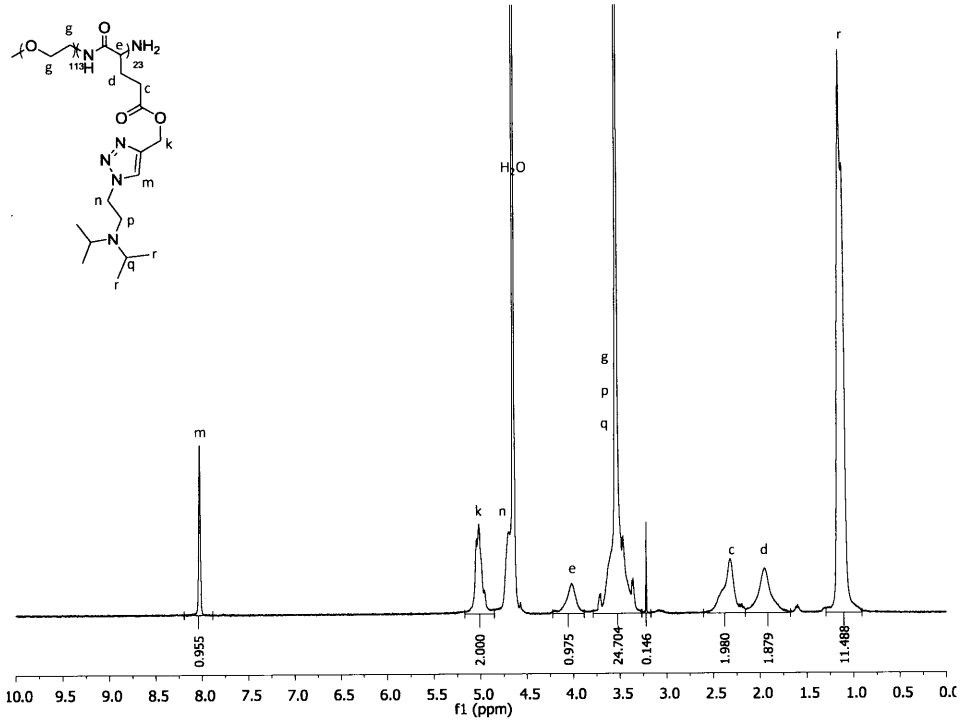

Figure 2-24. ^{1}H-NMR of PEG-b-PPLG functionalized with diisopropylamine (N-(2-azidoethyl)-N-isopropylpropan-2-amine) in D2O

2.9 DMF-GPC polymer analysis

2.9.1 PPLG homopolymer DMF-GPC traces

Although not a complete list of every PPLG homopolymer synthesized, the list below provides a summary of many different batches synthesized and analyzed by both ^{1}H-NMR and GPC. The labels ACE-X-Y refers to Amanda C. Engler (ACE), notebook number X, and page number Y. The degree of polymerization for each polymer was determined using two different NMR peaks from the heptylamine initiator, one containing eight protons and the other containing three protons on the last methyl group. The stoichiometry column refers to the feed ratio of initiator to monomer. The GPC traces of all the polymers are shown in Figure 2-25. Figure 2-26 shows a calibration-like curve for looking at the molecular weight predicted by ^{1}H-NMR

compared to the molecular weight obtained for the DMF-GPC using PMMA standards. From Figure 2-26, it appears that using only three protons could result in an over prediction of degree of polymerization if the polymer length is too long. The 8H peak was used to determine degree of polymerization in this thesis.

Table 2-1. Summary of polymers synthesized using a heptylamine initiator. Mn, Mw, Mp, and polydispersity were determined by DMF GPC. The stoichiometry refers to the feed ratio of initiator to monomer and the "by NMR" columns refer to the degree of polymerization determined by ^{1}H-NMR. The 8H peak appears around 1.3 ppm and the 3H peak appears at 0.8 ppm (ACE-5-28 is shown in Figure 2-5).

	Mn	Mw	Mp	Polydispersity	Stoichiometry	by NMR 8H	by NMR 3H
ACE-4-68	15617	17348	17643	1.11	75	69	80
ACE-5-7	9896	11141	11096	1.13	40	38	41
ACE-5-10	17929	20054	19754	1.12	75	72	78
ACE-5-26	6127	7644	8593	1.25	25	30	31
ACE-5-27	12666	14094	14714	1.11	50	56	58
ACE-5-28	17869	19426	19788	1.09	75	75	75
ACE-5-35	6898	8709	9590	1.26	40	41	42
ACE-5-58	42872	49968	53102	1.17	150	140	165
ACE-5-66	26247	29968	31082	1.14	100	98	107
ACE-5-67	16618	19270	18172	1.16	75	70	72

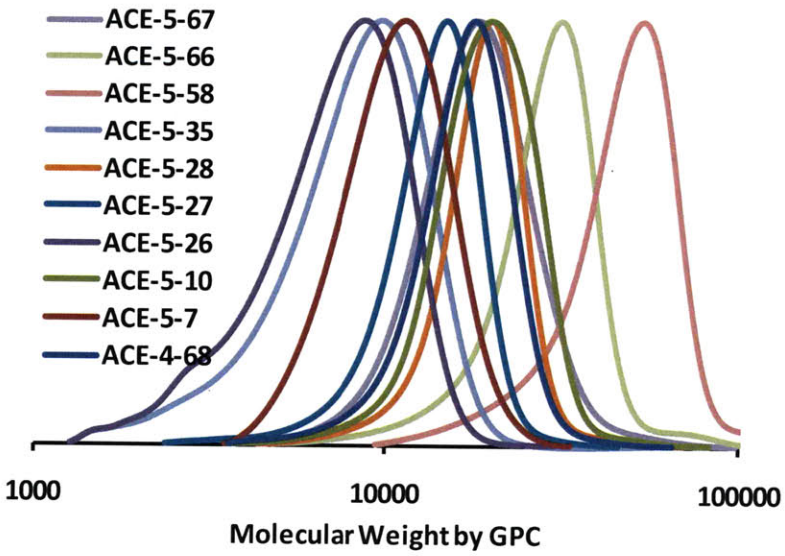

Figure 2-25. GPC traces of PPLG homopolymers

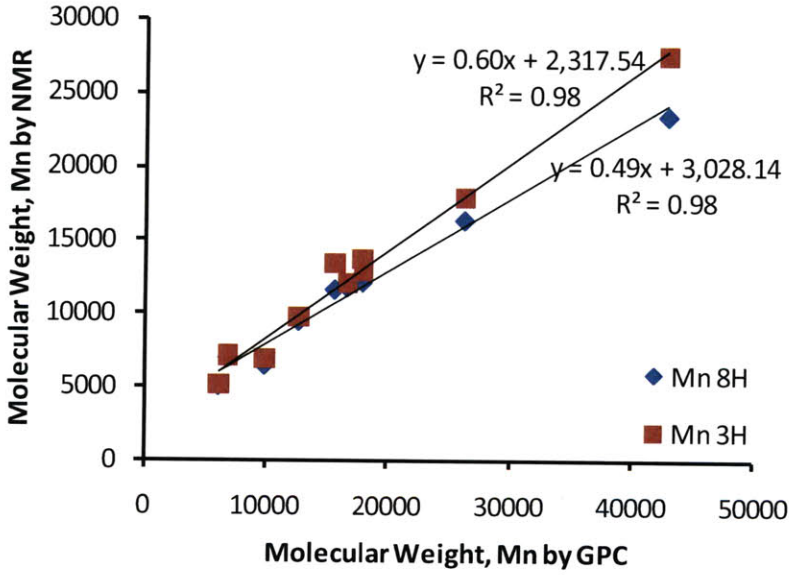

Figure 2-26. Comparison of Mn obtained by DMF-GPC with PMMA standards to Mn obtained from ^{1}H-NMR calculated using eight or three protons.

2.9.2 PEG-b-PPLG DMF-GPC analysis

Table 2-2 summarizes the molecular weights obtained from the vendor, ^{1}H-NMR, and GPC. The GPC trace shown in Figure 2-27 is representative of those obtained for all diblock polymers.

Table 2-2. Molecular weight summary for PEG and PEG-b-PPLG system.

	From Vendor	NMR	GPC			
	Mp	Mn	Mn	Mw	Mp	PDI
PEG (MW 5000)	5229		8627	9297	9759	1.08
PEG -b-PPLG		10500	19800	21983	22260	1.11

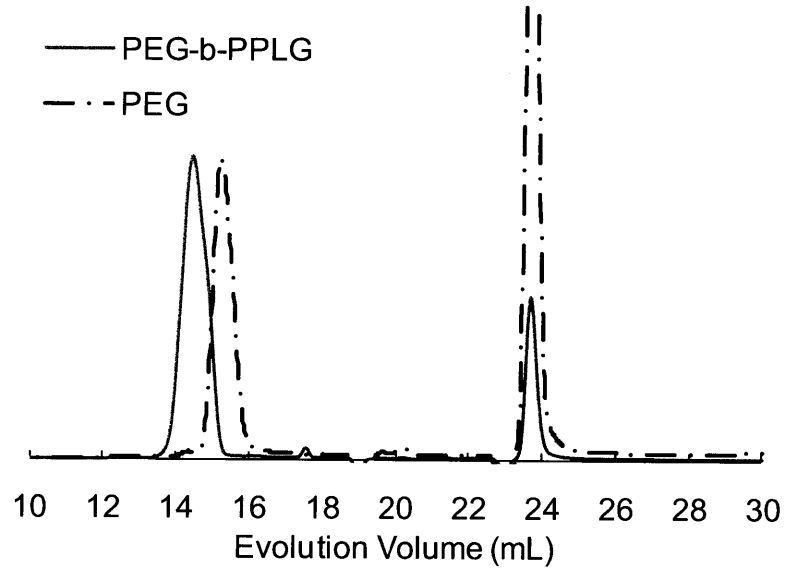

Figure 2-27. GPC traces for PEG_{114}-b-$PPLG_{26.6}$. The GPC trace of PEG-b-PPLG is the crude reaction solution before purification. The peak at 24 is toluene and the small peak at 17.5 is residual monomer.

2.10 References

1. Belshaw, P. J.; Mzengeza, S.; Lajoie, G. A., Chlorotrimethylsilane Mediated Formation of Omega-Allyl Esters of Aspartic and Glutamic Acids. *Synth. Commun.* **1990,** *20* (20), 3157-3160.

2. Poche, D. S.; Moore, M. J.; Bowles, J. L., An unconventional method for purifying the N-carboxyanhydride derivatives of gamma-alkyl-L-glutamates. *Synth. Commun.* **1999,** *29* (5), 843-854.

3. Kolb, H. C.; Finn, M. G.; Sharpless, K. B., Click chemistry: Diverse chemical function from a few good reactions. *Angewandte Chemie-International Edition* **2001,** *40* (11), 2004-2021.

4. Gao, H. F.; Matyjaszewski, K., Synthesis of molecular brushes by "grafting onto" method: Combination of ATRP and click reactions. *J. Am. Chem. Soc.* **2007,** *129* (20), 6633-6639.

5. Schutte, E.; Weakley, T. J. R.; Tyler, D. R., Radical cage effects in the photochemical degradation of polymers: Effect of radical size and mass on the cage recombination efficiency of radical cage pairs generated photochemically from the (CpCH2CH2N(CH3)C(O)(CH2)(n)CH3)(2)MO2(CO)(6) (n = 3, 8, 18) complexes. *J. Am. Chem. Soc.* **2003,** *125* (34), 10319-10326.

6. Carboni, B.; Benalil, A.; Vaultier, M., Aliphatic Amino Azides as Key Building-Blocks for Efficient Polyamine Syntheses. *J. Org. Chem.* **1993,** *58* (14), 3736-3741.

7. Calas, M.; Cordina, G.; Bompart, J.; BenBari, M.; Jei, T.; Ancelin, M. L.; Vial, H., Antimalarial activity of molecules interfering with Plasmodium falciparum phospholipid metabolism. Structure-activity relationship analysis. *Journal of Medicinal Chemistry* **1997,** *40* (22), 3557-3566.

8. Boyer, J. H.; Hamer, J., The Acid-Catalyzed Reaction of Alkyl Azides Upon Carbonyl Compounds. *J. Am. Chem. Soc.* **1955,** *77* (4), 951-954.

9. Banaszynski, L. A.; Liu, C. W.; Wandless, T. J., Characterization of the FKBP center dot Rapamycin center dot FRB ternary complex. *J. Am. Chem. Soc.* **2005,** *127* (13), 4715-4721.

10. Sechi, M.; Derudas, M.; Dallocchio, R.; Dessi, A.; Bacchi, A.; Sannia, L.; Carta, F.; Palomba, M.; Ragab, O.; Chan, C.; Shoemaker, R.; Sei, S.; Dayam, R.; Neamati, N., Design and synthesis of novel indole beta-diketo acid derivatives as HIV-1 integrase inhibitors. *Journal of Medicinal Chemistry* **2004,** *47* (21), 5298-5310.

11. Shukla, A.; Fleming, K. E.; Chuang, H. F.; Chau, T. M.; Loose, C. R.; Stephanopoulos, G. N.; Hammond, P. T., Controlling the release of peptide antimicrobial agents from surfaces. *Biomaterials* **2010,** *31* (8), 2348-2357.

12. Zhou, C. C.; Qi, X. B.; Li, P.; Chen, W. N.; Mouad, L.; Chang, M. W.; Leong, S. S. J.; Chan-Park, M. B., High Potency and Broad-Spectrum Antimicrobial Peptides Synthesized via Ring-Opening Polymerization of alpha-Aminoacid-N-carboxyanhydrides. *Biomacromolecules* **2010,** *11* (1), 60-67.

13. Merkel, O. M.; Mintzer, M. A.; Sitterberg, J.; Bakowsky, U.; Simanek, E. E.; Kissel, T., Triazine Dendrimers as Nonviral Gene Delivery Systems: Effects of Molecular Structure on Biological Activity. *Bioconjugate Chemistry* **2009,** *20* (9), 1799-1806.

3 An Introduction to Poly(γ-Propargyl-L-Glutamate): Highly Efficient "Grafting onto" a Polypeptide Backbone

3.1 Introduction

A cell's extracellular matrix consists of macromolecules (such as glycoproteins, proteoglycans, and collagen) that control both the mechanical structure and the microenvironment.[1] These properties provide physical cues that are necessary to induce various cell functions and morphologies. An important goal of tissue engineering is to mimic the environment of the extracellular matrix on several levels: mechanically, chemically, and architecturally.[2] To accomplish this goal, new synthetic methods are necessary in order to mimic the structure of these complex macromolecules. We have developed a synthetic method to form highly functionalized grafted polypeptides that can be made to mimic complex biomacromolecules such as glycoproteins and proteoglycans. Although these new synthetic polypeptides are much simpler than natural peptides, they still adapt the α-helical conformation of natural polypeptides; various chemical moieties can be attached to mimic the microenvironment of the extracellular matrix. These polymers have several features that make them very attractive for biological applications including low toxicity, biodegradability, tunable structures, and well-controlled dimensions.

These synthetic homopolymers of polypeptides have been synthesized using a well-studied N-carboxyanhydride (NCA) ring-opening polymerization (ROP) which can accommodate a wide variety of monomers containing various functional groups.[3-6] In particular, the carboxylic acid moiety (e.g. glutamate and aspartate) and amino (e.g. lysine) moiety of the amino acids have been used to add chemical complexities such as pharmaceutical drugs and

molecules that dictate hydrophobicity or pH responsiveness.[5, 7, 8] However, functionalization of polypeptides synthesized by NCA ROP has several limitations. Because of the nature of the polymerization, the type of monomer that can be used is limited to NCAs with alkyl end groups or NCAs where the functional group is protected. When creating polypeptides with functional carboxylic acid or amino groups, a three step process is often required: (1) polymerization with the protected functional group, (2) the deprotection of the functional group, and (3) the functionalization. If a high degree of functionalization is required, the added chemical moieties are limited to small molecules and low molecular-weight oligomers. The addition of polymeric side chains at a high grafting density using a "grafting onto" method has not yet been achieved. Li et al. reported a grafting efficiency of 36% for poly(γ-benzyl-l-glutamate)-g-poly(ethylene glycol) (PEG) with a PEG MW=350Da[9] and Feuz et al. reported a grafting efficiency of 48% for poly(L-lysine-g-PEG) with PEG MW=1, 2, and 5kDa.[10]

To overcome the limitations of NCA ROP, we have synthesized a new NCA monomer incorporating an alkyne group that is available for click chemistry. Click reactions, which were first described by Sharpless et al., refer to a series of highly efficient reactions that include the 1,3-dipolar cycloaddition reaction between an alkyne and an azide to form a triazole.[11] These reactions have received a significant amount of attention because of their high reaction efficiency, mild reaction conditions, functional group tolerance, and few byproducts.[11] In recent years, click chemistry has been used in a wide variety of polymer applications including functionalization of polymers with small molecules, formation of diblock polymers, formation of new dendrimers, formation of macromonomers, crosslinking of micelles, and the "grafting onto" method for the formation of molecular brushes.[12-20] In this chapter, the synthesis of poly(γ-propargyl-L-glutamate) (PPLG) and the attachment of different lengths of azide-terminated

polyethylene glycol (PEG) is reported. This model system, depicted in Figure 3-1, demonstrates the high efficiency of "grafting onto" polymer side chains, while maintaining the α-helical conformation of the polypeptide backbone.

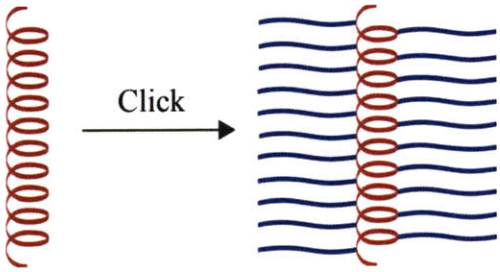

Figure 3-1. Schematic of grafting PEG side chains onto a PPLG backbone.

3.2 Results and Discussion

3.2.1 Synthesis of PPLG and PPLG-g-PEG

The synthetic strategy employed in our study is shown in Scheme 3-1. The alkyne containing monomer, γ-propargyl L-glutamate N-carboxyanhydride (2), was synthesized by a two-step process. γ-Propargyl L-glutamate hydrochloride (1) was prepared by the reaction of propargyl alcohol with glutamic acid, mediated by chlorotrimethylsilane.[21] 1 was then reacted with triphosgene in ethyl acetate to form the NCA monomer (2).[22] PPLG (3) was prepared by ROP of 2 initiated with heptylamine initiator in dimethylformamide (DMF). The polymerization was monitored by observing the disappearance of the NCA characteristic peaks (1790 and 1850 cm^{-1}) using an FTIR spectrometer.[7] After 2-3 days, the peaks disappeared and the polymer was purified by precipitation out of solution into diethyl ether. The resulting PPLG had a degree of polymerization of n = 40 (by GPC (DMF), Mn = 8513, PDI = 1.449, Figure 3-4A). The relatively broad molecular weight distribution is typical of a primary amine initiated NCA ROP. There are several strategies presented in the literature to minimize the side reactions associated

with this type of polymerization.[3, 23-28] The Deming group uses a nickel catalyst to achieve a living polymerization[3, 23]; however low-valent nickel catalysts may cause alkynes to cyclize forming functionalized benzyl rings.[25] Lu and Cheng use a silane mediated controlled polymerization.[28] Other strategies for obtaining a pseudo-living polymerization initiated with a primary amine include running the reaction under vacuum[26] and avoiding DMF by using very pure THF or dimethylacetamide (DMAC).[27] PPLG is completely soluble in dimethylacetamide but has limited solubility in THF. To best eliminate side reactions of the PPLG polymerization, we found using high purity components and running the reaction under dry, inert conditions significantly decreases side reactions.

Scheme 3-1. Synthesis of PPLG and side chain coupling via click chemistry

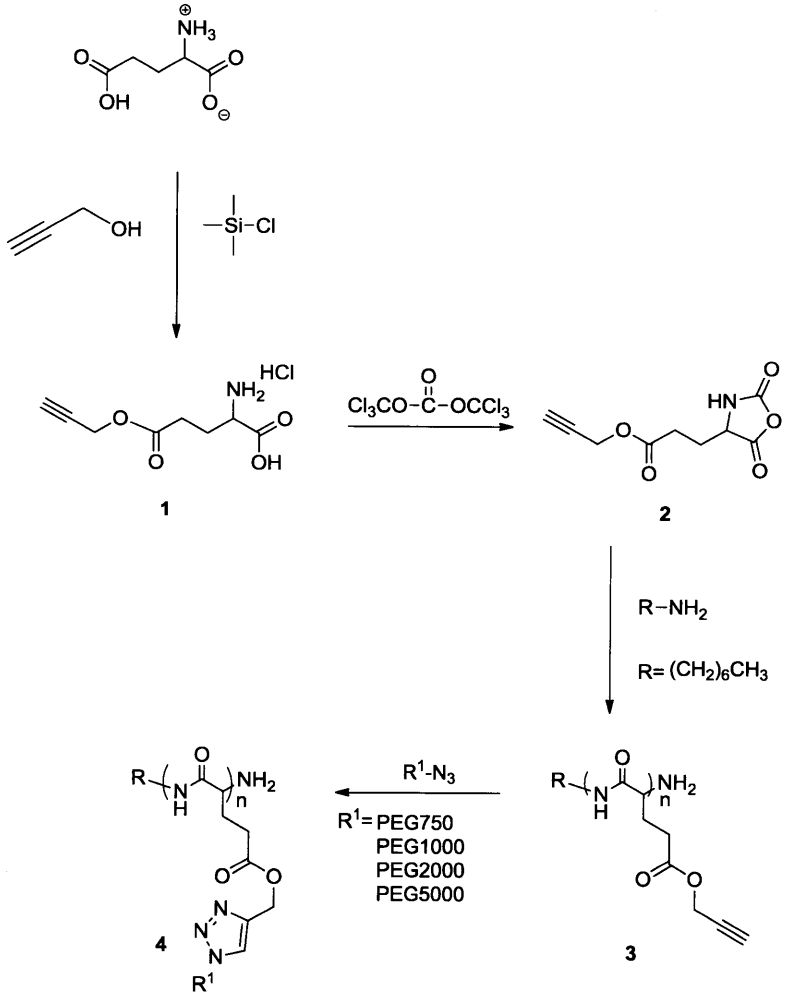

To synthesize PPLG-g-PEG, PPLG was coupled with PEG-N_3 using CuBr/ N,N,N,N',N'-Pentamethyldiethylenetriamine (PMDETA) as catalyst in DMF, with a molar ratio of alkyne/azide/CuBr/PMDETA equal to 1/2/0.33/0.33 for all molecular weights of PEG-N3 used, and at various ratios for PEG1000-N_3 to further characterize the side chain grafting. After the reaction was complete, the reaction solution was passed through a short alumina oxide column to remove the catalyst. The functionalized polymers were purified by dialysis and characterized by ^{1}H-NMR, FTIR spectrometry, GPC, and circular dichroism (CD).

3.2.2 Kinetics of PEG Grafting

The kinetics of the PEG-N_3 coupling reaction were determined using a PEG1000-N_3 side chain and a reaction molar ratio of alkyne/azide/CuBr/PMDETA equal to 1/1/0.1/0.1, using GPC. The molar ratios were lowered to slow down the kinetics such that they could be observed by GPC. Samples were taken from the reaction mixture (40μL) at various time points and GPC samples were prepared by dilution with 750μL DMF and addition of 5μL of a toluene standard. Conversion of the PEG-N_3 was determined by comparing the peak area of the PEG-N_3 curve to the toluene peak. Figure 3-2 shows the GPC traces (DMF) and conversion as a function of reaction time. As indicated by the overlap of the 125 min trace and the 35 minute trace, the reaction was complete after 35 minutes. The conversion of PEG-N_3 by GPC at 35 minutes was 95.8%.

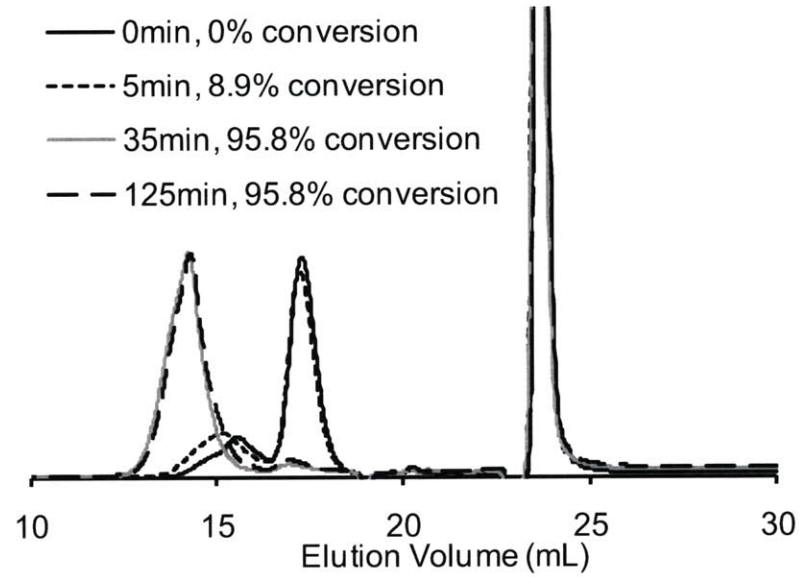

Figure 3-2. Evolution of GPC (DMF) traces as a function of reaction time

3.2.3 PPLG-g-PEG Characterization

We also used ^{1}H-NMR spectroscopy to monitor side chain grafting. Figure 3-3 shows the ^{1}H-NMR spectrum of PPLG, PPLG-g-PEG1000 at 50% functionalization, and PPLG-g-PEG at nearly complete functionalization. It can be seen from a comparison of Figure 3-3A to Figure 3-3B that the ester peak b has decreased and a new ester peak k has appeared; furthermore, the peak m representing the methyl group next to the nitrogen of the triazole group appears. The alkyne peak a is not observed because it overlaps with the PEG-N_3 peaks. In Figure 3-3B and Figure 3-3C, no peaks from the original backbone present that can be used to determine a grafting efficiency. Therefore, to determine the grafting efficiency, a small sample of the crude reaction solution was concentrated down to a solid, dissolved in DMF-d^7, and an ^{1}H-NMR spectrum was obtained. The conversion of the PEG-N_3 was determined by comparing the area under peaks m and f.[29] Based on the conversion of the azide to triazole (for PPLG-g-PEG1000, $y_{conversion}$ = 49.6%) and the initial feed ratio of PEG-N_3 to PPLG (1/2.01), the grafting efficiency was determined (y_{graft} = 99.6%). These results are consistent with those observed by GPC

(DMF) for the PPLG-g-PEG1000 system. Similar NMR spectra were observed for PPLG-g-PEG with PEG MW 1000, 2000, and 5000 g/mol. As shown in Table 3-1, the grafting efficiency (for a feed ratio of PPLG-alkyne/PEG-N_3 of ½) is close to 100% in each case.

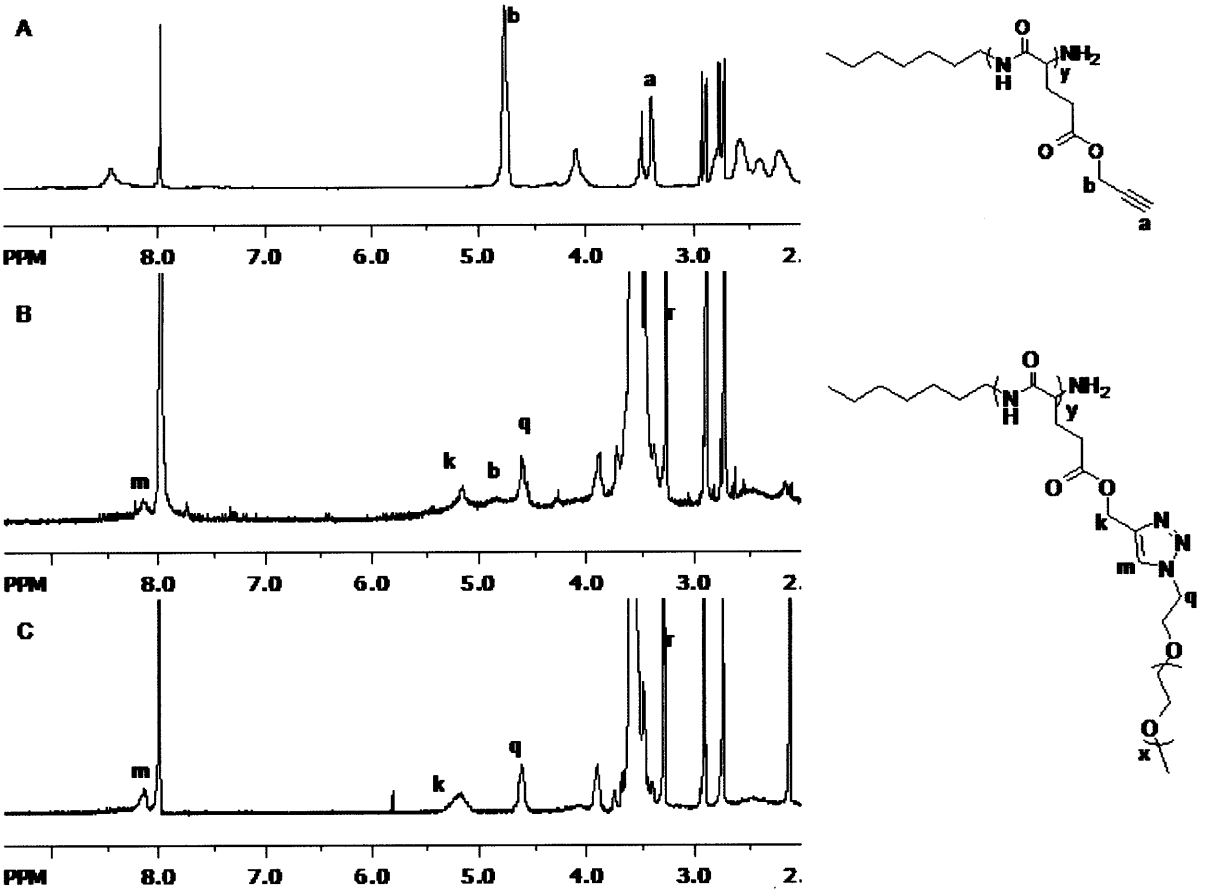

Figure 3-3. ^{1}H-NMR spectrum of (A) PPLG in DMF-d7 (B) PPLG-g-PEG 1000 with a feed ratio PPLG-alkyne/PEG-N_3 of 1/0.5 in DMF-d7 (C) PPLG-g-PEG 1000 with a feed ratio PPLG-alkyne/PEG-N_3 of 1/2 in DMF-d7

Figure 3-4A shows the GPC (DMF) traces of different molecular weight PPLG-g-PEG polymers prepared with a PPLG-alkyne/PEG ratio of 1/2. All of the grafted copolymers show an increase in molecular weight while maintaining a narrow molecular weight distribution. This molecular weight increase also indicates that the grafting method does not degrade the peptide

backbone. In Figure 3-4B, the PPLG-g-PEG molecular weight scales linearly with increasing side chain length, which indicates that the grafting efficiency remains consistent for different molecular weight side chains.

Table 3-1. Summary of GPC (DMF) results and grafting efficiency determined by NMR

Polymer	Mn (g/mol)	Mp (g/mol)	PDI	y_{graft}
PPLG	7043	6870	1.38	--
PPLG-g-PEG 750	14134	18080	1.42	98.9± 1.3%
PPLG-g-PEG 1000	14999	22223	1.40	96.3± 2.2%
PPLG-g-PEG 2000	34443	41884	1.22	Not Tested
PPLG-g-PEG 5000	97082	99058	1.19	97.4± 2.8%

The observed grafting efficiencies are higher than those of similar systems utilizing graft-onto approaches found in the literature, including those involving click chemistry. Gao and Matyjaszewski synthesized a similar system of PHEMA-g-PEG and the highest PEG-N_3 (MW=750) grafting efficiency obtained was 88.4% at an alkyne/azide ratio of 1/8.5.[29] They suggest that the grafting efficiency is lower than 100% as a result of steric congestion. Parrish and Emrick reported PEG-grafted aliphatic polyester systems with PEG molecular weights up to 1100 molecular weight and grafting efficiencies between 70-80%.[30] Parrish, Breitenkamp, and Emrick reported a Poly(α-Propargyl-δ-valerolactone)-g-PEG system where the PEG-N_3 1100 grafting efficiency obtained was 43%.[31]

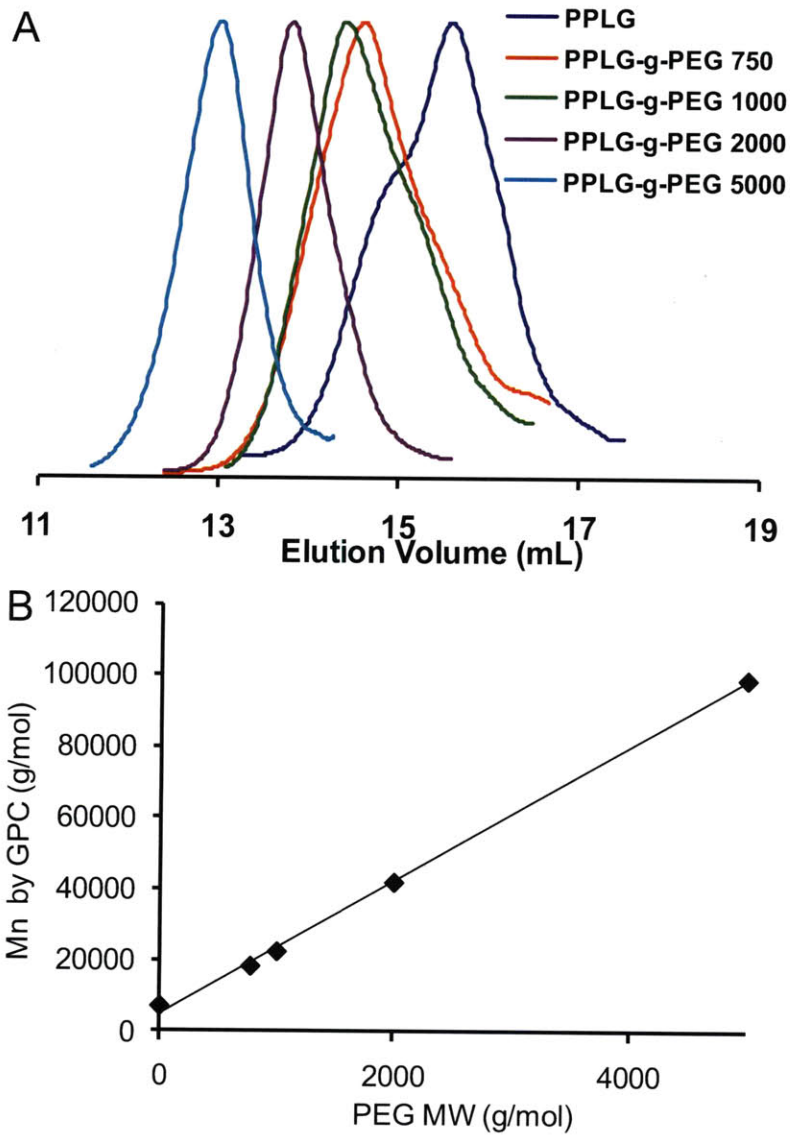

Figure 3-4. (A) GPC (DMF) traces for PPLG-g-PEG (B) PPLG-g-PEG molecular weight as a function of grafted PEG-N_3 molecular weight

We hypothesize that the high grafting efficiency achieved with PPLG (nearly 100%) is a result of the rigid α-helical structure of the polymer backbone. Synthetic peptides, in particular substituted poly(L-glutamates) form stable α-helix when in various organic solvents and when solvent cast from volatile organic solvents. [32, 33] This stable α-helical structure causes the alkyne-terminated side chains to protrude outward from each repeat unit thereby increasing their

availability for coupling. The α-helical structure is present throughout the reaction, initially from the PPLG backbone. Once the reaction reaches a high grafting density, the steric repulsion between the grafted PEG chains causes the graft polymer to develop the shape of a symmetrical brush polymer with the most favorable backbone conformation of an α-helix.[10]

3.3 Confirmation of α-Helical Structure of PPLG and PEG-b-PPLG

To confirm the hypothesis that PPLG adopts an α-helical structure, liquid phase FTIR was performed on PPLG in DMF. The α-helical conformation was identified by the strong C=O amide I absorption at 1658 cm^{-1} and the N-H amide II absorption at 1549 cm^{-1}, as shown in Figure 3-5. Furthermore, circular CD was performed in water (DMF is not a suitable solvent for CD) to confirm the presence of an α-helical structure in PPLG and PPLG-g-PEG at different grafting densities and with different molecular weight side chains. To obtain a CD spectra of PPLG, a block copolymer (PEG_{114}-b-$PPLG_{26.6}$) was synthesized and analyzed by CD (Figure 3-6). In all cases, the characteristic negative ellipticity of an α-helix was observed at 208 nm and 222 nm.[34, 35] As shown in Figure 3-7A, at 50% substitution and near 100% substitution the backbone has an α-helical conformation. The less pronounced minima at 209 nm and 222 nm are a result of an increased presence of PEG side chains, which decrease the concentration of α-helix backbone. In Figure 3-7B, the characteristic α-helix minimums were observed for all molecular weights of the PEG side chains. Thus, the characteristic α-helix peaks observed in FTIR and CD indicate that the polymer backbone does have an α-helix structure. The rotating helical arrangement of these groups increases their availability along the backbone for coupling with the PEG-N_3 side chains.

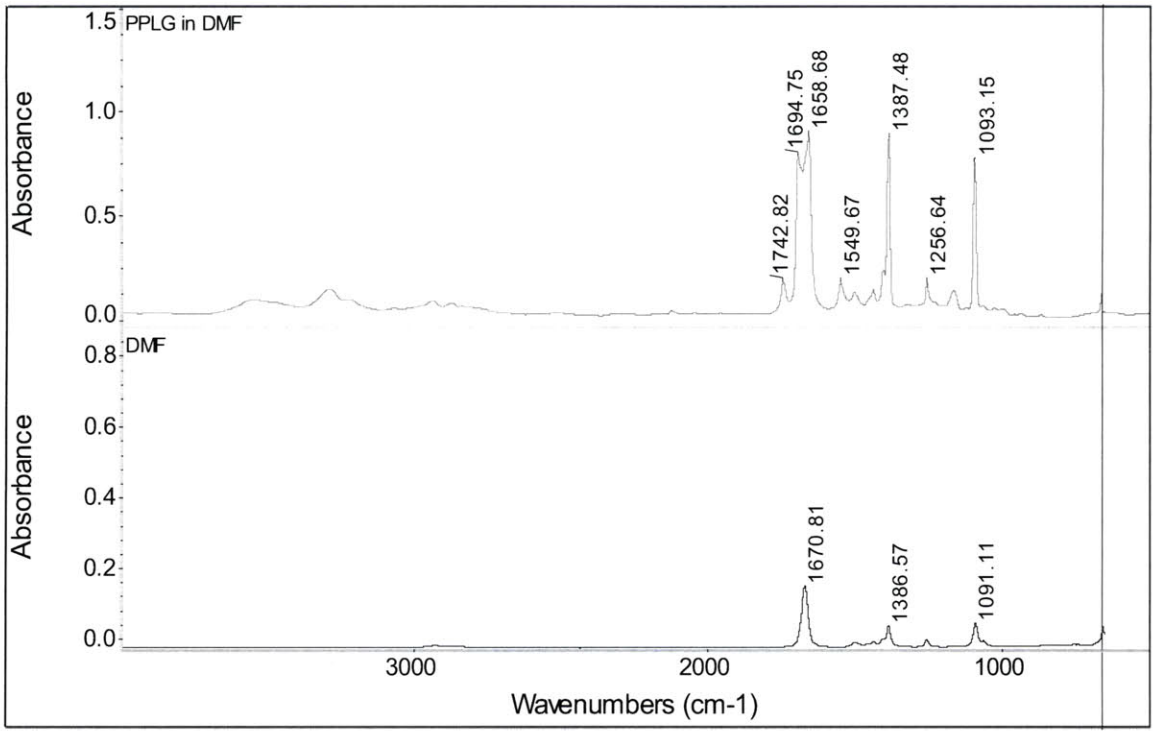

Figure 3-5. FTIR of DMF and PPLG in DMF, the peak at 1694 cm-1 is DMF

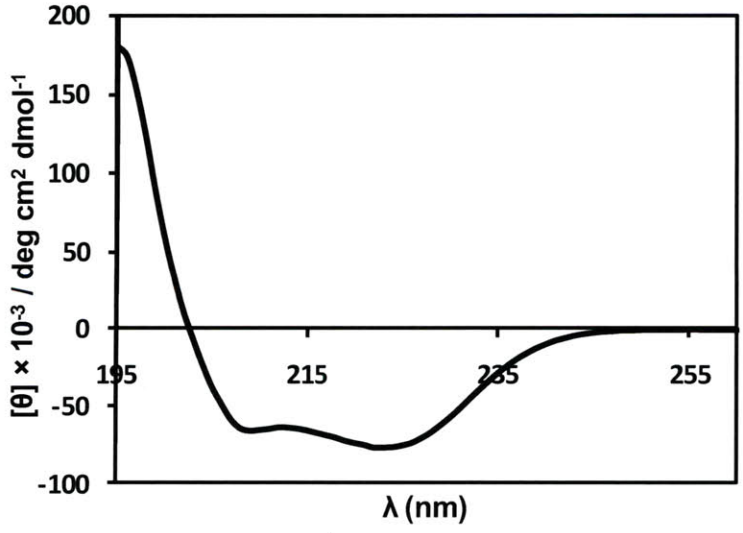

Figure 3-6. CD of PEG-b-PPLG in water at a concentration of 1 mg/mL. The minimums at 208 nm and 222 nm indicate that the polymer has an α-helical structure.

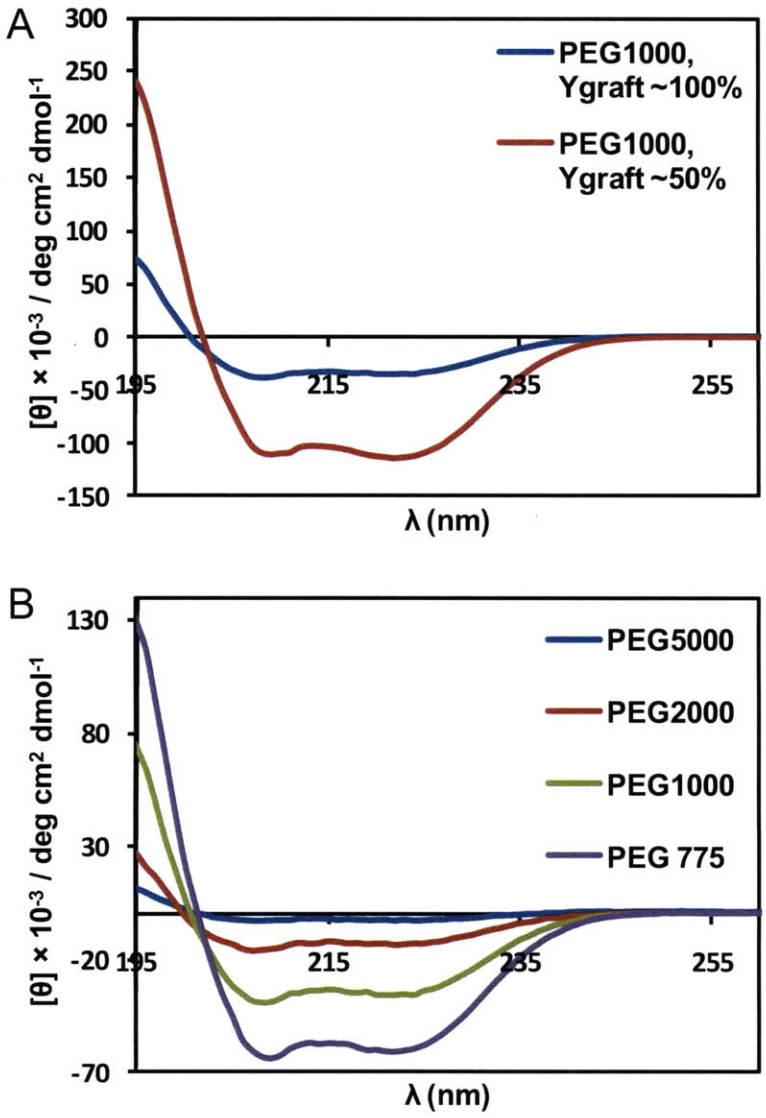

Figure 3-7. A) CD of PPLG-g-PEG 1000 (2.5 mg/mL) at ~50% and ~100% grafting in water B) CD of PPLG-g-PEG (2.5 mg/mL) at different molecular weights all with close to 100% grafting.

3.3.1 Particle Sizing of PPLG-g-PEG

Dynamic light scattering was also used to observe the size of the molecular brushes obtained when different molecular weight side chains were grafted onto the PPLG. Measurements were taken at a 15° and 90° and similar distributions were observed for both angles. A representative size distribution for PPLG-g-PEG (MW1000) is shown in Figure 3-8A.

Narrow size distributions were obtained for all graft systems and particle size increases as a function of molecular weight, as shown in Figure 3-8B.

3.4 Conclusion

In summary, we have described a new synthetic method to form highly functionalized grafted polypeptides. A new NCA monomer, propargyl-L-glutamate, and a new polymer, PPLG, have been synthesized. This new polymer provides a means of attaching a wide variety of molecules, which vary in both size and hydrophobicity, to a polypeptide using a single step click reaction. The combination of NCA ROP and click chemistry provides a versatile synthetic approach to develop molecules which mimic the complex architecture of natural peptides. We have shown that PEG chains with varying molecular weight from 750 g mol^{-1} to 5000 g mol^{-1} can be attached to the PPLG backbone at nearly perfect grafting densities. A grafting density of 95.8% was obtained at an alkyne/azide reaction ratio of 1/1 and a grafting density of 96.3-98.9% was obtained at reaction ratios of alkyne/azide of 1/2. These grafting efficiencies are higher than similar PEG grafting systems reported in the literature.[29-31] The extremely high efficiency achieved with PPLG is a result of the rigid α-helical structure of the polymer backbone, which causes the alkyne terminated side chains to protrude outward from each repeat unit, thus increasing their availability for coupling.

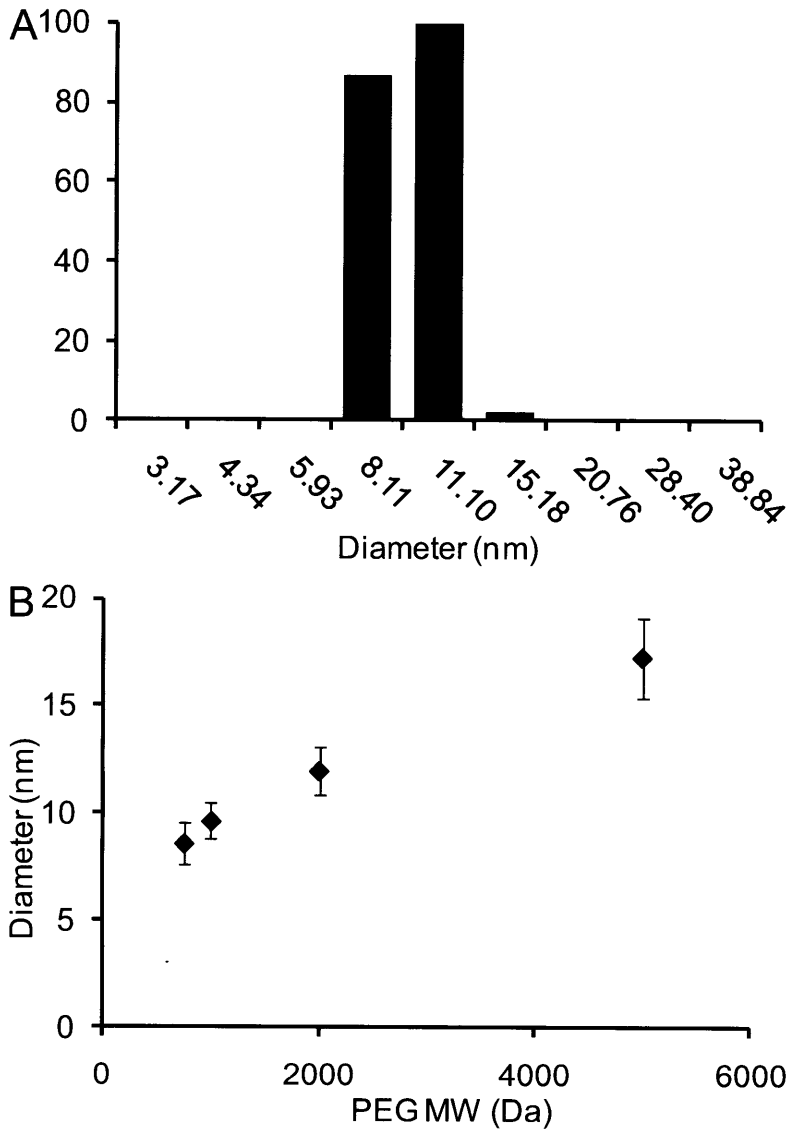

Figure 3-8. A) Particle size distribution for PPLG-g-PEG (MW2000) recorded at 90° B) Particle size as a function of PEG side chain molecular weight

3.5 References

1. Griffith, L. G.; Swartz, M. A., Capturing complex 3D tissue physiology in vitro. *Nat. Rev. Mol. Cell Biol.* **2006,** *7* (3), 211-224.

2. Benoit, D. S. W.; Schwartz, M. P.; Durney, A. R.; Anseth, K. S., Small functional groups for controlled differentiation of hydrogel-encapsulated human mesenchymal stem cells. *Nat. Mater.* **2008,** *7* (10), 816-823.

3. Deming, T. J., Synthetic polypeptides for biomedical applications. *Prog. Polym. Sci.* **2007,** *32* (8-9), 858-875.

4. Daly, W. H.; Poche, D., The Preparation of N-Carboxyanhydrides of Alpha-Amino-Acids Using Bis(Trichloromethyl)Carbonate. *Tetrahedron Letters* **1988,** *29* (46), 5859-5862.

5. Osada, K.; Kataoka, K., Drug and gene delivery based on supramolecular assembly of PEG-polypeptide hybrid block copolymers. In *Peptide Hybrid Polymers*, SPRINGER-VERLAG BERLIN: Berlin, 2006; Vol. 202, pp 113-153.

6. Tian, L.; Hammond, P. T., Comb-dendritic block copolymers as tree-shaped macromolecular amphiphiles for nanoparticle self-assembly. *Chemistry of Materials* **2006,** *18* (17), 3976-3984.

7. Yokoyama, M.; Kwon, G. S.; Okano, T.; Sakurai, Y.; Seto, T.; Kataoka, K., Preparation of micelle-forming polymer-drug conjugates. *Bioconjugate Chem.* **1992,** *3* (4), 295-301.

8. Lavasanifar, A.; Samuel, J.; Kwon, G. S., Poly(ethylene oxide)-block-poly(L-amino acid) micelles for drug delivery. *Advanced Drug Delivery Reviews* **2002,** *54* (2), 169-190.

9. Li, T.; Lin, J.; Chen, T.; Zhang, S., Polymeric micelles formed by polypeptide graft copolymer and its mixtures with polypeptide block copolymer. *Polymer* **2006,** *47* (13), 4485-4489.

10. Feuz, L.; Strunz, P.; Geue, T.; Textor, M.; Borisov, O., Conformation of poly(L-lysine)-graft-poly(ethylene glycol) molecular brushes in aqueous solution studied by small-angle neutron scattering. *Eur. Phys. J. E* **2007,** *23* (3), 237-245.

11. Kolb, H. C.; Finn, M. G.; Sharpless, K. B., Click chemistry: Diverse chemical function from a few good reactions. *Angewandte Chemie-International Edition* **2001,** *40* (11), 2004-2021.

12. Hawker, C. J.; Wooley, K. L., The convergence of synthetic organic and polymer chemistries. *Science* **2005,** *309* (5738), 1200-1205.

13. Wu, P.; Malkoch, M.; Hunt, J. N.; Vestberg, R.; Kaltgrad, E.; Finn, M. G.; Fokin, V. V.; Sharpless, K. B.; Hawker, C. J., Multivalent, bifunctional dendrimers prepared by click chemistry. *Chem. Commun.* **2005,** (46), 5775-5777.

14. Joralemon, M. J.; O'Reilly, R. K.; Hawker, C. J.; Wooley, K. L., Shell Click-crosslinked (SCC) nanoparticles: A new methodology for synthesis and orthogonal functionalization. *J. Am. Chem. Soc.* **2005,** *127* (48), 16892-16899.

15. Helms, B.; Mynar, J. L.; Hawker, C. J.; Frechet, J. M. J., Dendronized linear polymers via "click chemistry". *J. Am. Chem. Soc.* **2004,** *126* (46), 15020-15021.

16. Wu, P.; Feldman, A. K.; Nugent, A. K.; Hawker, C. J.; Scheel, A.; Voit, B.; Pyun, J.; Frechet, J. M. J.; Sharpless, K. B.; Fokin, V. V., Efficiency and fidelity in a click-chemistry route to triazole dendrimers by the copper(I)-catalyzed ligation of azides and alkynes. *Angewandte Chemie-International Edition* **2004,** *43* (30), 3928-3932.

17. Gondi, S. R.; Vogt, A. P.; Sumerlin, B. S., Versatile Pathway to Functional Telechelics via RAFT Polymerization and Click Chemistry. *Macromolecules* **2007,** *40* (3), 474-481.

18. Vogt, A. P.; Sumerlin, B. S., An Efficient Route to Macromonomers via ATRP and Click Chemistry. *Macromolecules* **2006,** *39* (16), 5286-5292.

19. Sumerlin, B. S.; Tsarevsky, N. V.; Louche, G.; Lee, R. Y.; Matyjaszewski, K., Highly Efficient "Click" Functionalization of Poly(3-azidopropyl methacrylate) Prepared by ATRP. *Macromolecules* **2005,** *38* (18), 7540-7545.

20. Riva, R.; Schmeits, S.; Jerome, C.; Jerome, R.; Lecomte, P., Combination of Ring-Opening Polymerization and "Click Chemistry"; Toward Functionalization and Grafting of Poly(ε-caprolactone). *Macromolecules* **2007,** *40* (4), 796-803.

4 The Synthetic Tuning of Clickable pH Responsive Cationic Polypeptides and Block Copolypeptides

4.1 Introduction

Synthetic polypeptides have received attention because of their unique structural properties and biocompatibility.[1-4] Like their naturally occurring analogs, these molecules have a poly(amino acid) backbone and possess the ability to fold into stable secondary structures. Helical structures, in particular, allow for proteins to optimally display surface moieties that dictate cell signaling and molecular docking.[5] This property gives synthetic polypeptides an advantage over other synthetic polymers that can only adopt a random coil structure. A considerable amount of research has been performed on synthetic polypeptides to better understand the complex features of proteins and to gain insight into their secondary structures.[6-10] Synthetic polypeptides can be synthesized on a large scale by the ring opening polymerization (ROP) of N-carboxyanhydrides (NCA) formed from naturally occurring amino acids. These simple homopolypeptides are able to arrange into or change their secondary structure based on solution conditions. [7-10] Although these macromolecules' secondary structure can be controlled to some extent, we are limited by the given side chain, which dictates polymer function, structure, and responsive behavior to temperature or pH among many other properties.

By employing our PPLG platform, described in Chapter 3, for the click chemistry of amino-functional groups, we have developed several new pH responsive macromolecules. A unique aspect of these new amine-functionalized polypeptides is the ability to buffer and, in some cases, undergo a solubility phase transition with degree of ionization while adopting an α-helical structure over biologically relevant pHs. These polymers include both poly(γ-propargyl

L-glutamate) (PPLG) based homopolymers and poly(ethylene glycol-b-γ-propargyl L-glutamate) (PEG-b-PPLG) block copolymers substituted with various amine moieties that range in pKa and hydrophobicity, providing the basis for a library of new synthetic structures that can be tuned for specific interactions and responsive behaviors.

The new PPLG based cationic polypeptides have the potential to be used for many different applications. Polypeptides have been investigated as smart molecules in lipid membranes,[11-13] liquid crystals used in optical storage and display devices,[4] drug delivery,[3, 14, 15] gene delivery,[3, 16-21] anti-fouling coatings,[22] tissue engineering, biosensors, and synthetic mimics of naturally occurring molecules. [1, 3, 23-26] We have characterized the pH responsive behavior of the new polypeptides, the pH-dependent hydrolysis rate of the ester containing amine side chains, and have performed preliminary experiments that demonstrate the potential use of these new materials for systemic drug and gene delivery. More specifically, for pH responsive drug delivery, one could design a micellar system that forms stable micelle drug carriers in the blood stream and normal tissue at extracellular conditions (pH 7.00-7.45)[27] but destabilizes in the endosome (early endosome pH 5.5-6.3 and late endosome pH < 5.5)[28] or in hypoxic regions of tumors (pH approaching 6.0)[27], to release the drug. To achieve this behavior, a pH responsive polypeptide is needed that is fully soluble at endosomal or tumor pH and insoluble at extracellular pH. We have determined the solubility behavior of the amine functionalized PPLG and the self-assembly behavior of the amine functionalized PEG-b-PPLG as a function of pH. For gene delivery, it is critical that the polymers complex with siRNA or DNA to form protective polymer-gene complexes (polyplexes); these polyplexes must escape the endosomal compartments into which they are initially trafficked upon internalization. [29, 30] One such mode of endosomal escape is through the so-called "proton effect" in which the basic polymer buffers

the endosome during acidification leading to osmotic swelling and rupture.[29, 31] The buffering capacity of the new polypeptides has been explored using titrations to determine the pH range at which these polymers buffer. In addition, siRNA complexation studies have been performed to determine if these polymers complex with siRNA to form polyplexes. Preliminary cell uptake studies, endosomal buffering studies, and transfection studies have also been performed on the polyplexes.

A unique aspect of these new polypeptides is that there is an ester linkage between the amine and the polymer backbone. These ester side chains can be hydrolyzed, leaving behind a carboxylic acid moiety, thus creating a charge shifting polymer (shifting with hydrolysis from positive to negative net charge). We have examined the rate of hydrolysis of the ester side chain at various pH conditions and the role the shift in overall polymer charge plays on disrupting the secondary structure. This hydrolysis and overall shift in charge from positive to negative could play a role in improving the safety and biodegradability of these substituted poly(γ-glutamic acid) based polymers[32-34], and may also aid in the delivery and subsequent unpackaging and release of nucleic acid based cargos that are delivered using these systems.

4.2 Results and Discussion

4.2.1 Polymer Synthesis

The PPLG polymers were prepared as previously described in Chapter 1.[35] Briefly, γ-propargyl L-glutamate was reacted with triphosgene to form the NCA. PPLG and PEG-b-PPLG were prepared by ring opening polymerization in dimethylformamide (DMF) at room temperature by initiation with heptylamine and PEG-NH_2 (MW=5000), respectively. Table 5-1 summarizes the stoichiometric feed ratio of each polymerization, the degree of polymerization

characterized by ^{1}H-NMR, and the molecular weight and molecular weight distribution characterized by gel permeation chromatography (GPC) with DMF as the carrier solvent. The narrow polydispersities (1.09-1.25) and reaction feed ratio compared to the degree of polymerization by ^{1}H-NMR indicate that the polymerization is well controlled. Furthermore, this polymerization route allows for high molecular weight polymers with a degree of polymerization as high as 140. As indicated by Poché et al., a high degree of polymerization can be obtained if the NCA monomer purity is high; the washing strategy employed in this NCA monomer preparation does significantly improve the monomer purity by removing residual HCl.[36]

Table 4-1. Summary of polymerization feed NCA-monomer/initiator, degree of polymerization by ^{1}H-NMR, molecular weight and polydispersity determined by DMF GPC with PMMA standards.

			DMF GPC with PMMA Standards		
Polymer	Feed ratio	DP by NMR	Mn	Mw	Polydispersity
PPLG	25	30	6100	7600	1.25
PPLG	50	56	12700	14100	1.11
PPLG	75	75	17900	19400	1.09
PPLG	150	140	42900	50000	1.17
PEG-NH_2	--	--	10000	11500	1.14
PEG-b-PPLG	25	23	14600	15800	1.08

Six different amine moieties ranging in pKa (1°, 2°, and 3° amines) and hydrophobicity (dimethylethanamine, dimethylpropanamine, diethylamine, and diisopropylamine) were attached to four different molecular weight PPLG backbones and a PEG-b-PPLG diblock copolymer through the copper-mediated 1,3 cycloaddition between the alkynes on the PPLG backbone and the azide bearing amine groups, shown in Scheme 4-1. The PPLG was coupled with azido amines using CuBr/PMDETA as a catalyst in DMF with a molar ratio of alkyne/azide/CuBr/PMDETA equal to 1/1.2/0.1/0.1. After the reaction was complete, the

polymer was purified by dialysis against water acidified with HCl (pH $\leq$ 4) to remove any unreacted amino azides and the copper catalyst. The polymer structures were confirmed using ^{1}H-NMR. Representative ^{1}H-NMR of the diethylamine and diisopropylamine substituted PPLG compared to the ^{1}H-NMR of PPLG are shown in Figure 4-1. For all amine groups, the coupling efficiency was near quantitative as indicated by the disappearance of the PPLG alkyne peak (a, 3.4ppm) and ester peak (b, 4.7ppm) and the appearance of a new ester peak (k, 5.2ppm) and the triazole ring peak (m, 8.15ppm). Furthermore, the peak integration for all samples tested were as expected for near quantitative substitution without hydrolysis of the ester group on the polymer side chains. Representative ^{1}H-NMR for the remaining amine functionalized PPLG and PEG-b-PPLG can be found in the supporting information.

Scheme 4-1. Functionalization of PPLG by the Click reaction and the pH responsive side groups.

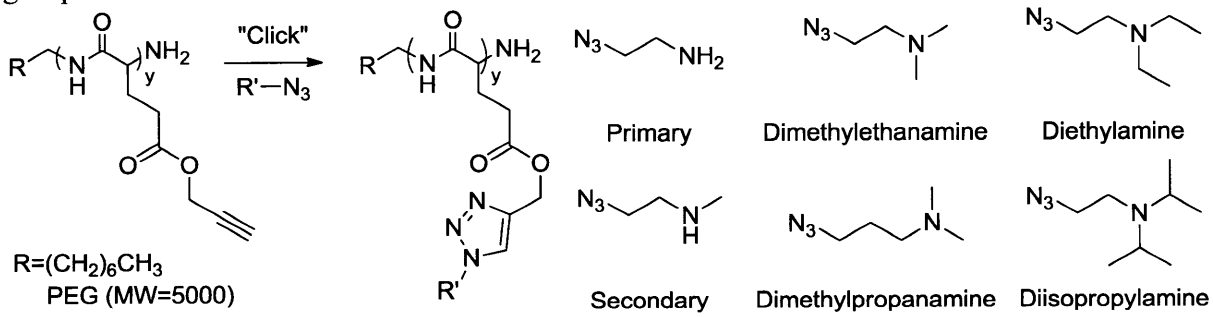

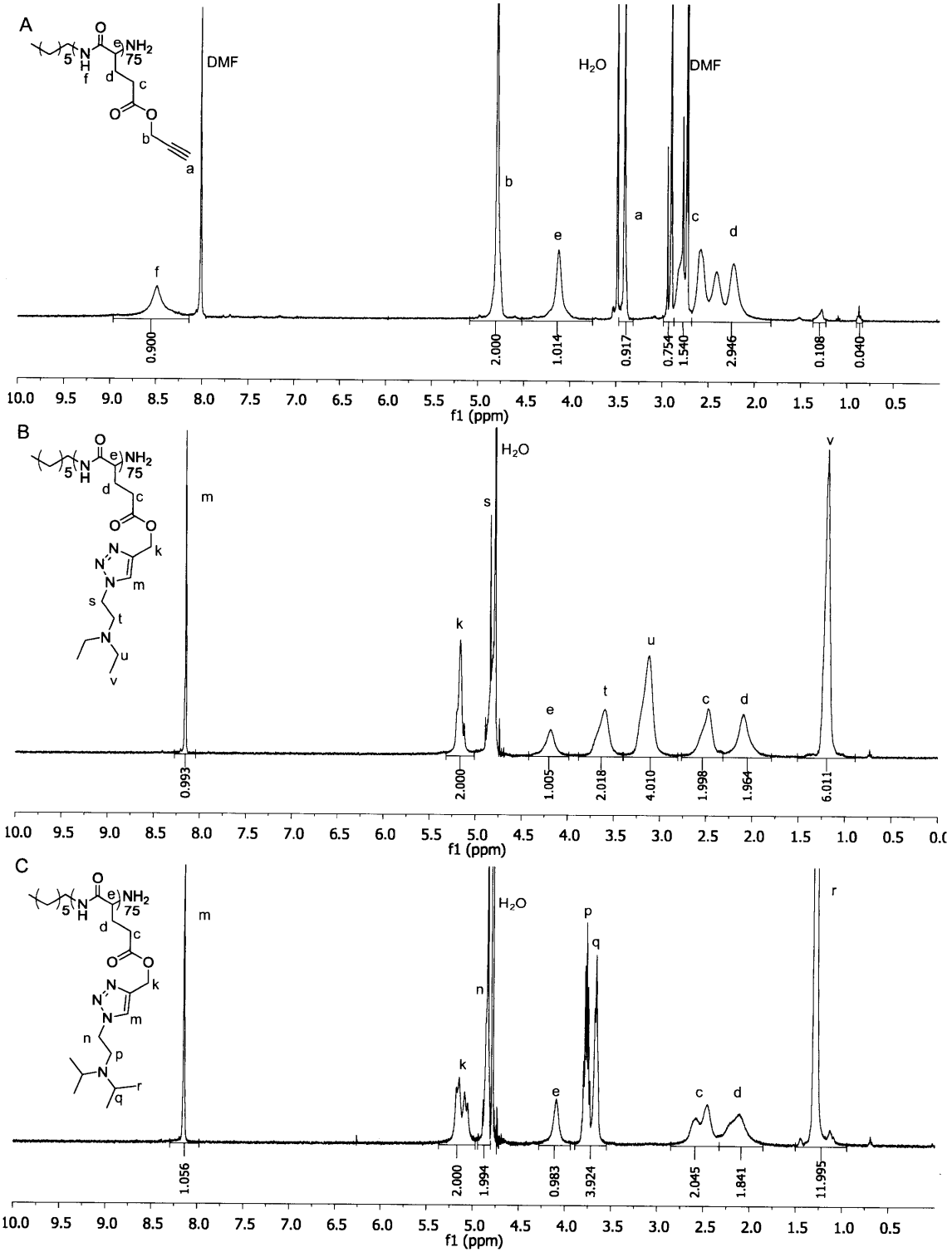

Figure 4-1. A) PPLG in DMF-d_7, B) PPLG functionalized with diethylamine in D_2O, and C) ^{1}H-NMR of PPLG functionalized with diispropylamine in D_2O. The PPLG backbone has a degree of polymerization of 75.

4.2.2 Investigation of Polymer Buffering and Solubility.

To investigate pH responsiveness and the buffering behavior of these polypeptide systems, titrations were performed on all polymers. Polymers were dissolved in 125 mM NaCl at 10 mM polypeptide-amine (molarity based on repeat unit), titrated with increasing pH to pH of 10-10.5 using 0.1 M NaOH, and subsequently titrated with decreasing pH using 0.1 M HCl. After titrations were complete, representative samples were freeze dried, dissolved in D_2O, and analyzed using ^{1}H-NMR. From the ^{1}H-NMR, the spectra were nearly identical to those obtained before titrations, indicating that hydrolysis did not occur during the 2-3 hour titration process (see supporting information, Figure 4-22). Representative titrations with increasing pH are shown in Figure 4-2, where Figure 4-2A consists of the dimethylethanamine polymers at varying degrees of polymerization, and Figure 4-2B consists of titrations of each polymer side functional group with a degree of polymerization of NCA backbone of 75 (titrations of additional polymers can be found in supporting information, Figure 4-21). All polymers appear to have strong buffering capacity in the pH range of 5-7.35, which scales with the pH range of typical extracellular tissue to late endosomal pH. [27, 28] The diisopropylamine polypeptide exhibits the sharpest buffering transition at pH 5.25; the diethylamine polymer also buffers in this range, but with a broader transition that has a midpoint at the slightly higher pH of approximately 6.5. The primary and secondary amine functional polymers interestingly exhibit similar broad buffering behavior beginning at pH 5.5 with a midpoint at 7.25. One would typically expect buffering at higher pH for primary and secondary amines (pKa approximately 9-11),[37, 38] although some buffering is observed in these polymers from pH 8 to 10. Polyelectrolytes typically exhibit broad buffering behavior and shifted pKa values due to segmental charge repulsion. For the dimethyl substituted amines, the dimethylethanamine exhibits buffering behavior starting at the same pH

as the primary and secondary amines with a midpoint falling between 6.5 to 7.0. These values are consistent with the series of polymers with ethylene linker groups to the triazole ring while the dimethylpropanamine polymer exhibits buffering at higher pHs. The additional carbon between the amine group and the triazole ring results in a higher pKa for the dimethylpropanamine. This shift in pKa could be the result of the amine group being further removed from the electron withdrawing triazole ring or from the decreased crowding experienced by the amine group. All of the polymers exhibit a small amount of buffering at the start of the titration curve, at pH 3-4; the buffering in this region could be a result of the triazole ring generated during the click reaction; triazoles exhibit pKa's of less than 3.0.[37, 39] The polymer buffering appears to have little dependence on polymer molecular weight, as indicated in Figure 4-2A.

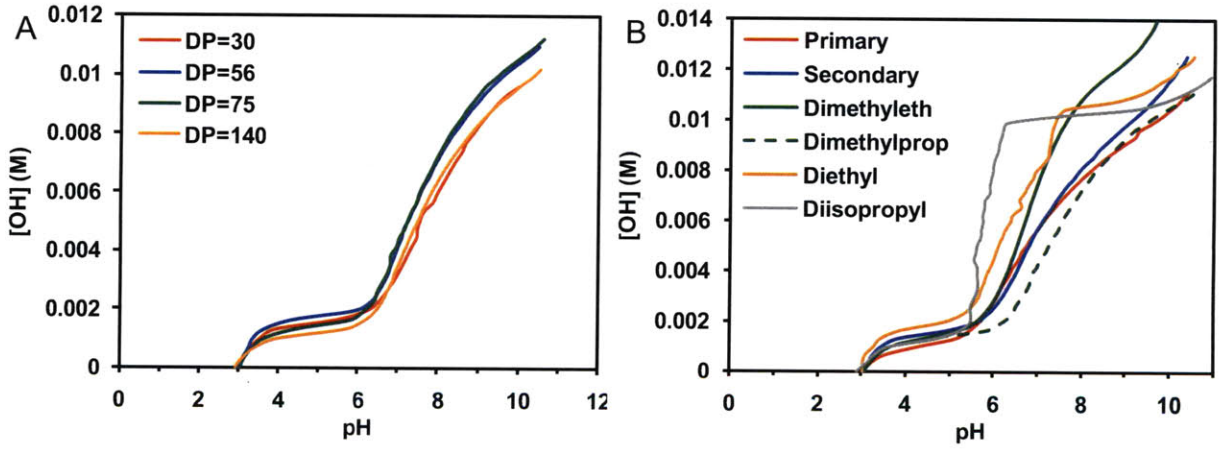

Figure 4-2. Titrations of polymers at a concentration of 10mM using 0.1M sodium hydroxide. A) PPLG polymers functionalized with dimethylethanamine with varying degrees of polymerization, and B) PPLG polymers with a degree of polymerization of 75.

The primary, secondary, and dimethyl polypeptides remain water soluble over the entire pH range; however as the cationic diethylamine and diisopropylamine functionalized polypeptides are titrated from acidic to basic conditions, the amines become deprotonated. The

resulting uncharged polypeptide is no longer soluble in water, leading to precipitation of the polypeptide from aqueous solution. For the diethylamine and diisopropylamine functionalized PPLG, polymer precipitation was observed at various pH values depending on polymer molecular weight. To determine the pH where precipitation occurs, turbidity measurements were performed on the diethylamine and diisopropylamine functionalized PPLGs by monitoring polymer solution transmission at 550nm, shown in Figure 4-3. When the polymers begin to precipitate out of solution, there is a sharp drop in transmission. For the diethylamine functionalized PPLG (Figure 4-3, solid lines), precipitation occurred between 6.80 and 7.45 depending on the degree of polymerization and for the diisopropylamine functionalized PPLG (Figure 4-3, dashed lines), precipitation occurred between 5.23 and 5.59. These values are consistent with the titration data shown in Figure 4-2 and in the supporting information section 4.4. In general we see the anticipated trend that increased molecular weight leads to precipitation at lower pH values and higher degrees of ionization of the polymer functional group. It is notable that the diethylamine series is more sensitive to molecular weight than the diisopropylamine series, which seems to approach a limiting minimum pH value for precipitation. This result may be due to the greater hydrophobicity of the diisopropylamine group as opposed to the diethylamine, which would lead to a lower degree of solubility of the amine side chain and a decreased dependence on molecular weight.

The pH transition observed for both the diisopropylamine and diethylamine functionalized polymers can be utilized for the design of a pH responsive drug carrier in which the responsive PPLG block would be the interior, pH responsive block of a micellar system. To determine if the precipitation pH could be tuned, a 50:50 mixture of diethylamine and diisopropylamine side groups was attached to PPLG (DP = 140) to generate a random

Table 4-2. CMC values for PEG-b-PPLG in water and amine functionalized PEG-b-PPLG in pH 5 and pH 9 buffer

	Solvent	CMC (mg/mL)	CMC (M)
PEG-b-PPLG	Milli-Q water	3.75×10^{-4}	3.74×10^{-8}
Diethylamine	pH 9 buffer	1.01×10^{-2}	7.41×10^{-7}
	pH 5.5 buffer	--	--
Diisopropylamine	pH 9 buffer	3.93×10^{-3}	2.77×10^{-7}
	pH 5.5 buffer	--	--

4.2.4 Secondary Structure.

Circular dichroism (CD) was used to probe the secondary structure of the various polymers as a function of pH. Polymer dissolved at 1 mg/mL was brought down to a pH of 3, titrated to a pH higher than 10, and then immediately titrated back to a pH of 3. A sample CD titration of a secondary amine polypeptide with DP = 75 is shown in Figure 4-6. When initially brought down to a pH of 3, the sample adopts a mixture of α-helix and random coil conformations, as indicated by the minimum at 222 nm, which is characteristic of an α-helix and the second, more negative minimum at 204 nm, which is indicative of a combination of α-helix and random coil. As the sample pH is increased, the sample adopts an all α-helical structure at high pH values (pH > 6.36), as indicated by the minimums at 208 nm and 222 nm.[41] When the pH is decreased stepwise back down to acidic pH, this α-helical structure transitions back to a mixture of α-helix and random coil. The α-helix to random coil transition correlates well with the pKa observed in the polymer titrations. In summary, the α-helix structure appears to correlate with the uncharged polymer backbone; as the backbone becomes charged, the helical structure becomes reversibly disrupted and exhibits some random coil structure.

copolymer. As shown in Figure 4-3, the copolymer precipitation pH (dotted-gray line) falls between the precipitation pH values observed for the diethylamine and diisopropylamine substituted PPLG (DP = 140), indicating that the pH responsiveness of the amine substitute PPLG block can be fine tuned by changing the ratio of side groups. One could also envision using this strategy to incorporated side groups that will improve the loading of a specific drug or increase polymer-gene complexation efficiency.

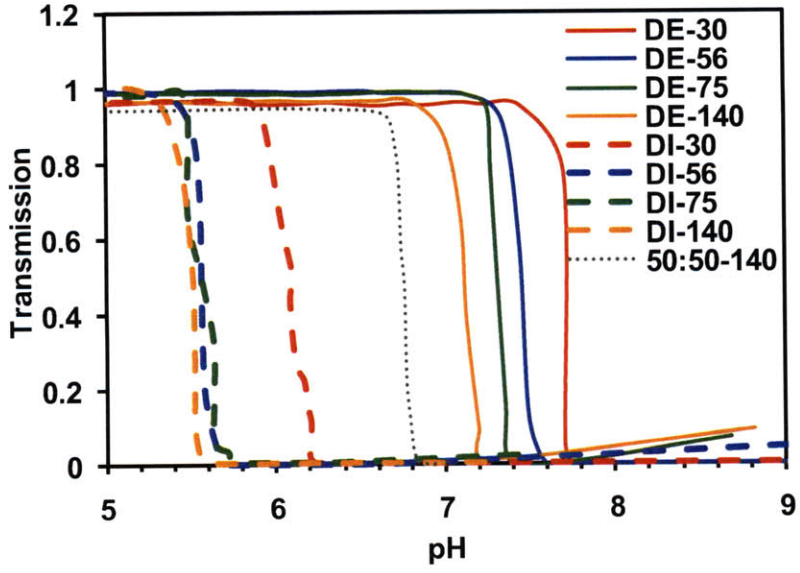

Figure 4-3. Transmission as a function of pH for all diethylamine and diisopropylamine functionalized polymers. Diethylamine is abbreviated DE and diisopropylamine is abbreviated DI.

The buffering and the precipitation behavior was found to be fully reversible, as indicated by reverse titrations that were performed on all polymers (reverse titrations can be found in the supporting information, Figure 4-23). For the completely water soluble primary, secondary, and dimethyl polymers, the reverse titration curve has the same shape as the original titration with no signs of hysteresis. For tertiary amine polymers that precipitated out of solution, hysteresis was often observed for the larger degrees of polymerization, such that the pH value for which the

polymers re-dissolved was often lower than the value observed for precipitation. For the shortest degree of polymerization (DP = 30), the polymers returned to solution at nearly the same pH as when the precipitation was initially observed (Figure 4-4).

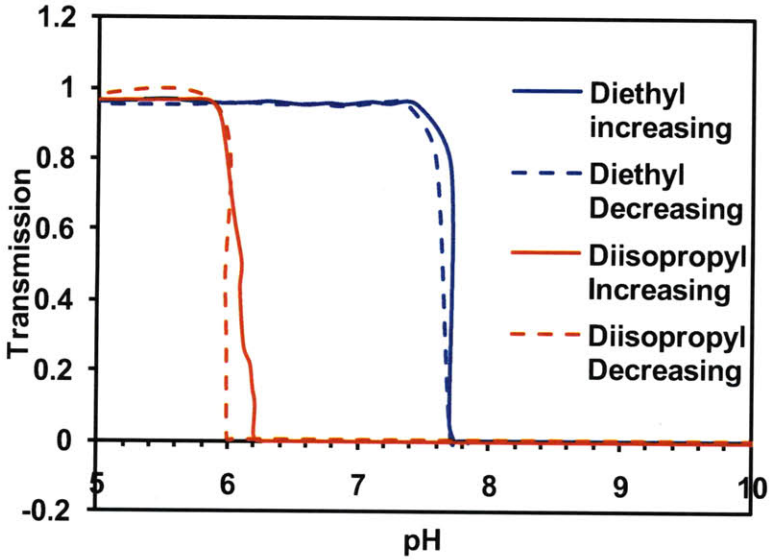

Figure 4-4. Transmission as a function of increasing and decreasing pH for diethylamine and diisopropylamine with DP = 30.

4.2.3 Functionalized PEG-b-PPLG Self-Assembly.

The self assembly of PEG-b-PPLG functionalized with diethylamine and diisopropylamine was studied as a function of pH. The critical micelle concentration (CMC) was determined for PEG-b-PPLG in water and amine functionalized PEG-b-PPLG in buffer solutions at pH 9 and pH 5.5. The CMC was determined by fluorometry using a pyrene probe. A representative example of the diisopropylamine functionalized PEG-b-PPLG is show in Figure 5 (diethylamine substituted PEG-b-PPLG can be found in the supporting information, Figure 4-24). As shown in Figure 5A, there is a clear break in the emission ratio indicating a CMC for the amine functionalized PEG-b-PPLG in pH 9 buffer. In pH 5.5 buffer, no break in emission

ratio was observed for the functionalized polymer indicating that these macromolecules do not self-assemble at all at this acidic pH but remain completely soluble in water. The observed CMC values for all diblock polymers tested (Table 5-1) are of the same order of magnitude of PEG-b-PBLA[15] and are several orders of magnitude lower than Pluronic micelle CMC values.[40] To further verify that the self-assembled structures were micelles, AFM was performed on diethylamine and diisopropylamine substituted PEG-b-PPLG cast from a water solution adjusted with 0.1M NaOH to pH~9. Spherical micelles were observed for the amine substituted PEG-b-PPLG; Figure 5B shows an AFM image of the diisopropylamine functionalized diblock copolymer. The micelles are thus able to form at moderate to high pH but become completely destabilized at low pH, making them of interest for drug release in which a pH triggered rapid disassembly of drug carrier can be designed to take place within acidic compartments to release a drug.

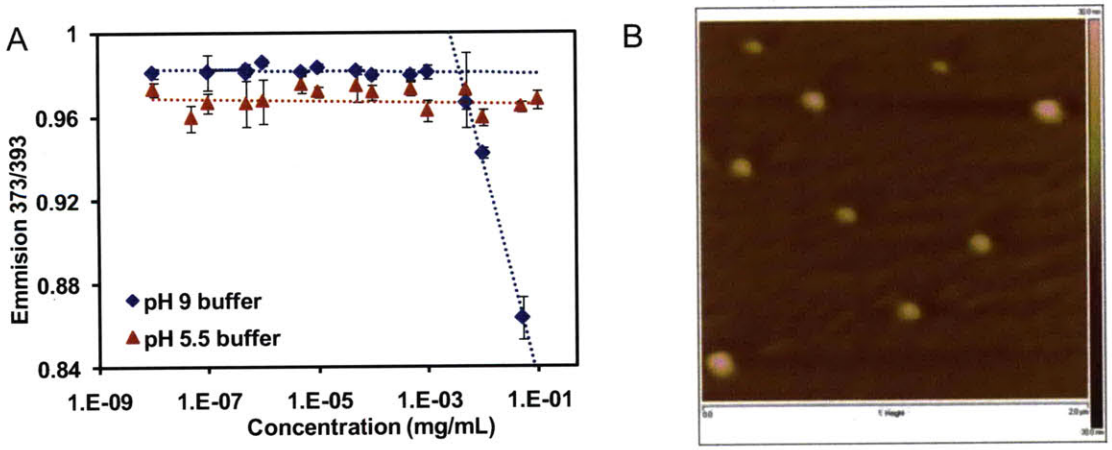

Figure 4-5. CMC determination by fluorometry using a pyrene probe for A) diisopropylamine substituted PEG-b-PPLG in pH 5.5 and 9 buffer and B) AFM image of diisopropylamine substituted PEG-b-PPLG at pH 8.88. The AFM images are 2 by 2 μm with a height range from -30 μm to 30 μm.

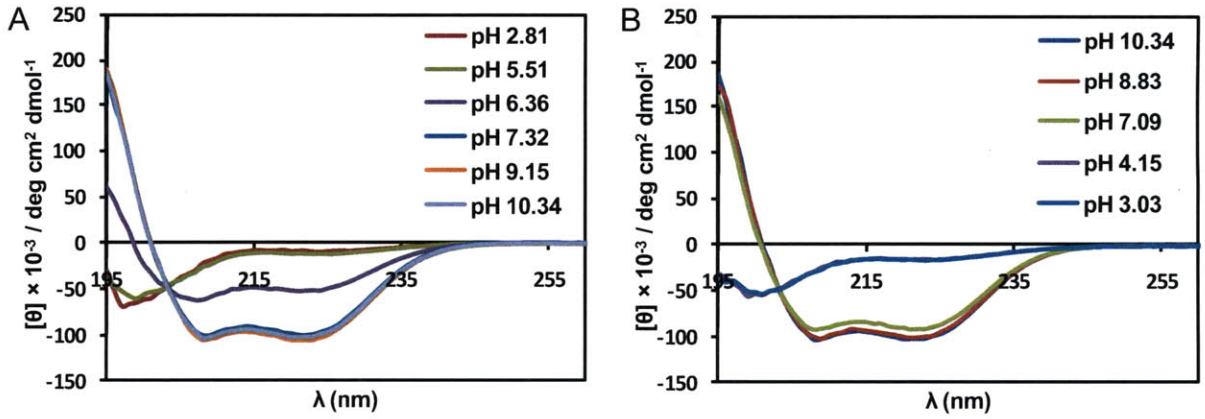

Figure 4-6. A) Increasing pH CD titrations and B) decreasing pH CD titrations for secondary amine, DP = 75

4.2.5 Impact of pH on Side Chain Hydrolysis.

The functional groups introduced along the PPLG backbone are esters that can undergo hydrolysis under basic conditions, yielding the loss of the amino side group and the introduction of the carboxylate anion, thus introducing negative charge to the polyelectrolyte backbone. Slow or moderate changes in the polypeptide backbone may be of interest for drug delivery, gene delivery, tissue engineering, and coating applications.[22, 34, 42, 43] Specifically, for systemic use, positively charged polymers such as poly(L-lysine) and poly(ethylene imine) often exhibit cytotoxicity.[33] The introduction of a mechanism that eliminates the multivalent positive charge and transforms the polymer into the natural poly(γ-glutamic acid), which is biodegradable, enhances the long-term biocompatibility of these polymers. [32, 33] To determine the side chain ester hydrolysis rate and the change in polymer secondary structure, ^{1}H-NMR and CD measurements were taken at various time points and pH conditions.

For ^{1}H-NMR, polymer samples (PPLG DP = 75 with secondary amine and PEG-b-PPLG with diethylamine and diisopropylamine), were dissolved in various pH buffers to a

concentration of 0.5-1 mg/mL and left to hydrolyze at room temperature. At various time points, samples were freeze dried, concentrated in D_2O, acidified with trifluoroacetic acid to stop any additional hydrolysis from occurring, and analyzed by ^{1}H-NMR. The amount of ester hydrolyzed was determined by observing the reduction in the triazole peak from the ester side chain (8.15 ppm) and the appearance of new triazole peak from the alcohol side chain byproduct (8.07 ppm). A sample ^{1}H-NMR for PEG-b-PPLG functionalized with diethylamine hydrolyzed at pH 9 is shown in Figure 4-7. The peak integration for the triazole ring was used to calculate the percentage of hydrolysis of the ester side chain; representative ester hydrolysis plots are shown in Figure 4-8. For all polymers, the rate of ester hydrolysis was highest at pH 11 and was increasingly slower as the pH was decreased. For example, in all cases complete hydrolysis was observed at pH 11 (at 2 days for the secondary amine and diethylamine and 11 days for the diisopropylamine), but at pH 5.5 after 15 days, all samples were less than 2% hydrolyzed. The rate of hydrolysis at pH 7.4, 9, and 11 was fastest for PPLG functionalized with secondary amine and slowest for PEG-b-PPLG functionalized with diisopropylamine. For the diblock polymers, the polypeptide is encapsulated as the inner core of a micelle, and is partially protected from hydrolysis, thus greatly slowing the rate of hydrolysis. The slower hydrolysis of the diisopropylamine is a likely result of the increased hydrophobicity of the diisopropylamine, slowing the rate of hydrolysis.

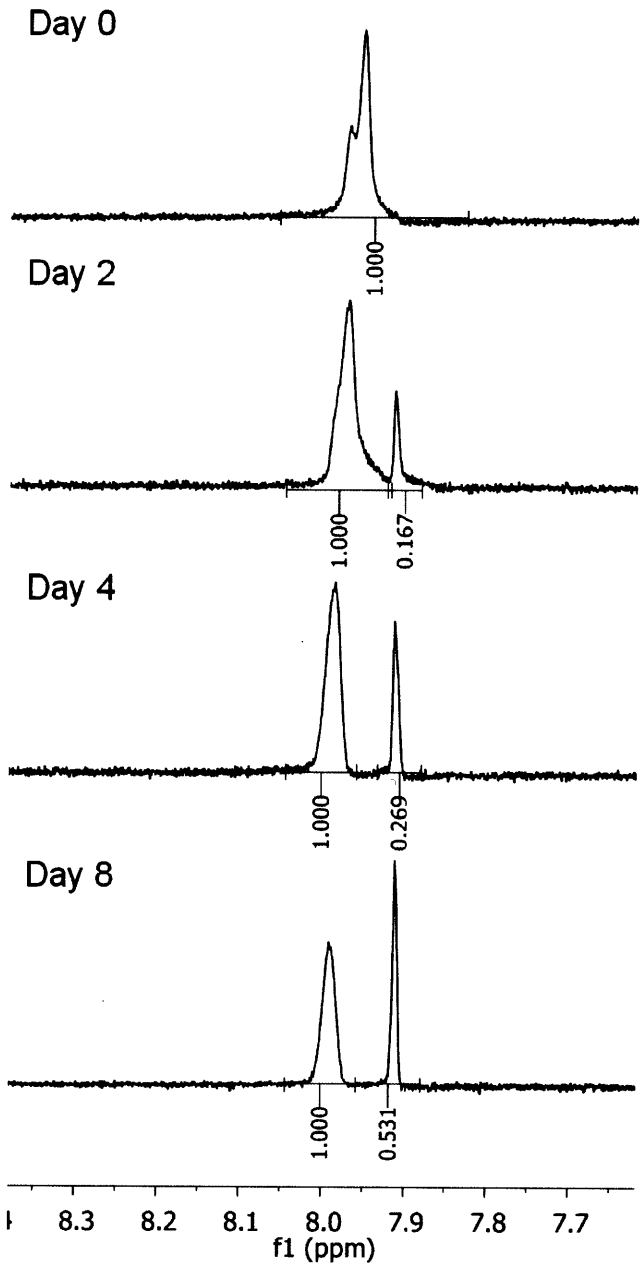

Figure 4-7. ^{1}H-NMR for PEG-b-PPLG functionalized with diethylamine hydrolyzed at pH 9 at various time points

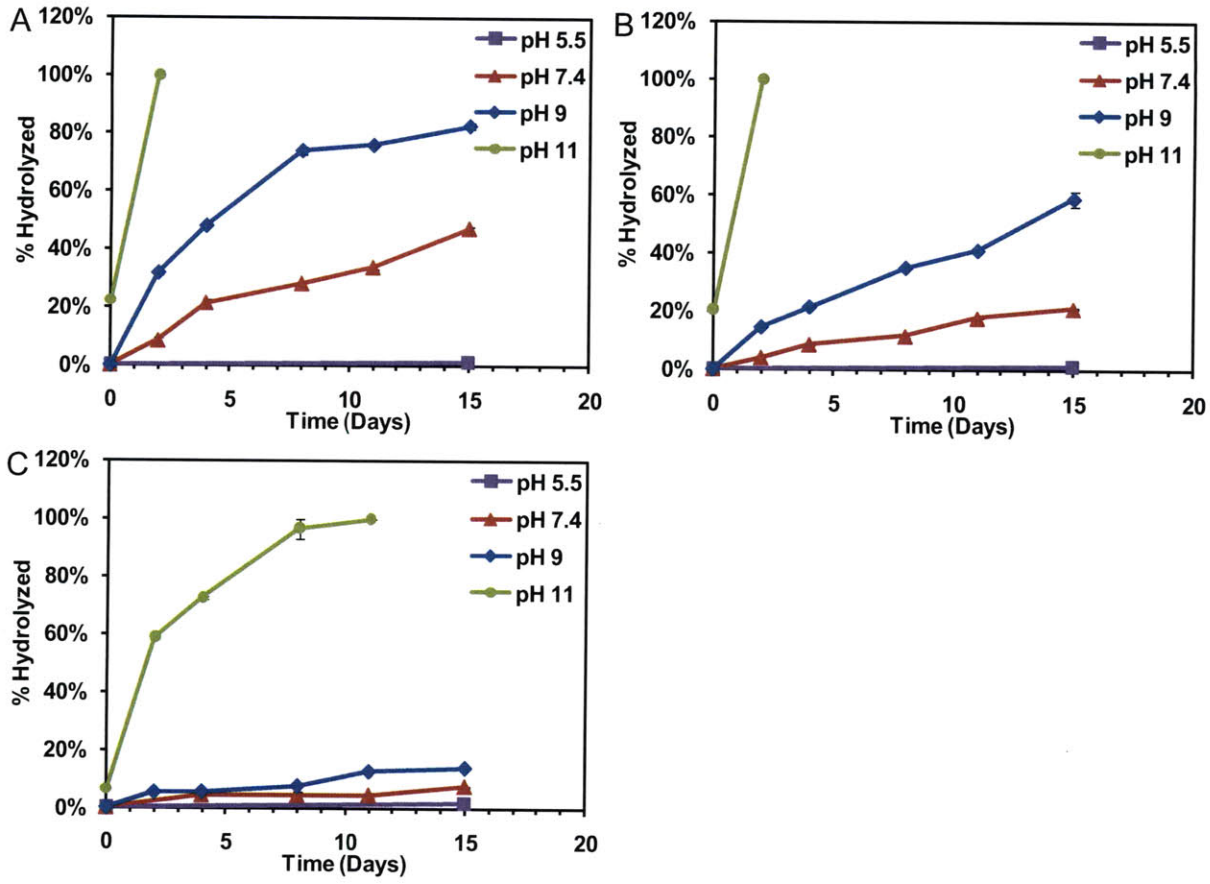

Figure 4-8. A) Percentage of ester side chains hydrolyzed as a function of time for PPLG (DP = 75) functionalized with secondary amine, B) PEG-b-PPLG functionalized with diethylamine, and C) PEG-b-PPLG functionalized with diisopropylamine.

When the polyamide backbone, which maintains an α-helical structure when at equilibrium at all pH conditions investigated (pH 7.4, 9, and 11), undergoes hydrolysis, a glutamic acid residue is generated. Poly(γ-glutamic acid), like poly(L-lysine), maintains an α-helix in the uncharged state, and is a random coil in the charged state;[44] thus as hydrolysis occurs at more basic conditions we observe the loss of the α-helical polymer structure (Figure 4-9A). CD was used to observe the change in polymer secondary structure at pH 7.4, 9, and 11 as a function of time and hydrolysis of the ester side chains. In Figure 4-9, the value observed at 222 nm is plotted for various pH values as a function of time for PPLG (DP = 75) functionalized with

a secondary amine and PEG-b-PPLG functionalized with diethylamine and diisopropylamine. At 222 nm, a shift from a strong negative value towards a small positive value is indicative of a secondary structure shift, in this case, a shift from an α-helix to a random coil (representative full spectra and plots for PPLG functionalized with secondary amine at pH 7.4 and pH 9 can be found in the supporting information, Figure 4-25). For PPLG (DP = 75) functionalized with secondary amine (Figure 4-9B), the polymer adopts a random coil after 1 day (24 hours) in pH 11 buffer solution, at pH 9, the polymer gradually adopts a random coil over several days, and at pH 7.4 the polymer primarily maintains an α-helical structure for multiple days. When compared to the ^{1}H-NMR data, at pH 11, the ester side chains have completely hydrolyzed in two days, leaving poly(γ-glutamic acid) which is in a random coil conformation. For pH 9, at day 4, the polymer is 50% hydrolyzed, and the polymer structure is nearly all random coil. This observation indicates that not all the ester side chains need to be hydrolyzed for the α-helix to be disrupted. Similar CD trends were observed for PPLG (DP = 75) functionalized with a primary amine and dimethylpropanamine (Supporting Information Figure 4-26, dimethylethanamine was not tested). As shown in Figure 4-9B, the block copolymer PEG-b-PPLG functionalized with a diethylamine follows a very similar trend, only at a slower rate due to the decreased rate of ester hydrolysis. For PPLG functionalized with diisopropylamine, minimal hydrolysis and therefore minimal change in structure was observed at pH 7.4 and pH 9. At pH 11, a conformational change is observed, but is much slower than that of the homopolymers and the diethylamine functionalized diblock copolymer because of the slower rate of ester hydrolysis. In summary, as more glutamic residues are generated on the polymer backbone, the secondary structure changes from α-helix to random coil.

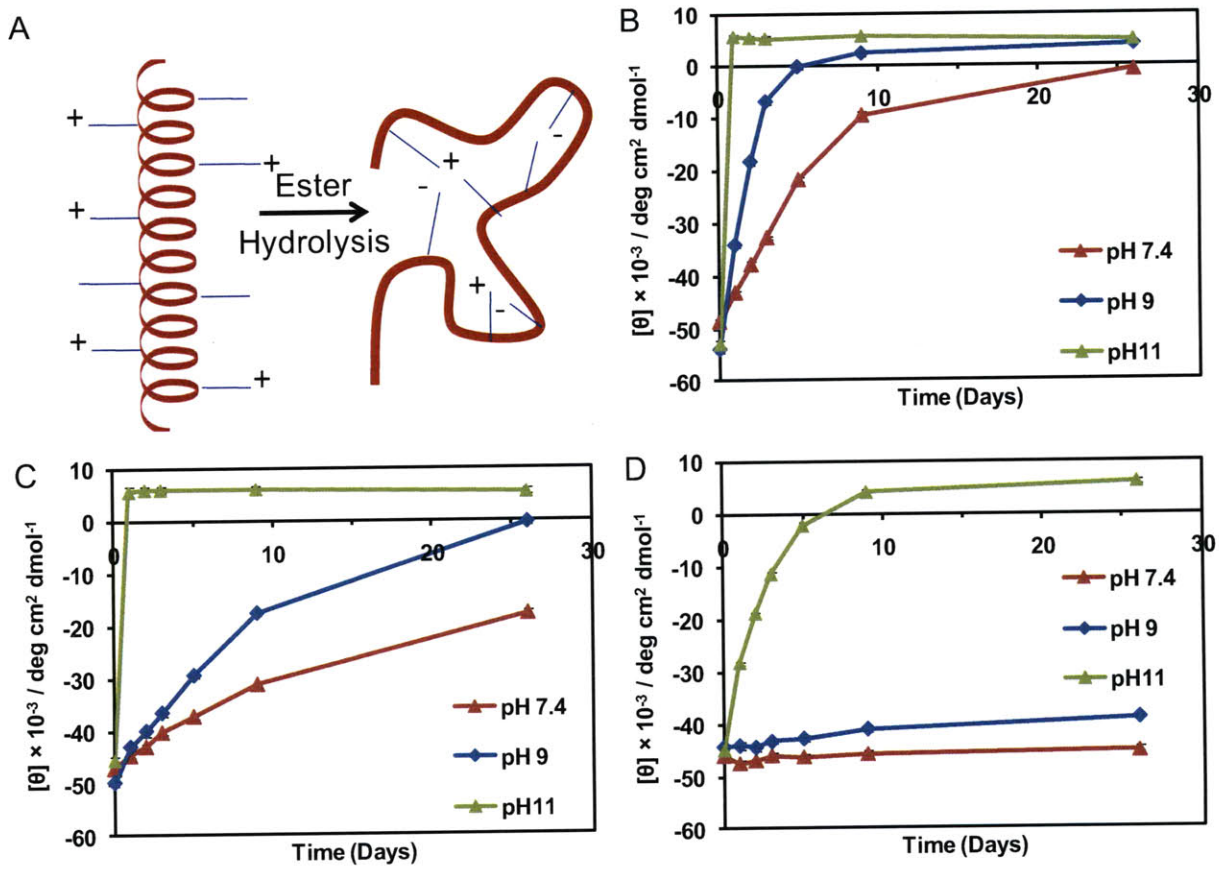

Figure 4-9. A) Schematic of polypeptide backbone conformational change as the ester side chains are hydrolyzed B) Value observed at 222 nm at various pH values as a function of time for (DP = 75) functionalized with secondary amine, C) value observed at 222 nm at various pH values as a function of time for PEG-b-PPLG functionalized with diethylamine, and D) value observed at 222 nm at various pH values as a function of time for PEG-b-PPLG functionalized with diisopropylamine. The error bars are not visible because they overlap with the points.

4.2.6 siRNA complexation studies

Studies have been performed to determine if the amine functionalized homopolymers complex siRNA into protective polyplexes. Polymers were mixed with siRNA at various PPLG polymer to siRNA charge ratios (N/P) ranging from 1:1 to 25:1 in either sodium acetate buffer (pH 5.5) or PBS (pH 7.4). Ribogreen was used to determine the complexation efficiency of each polymer at the various ratios, shown in Figure 4-10. As shown in Figure 4-10A and C, all amine

functionalized PPLG homopolymers prevent dye access to more than 90% of siRNA at charge ratios above 4:1 in sodium acetate. Additionally PPLGs with primary amine substituents are able to completely complex siRNA at a charge ratio that is two-fold lower, indicating the strength of primary amines for complexation. At the higher pH of PBS (7.4), fewer amines are charged, particularly in the case of the dimethylethanamine, diethylamine, and diisopropylamine substituents, leading to looser complexes and greater dye access. This manifest itself both at low polymer:siRNA ratios for all of the polymers, and most noticeably for the dimethylethanamine, diethylamine, and diisopropylamine PPLGs (see Figure 4-10B and D). While these tertiary amine substituents may be useful for stimulating endosomal escape, the copolymers with primary and secondary amines are more likely to exhibit properties that enable full encapsulation of siRNA and buffering effects *in vivo*. AFM was used to image the polyplexes. Representative AFM images for PPLG (DP = 75 and DP = 140) substituted with dimethylethanamine are shown in Figure 4-11. The particles range in size from 75 nm to 150 nm in diameter. Similar results were observed for the diblock polymers when complexed in sodium acetate buffer, as shown in Figure 4-12 (only select diblock polymers were tested).

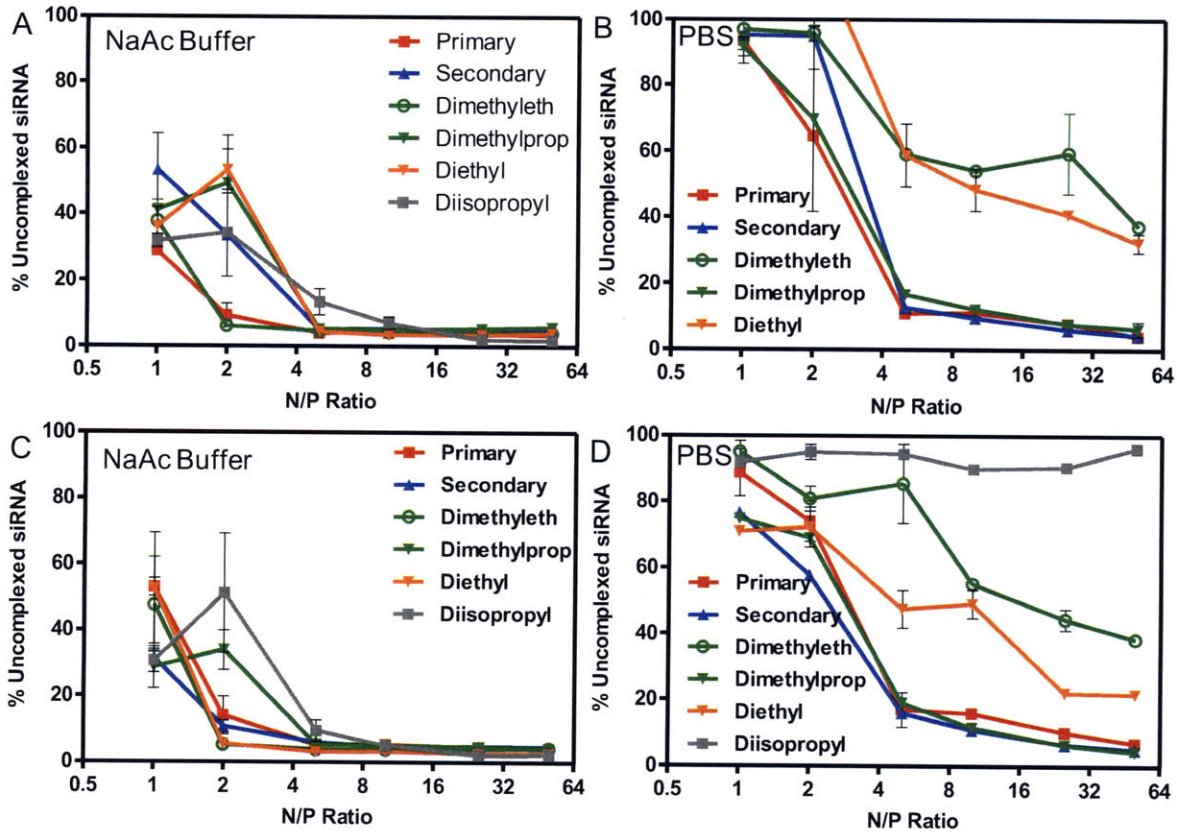

Figure 4-10. Percentage of uncomplexed siRNA as a function of siRNA:Polymer (w/w) ratio for each amine substituted PPLG for degree of polymerization 140 (A,B) and 75 (C,D). Polyplexes were formed in either sodium acetate buffer (A,C) or PBS (B,D). The DP140 diisopropylamine sample was insoluble in PBS.

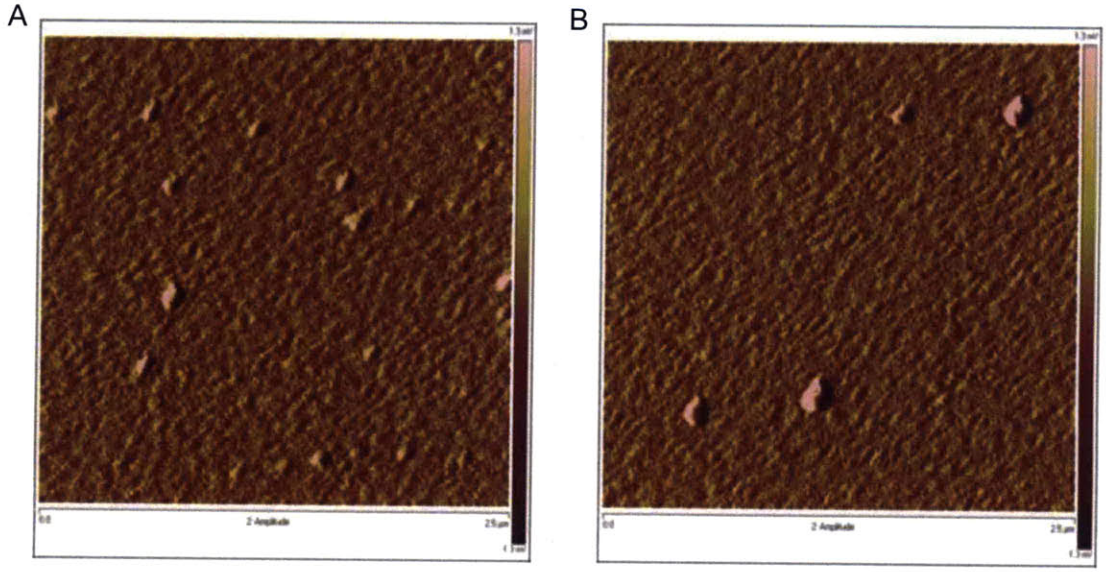

Figure 4-11. Amplitude AFM images (2 μm by 2 μm with a z scale of 1.5 nm) of polyplexes formed with dimethylethanamine PPLG with degree of polymerization of A) 75 and B) 140.

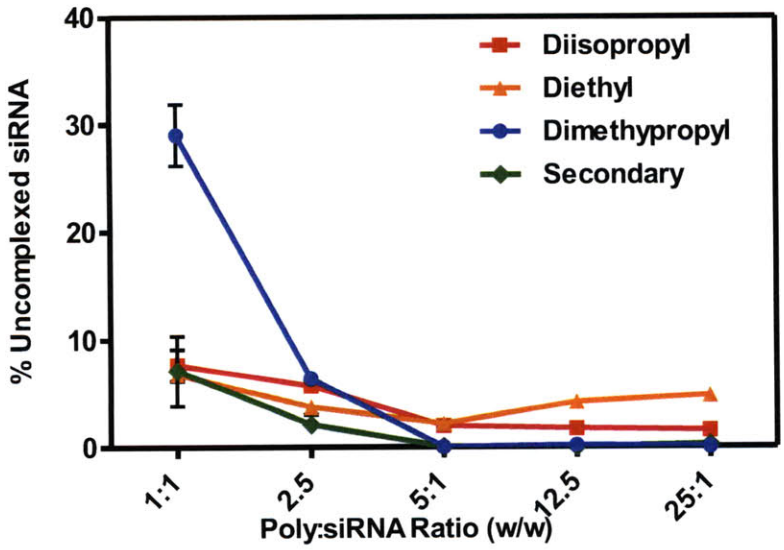

Figure 4-12. Percentage of uncomplexed siRNA as a function of siRNA:Amine Polymer (w/w) ratio for each amine substituted PEG-b-PPLG

Polyplexes can be disrupted by the addition of a competing polyanion, such as heparin. In Figure 4-13A, PPLGs (DP = 140) with primary amine substituents were complexed at low (5:1) and high (25:1) polymer: siRNA ratios (N/P) in either sodium acetate or PBS, along with PEI and Lipofectamine 2000 as controls. As anticipated, relatively low levels of heparin were required to dissociate PPLG complexes formed at 5:1 as compared with those complexes formed at the 25:1 N/P ratio. PPLG complexes formed in PBS were more easily disrupted than those formed at low pH, most likely because those formed at low pH contained more highly charged amines, and were thus more tightly complexed. Figure 4-13B demonstrates this concept with different amine substituents. In the DP75 polymers (red), the tertiary amine in the dimethylpropanamine group forms a looser polyplex and is disrupted more readily than the secondary and primary amines. However, for DP140, the dimethylpropanamine polyplexes begin to dissociate with the same amount of added heparin as the primary and secondary polyplexes, indicating that molecular weight is also a factor in polyplex stability. In summary,

the siRNA complexation behavior of these systems is tunable, and can be altered through the introduction of different buffering amine functionalities, molecular weight and pH conditions of complexation.

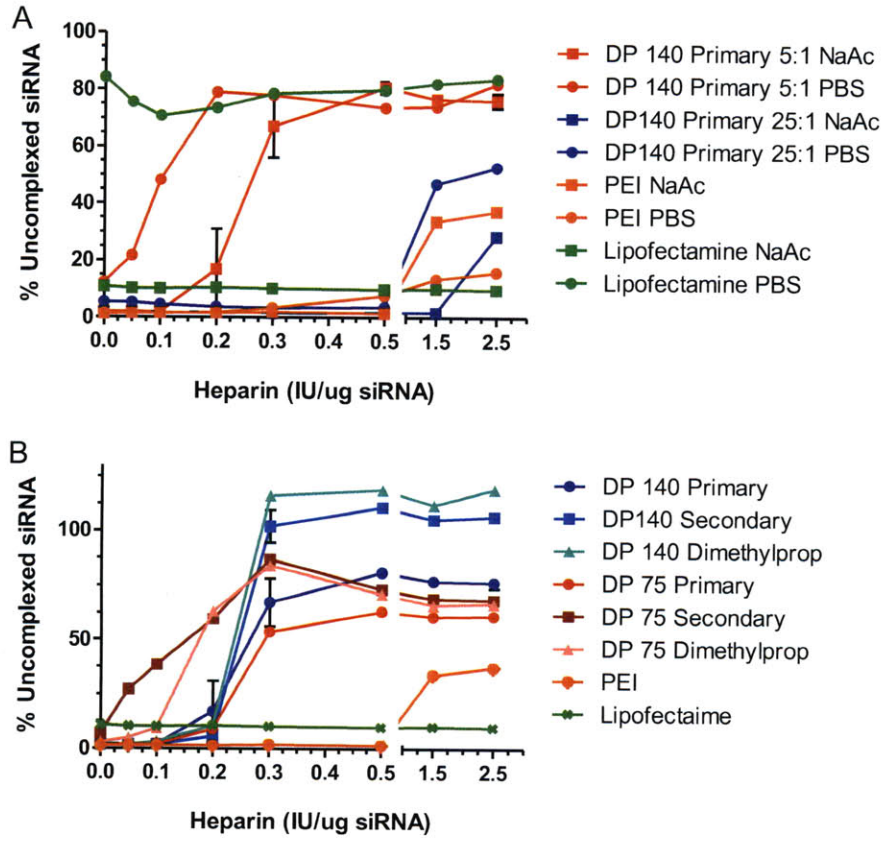

Figure 4-13. Percentage of uncomplexed siRNA as a function of added heparin for various complexation conditions. A) Complexes were formed in pH 5.5 Sodium Acetate buffer (squares) or PBS (circles) at two different polymer:siRNA ratios (w/w). B) PPLGs with primary (circle), secondary (square), or dimethylpropanamine (triangle) substitutions were complexed in sodium acetate buffer prior to dissociation with heparin.

4.2.7 Toxicity of polyplexes

As a measure of biocompatibility, we determined the viability of HeLa cells when exposed to the polyplexes at the concentrations used for transfection studies using an MTT assay. The MTT assay measures the effect of the polyplexes on cell metabolism and growth, and

it is a common measure of toxicity. As shown in Figure 4-14, all polyplexes formed were relatively non cytotoxic at an siRNA dose of 50 ng/well, indicating that these polyplexes are safe at the dosing concentration.

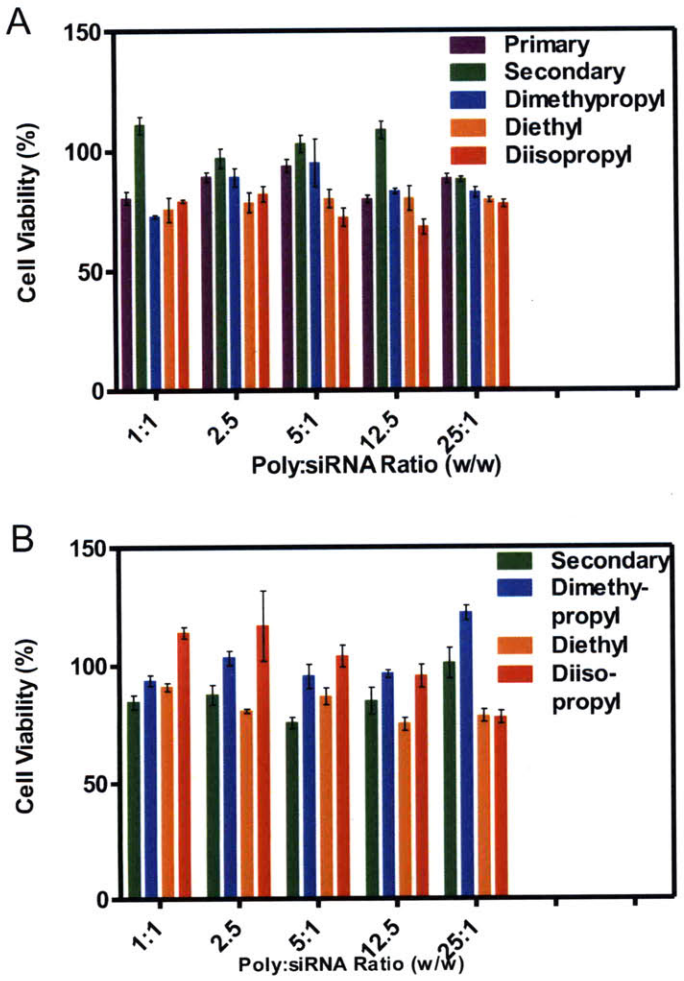

Figure 4-14. MTT assay for cellular toxicity of homopolymers (A) and diblock polymers (B) on HeLa cells at an siRNA concentration of 50 ng/well siRNA.

4.2.8 Transfection

Knockdown studies were performed using a Dual-Glo Luciferase Assay on homopolymers and diblock polymers to determine if the siRNA delivered to cell resulted in transfection. As shown in Figure 4-15, the lipofectamine control is reducing Luciferase

expression, indicating that the assay is viable. In both the diblock and homopolymers, Luciferase expression is still at around 100% indicating that the polyplexes are not transfecting. To determine the rate limiting step in transfection of these polyplexes, additional studies were performed to determine if the polyplexes were being taken up by the cells and escaping the endosome.

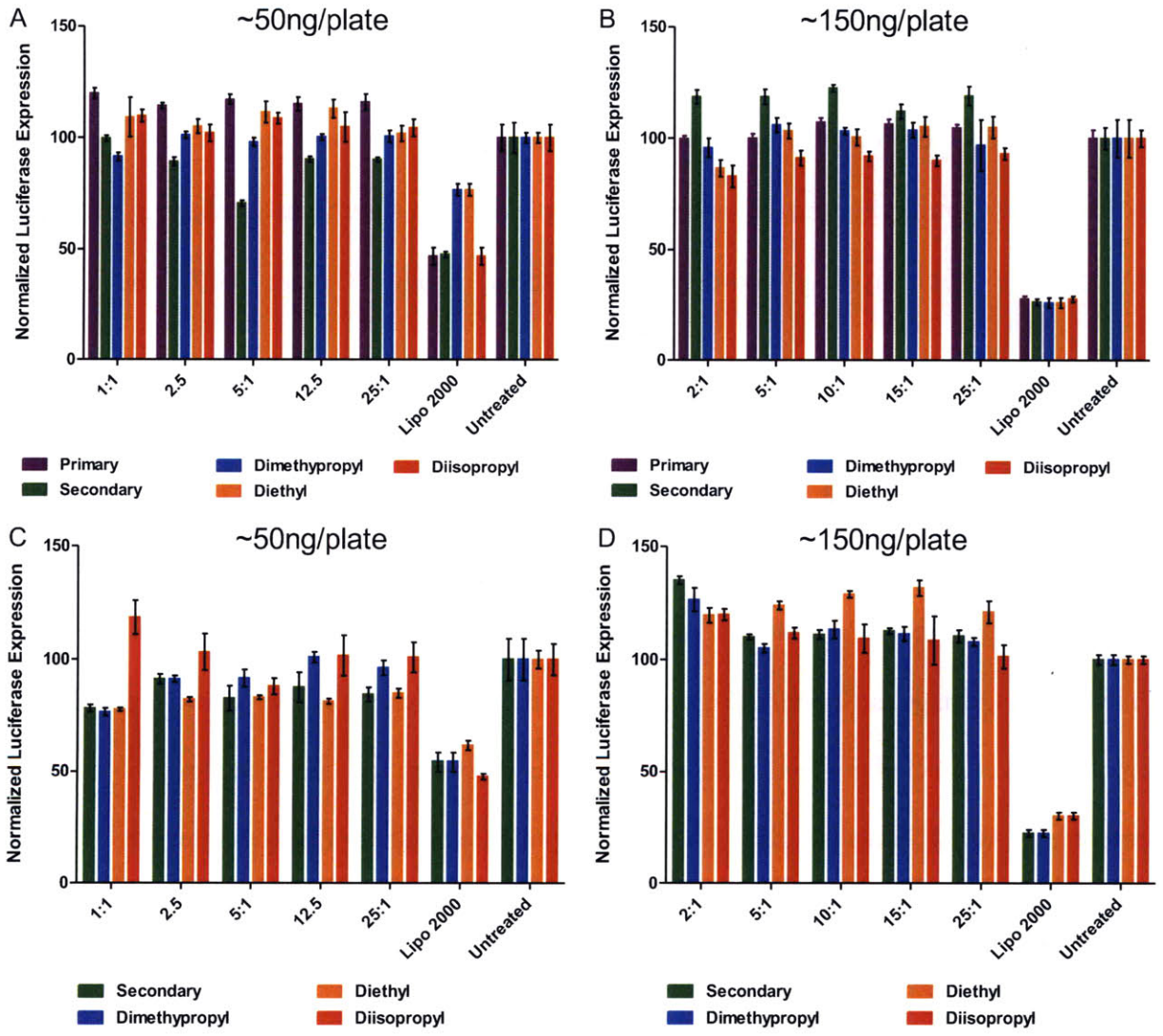

Figure 4-15. Transfection studies at 50 ng/well (A,C) and 150 ng/well (B,C) for homopolymers (A,B) and diblock polymers (C,D)

4.2.9 Cell Uptake

Cellular uptake studies were performed on amine functionalized PPLG (DP = 75) and PEG-b-PPLG functionalized with diethylamine. Labeled siRNA was complexed with the polymers at N/P ratios of 5:1 and 25:1 and flow cytometry was used to determine if cells were taking up the polyplexes (Figure 4-16). When comparing the mean fluorescence intensity of the homopolymers at a 5:1 ratio to the Lipofectamine control and the naked siRNA, the intensity falls between the two indicating that the additional polymer is aiding in enhancing uptake. At a ratio of 25:1, all the homopolymers except the diisopropylamine have greater uptake than the Lipofectamine control. For the diblock polymer, uptake is not significantly enhanced because of the protective PEG layer. Fluorescent microscope images (Figure 4-17) and confocal microscope images (Figure 4-18) were obtained of the diethylamine polymer. Figure 4-17A is an image of uncomplexed red labeled siRNA uptake in HeLa cells and Figure 4-17B is an image of the uptake of PPLG with diethylamine complexed red labeled siRNA. The increase in red fluorescence (shown in bright spots in the cells near the cell nucleus (blue)) in Figure 4-17B in comparison to Figure 4-17A indicates that the polyplexes enhance cellular uptake of the siRNA. In the confocal image, at 0 hours (Figure 4-18A), the polyplexes (bright yellow-green because the polymer was labeled in green and the siRNA was labeled in red) are seen along the outer cell membrane. At 24 hours (Figure 4-18B), the polyplexes are trafficked into the cells into compartments close to the nucleus (blue), as indicated by the bright green spots. These bright punctated spots indicate that the polyplexes may not be escaping the endosome.

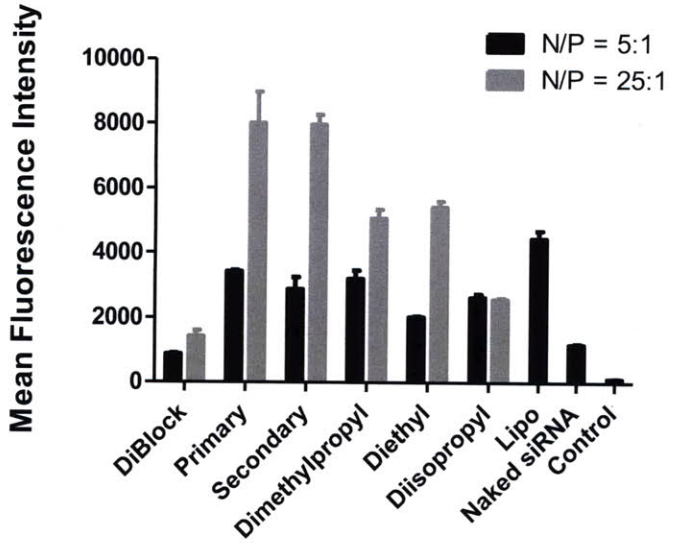

Figure 4-16. Polyplex uptake studies with siRNA:polyplex N/P ratios of 5:1 and 25:1.

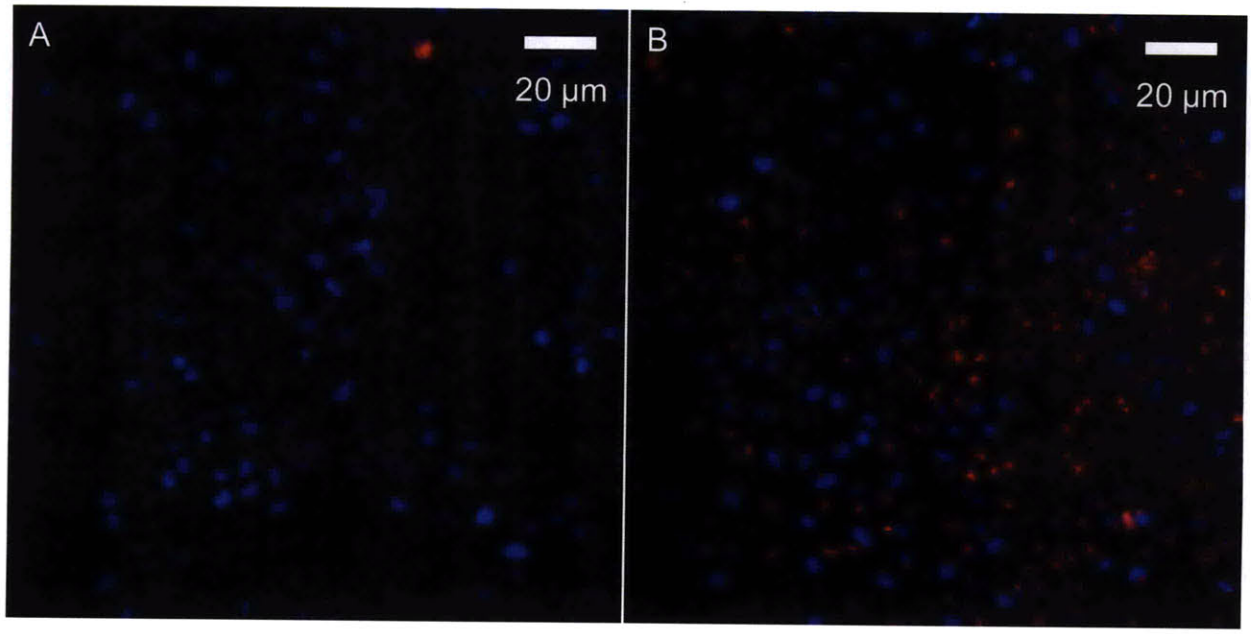

Figure 4-17. Fluorescent microscope images of cell uptake of fluorescently labeled siRNA with A) uncomplexed siRNA and B) complexed siRNA with diethylamine PPLG (DP = 75).

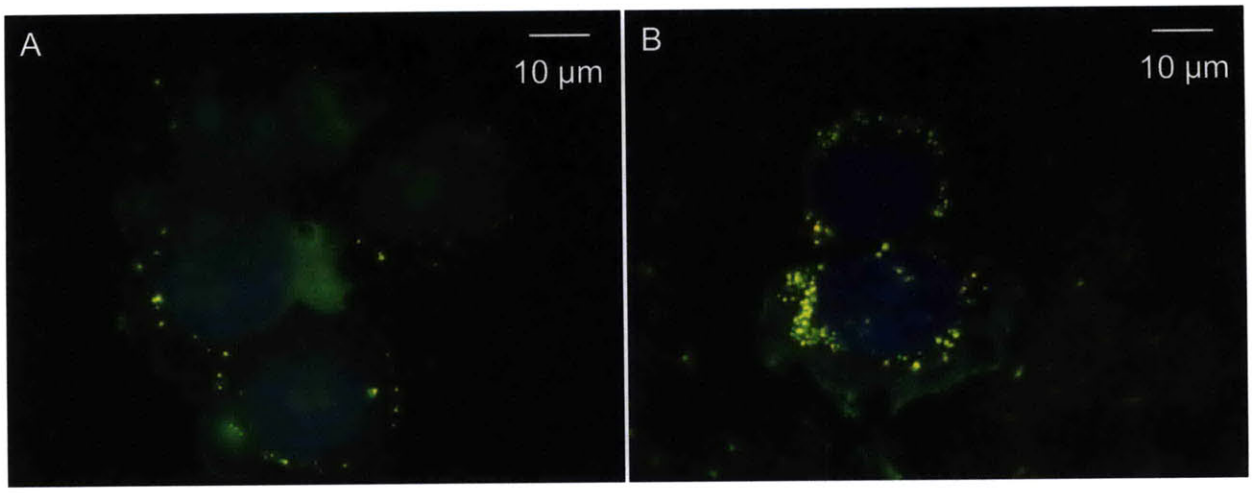

Figure 4-18. Confocal images of red labeled siRNA complexed with green labeled diethylamine PPLG (DP = 75) at A) 1 hour and B) 24 hours.

4.2.10 Endosomal escape

A high throughput endosomal escape assay was conducted on PPLG (DP = 75) with diethylamine to determine the amount of polymer necessary to trigger endosomal escape. From Figure 4-19, at 15 µg/well pure polymer exhibits 70% escape but when the polymer is complexed at a 5:1 ratio, less than 20% of the polymer is escaping the endosome. This result indicates that having free tertiary amine is required for endosomal escape. Furthermore, the free amine required for endosomal escape is significantly larger than the dose typically given to cells. When compared to PEI, the charge density per molecular weight of the polymer is 4 times less than that of the PEI. In order for this system to work, large doses of free polymer are necessary for endosomal escape or the dose size must be significantly increased. Another strategy could be to mix different side groups. Some that are specifically designed to complex the genetic material and others that are specifically designed for endosomal buffering and escape.

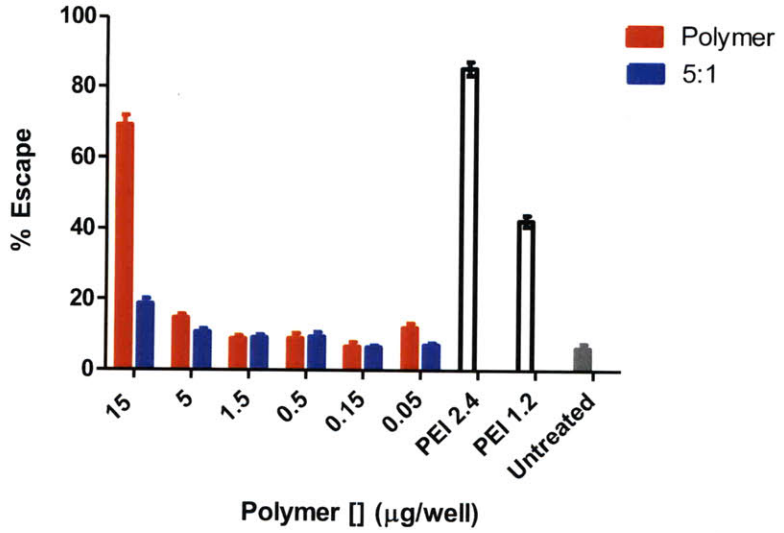

Figure 4-19. Endosomal escape of PPLG (DP = 75) naked polymer and siRNA at a 5:1 N/P ratio

4.2.11 Mixing primary amine and diethylamine click groups

The flexibility of this system allows for easy mixing of side group functionality. We mixed the primary amine side group, which complexes well with siRNA and diethylamine amine side group, which has strong buffering, at a 50:50 ratio to see if combining the two groups decreases Luciferase expression. The polyplexes were formed in either PBS or sodium acetate buffer to determine if the pH of polyplex formation at different N/P ratios effects transfection. Similar to what was observed for the homopolymers, knockdown of Luciferase expression was not observed, as shown in Figure 4-20. This result is most likely a result of the limited amount of charge on the cationic polymer. The amount of tertiary amine could be increased on the backbone and that could possibly improve endosomal buffering. See Chapter 6 for more discussion on this topic.

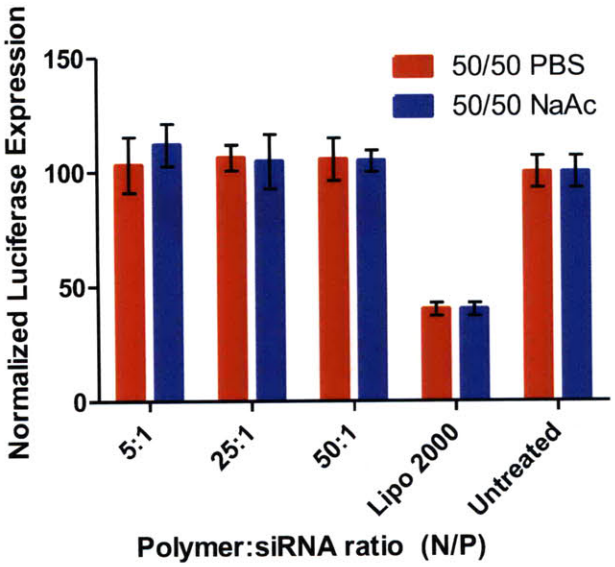

Figure 4-20. Transfection studies at 50 ng/well for PPLG (DP = 140) functionalized with 50:50 primary amine:diethylamine. Complexes were formed in PBS and sodium acetate buffer.

4.3 Conclusion

We have developed a new library of pH responsive polypeptides based on the combination of NCA polymerization and click chemistry. PPLG homopolymers and PEG-b-PPLG block copolymers were substituted with various amine moieties that range in pKa and hydrophobicity and can be tuned for specific interactions and responsive behaviors. We have demonstrated that these new amine-functionalized polypeptides change solubility, or self assemble into micelles for the case of diblock polymers, with degree of ionization and adopt an α-helical structure at biologically relevant pHs. The impact of side chain hydrolysis was also explored to determine the hydrolysis rate as a function of pH and the impact of hydrolysis on polymer side chain conformation. These properties are of interest for a number of applications, here we have performed preliminary experiments that demonstrate that these polymers are strong candidates for drug and gene delivery.

4.4 Supporting information

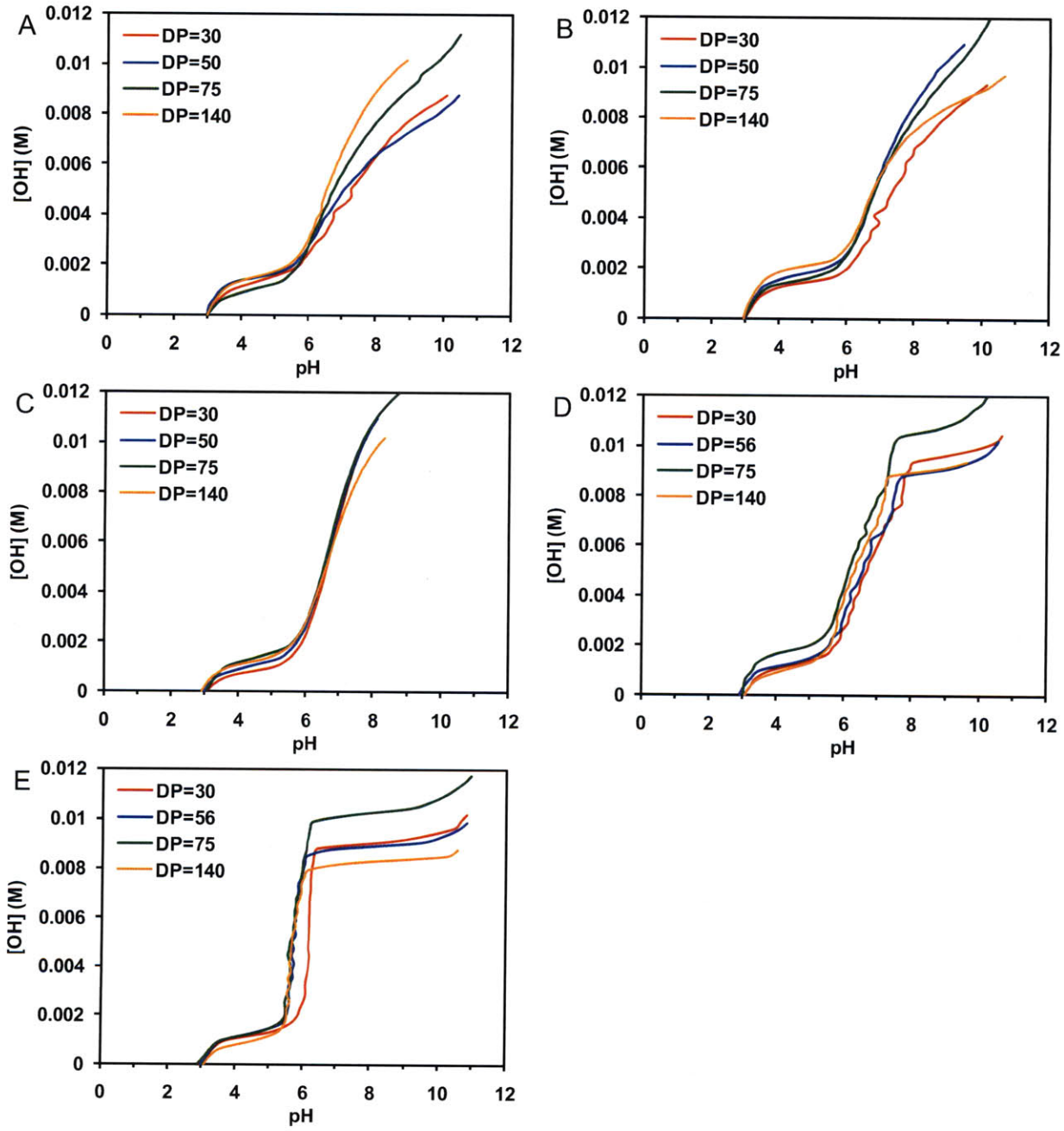

Figure 4-21. Titrations with increasing pH A) primary amine, B) secondary amine, C) dimethylethanamine, D) diethylamine, and E) diisopropylamine.

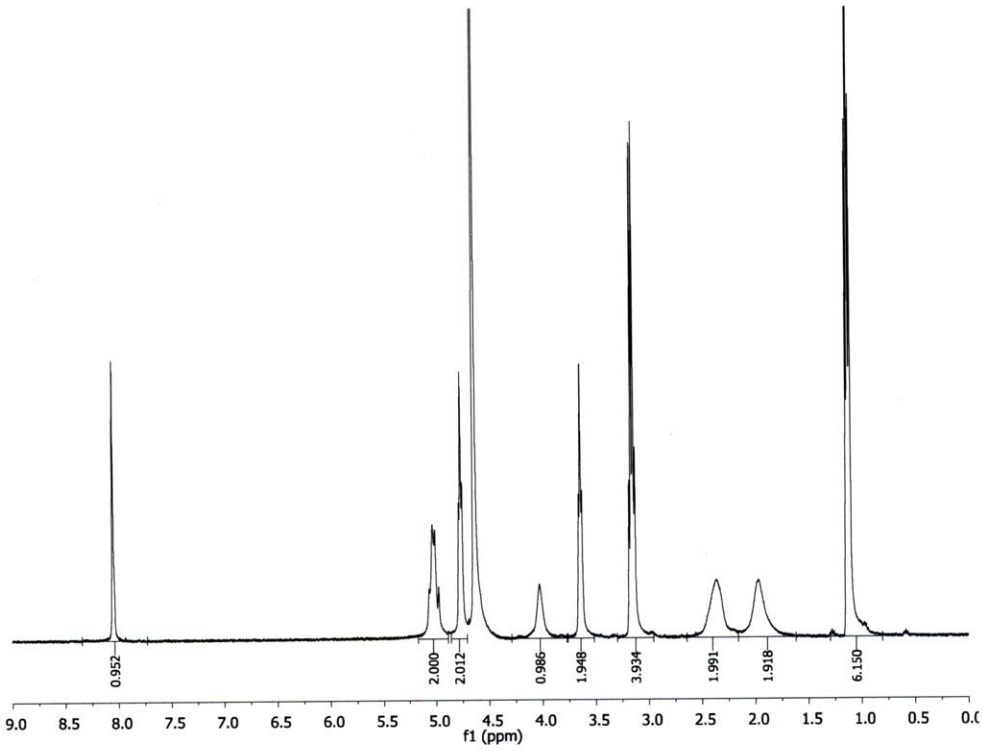

Figure 4-22. PPLG (DP = 75) functionalized with diethylamine in D_2O after titration

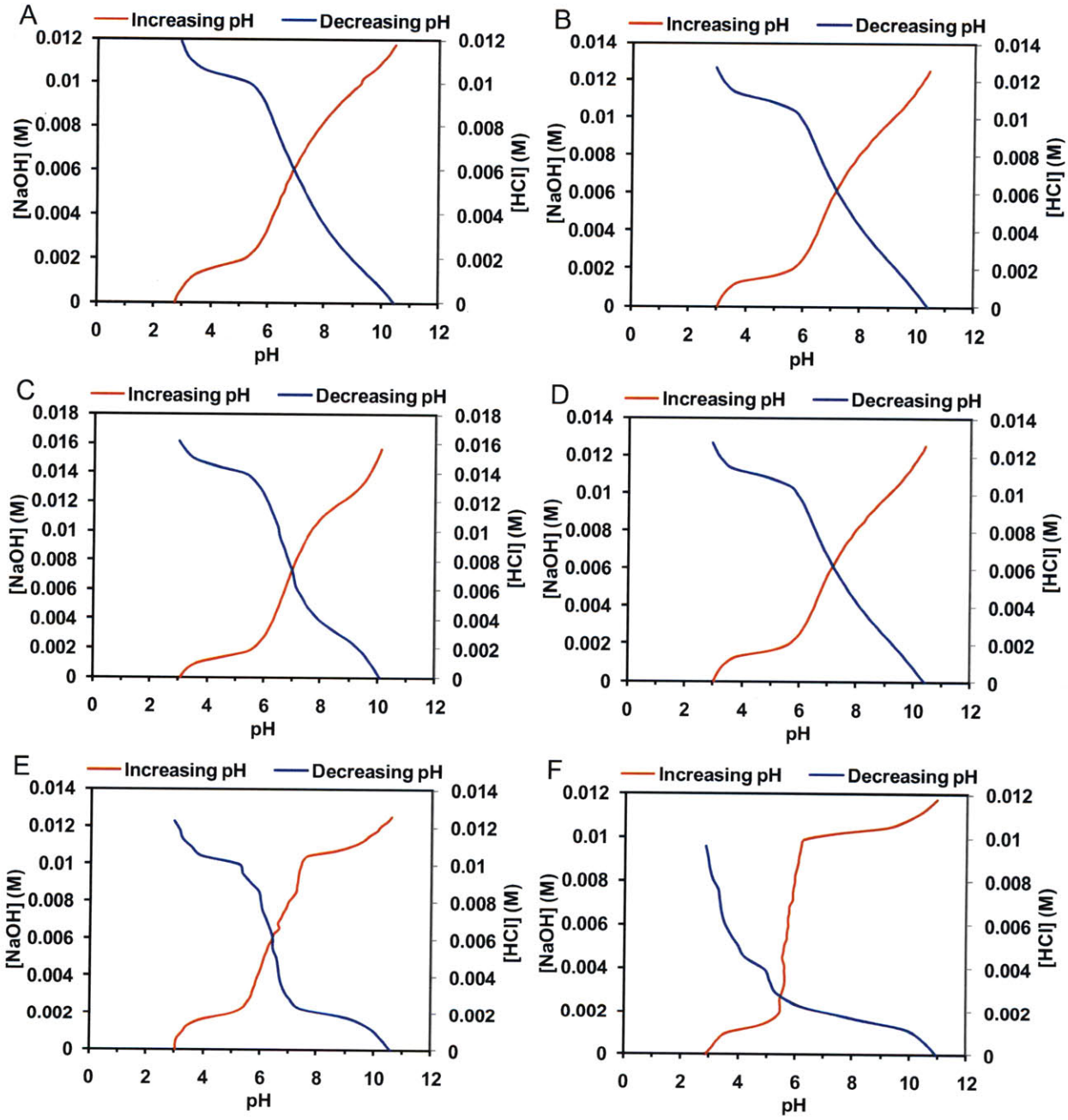

Figure 4-23. Titrations with increasing pH and decreasing pH for PPLG (DP = 75) functionalized with A) primary amine, B) secondary amine, C) dimethylethanamine, D) dimethylpropanamine, E) diethylamine, and F) diisopropylamine.

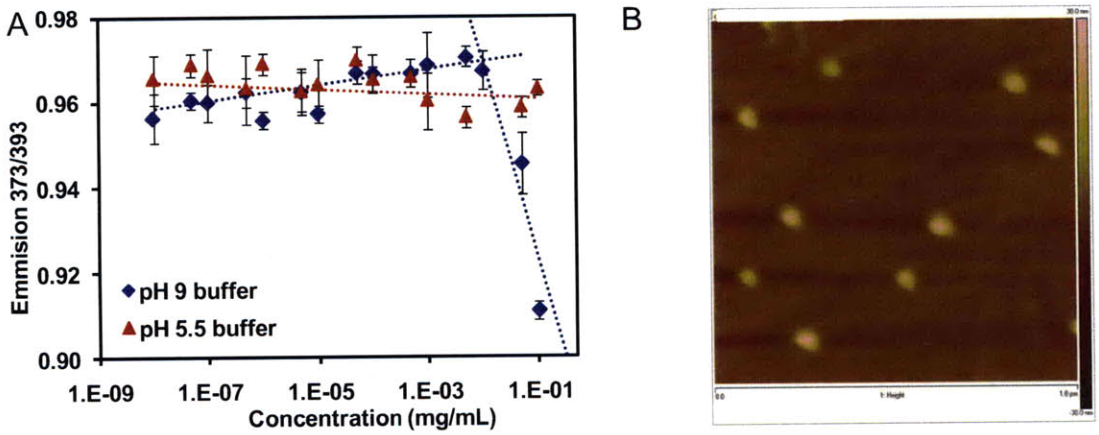

Figure 4-24. A) CMC determination by fluorometry using a pyrene probe for diethylamine substituted PEG-b-PPLG in pH 5.5 and 9 buffer and B) AFM image of diethylamine substituted PEG-b-PPLG at pH 9.21 and The AFM image is 1.8 by 1.8 μm.

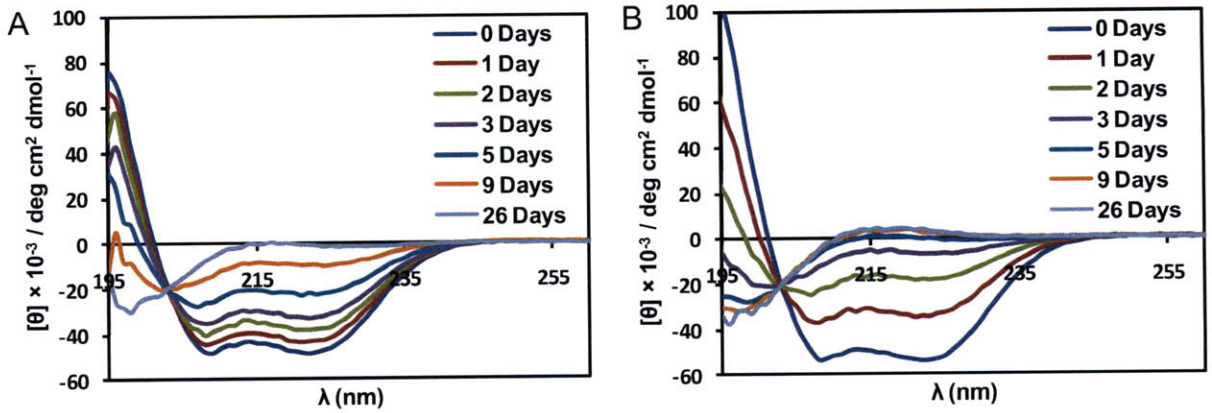

Figure 4-25. CD spectra of PPLG (DP = 75) functionalized with secondary amine taken at various time points at A) pH 7.4 and B) pH 9.

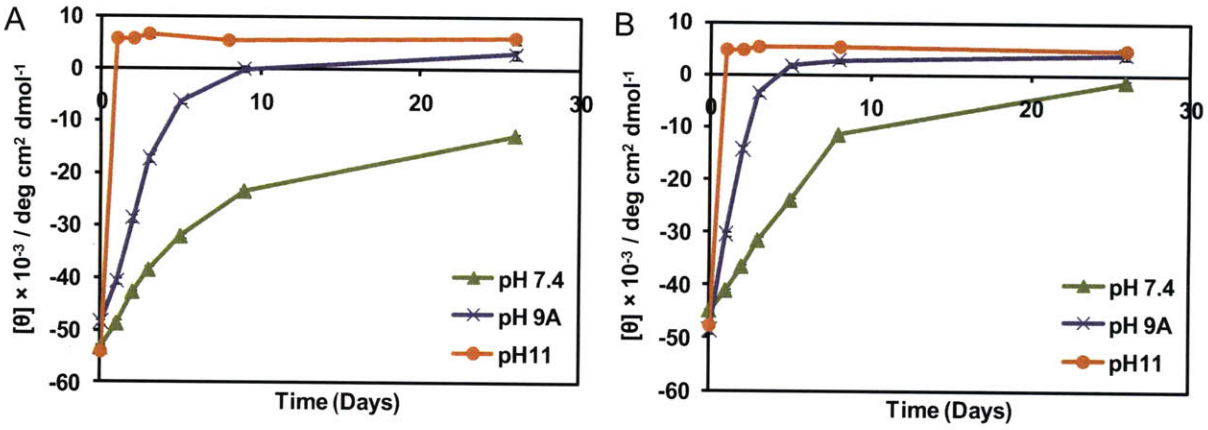

Figure 4-26. A) Value observed at 222 nm at various pH values as a function of time for (DP = 75) functionalized with primary amine and B) Value observed at 222 nm at various pH values as a function of time for (DP = 75) functionalized with dimethylpropanamine.

4.5 References

1. Deming, T. J., Synthetic polypeptides for biomedical applications. *Prog. Polym. Sci.* **2007,** *32* (8-9), 858-875.

2. Deming, T. J., Polypeptide and polypeptide hybrid copolymer synthesis via NCA polymerization. *Peptide Hybrid Polymers* **2006,** *202*, 1-18.

3. Osada, K.; Kataoka, K., Drug and gene delivery based on supramolecular assembly of PEG-polypeptide hybrid block copolymers. In *Peptide Hybrid Polymers*, SPRINGER-VERLAG BERLIN: Berlin, 2006; Vol. 202, pp 113-153.

4. Daly, W. H.; Poche, D.; Negulescu, I. I., Poly(Gamma-Alkyl-Alpha, L-Glutamate)s Derived from Long-Chain Paraffinic Alcohols. *Prog. Polym. Sci.* **1994,** *19* (1), 79-135.

5. Bromley, E. H. C.; Channon, K.; Moutevelis, E.; Woolfson, D. N., Peptide and Protein Building Blocks for Synthetic Biology: From Programming Biomolecules to Self-Organized Biomolecular Systems. *ACS Chemical Biology* **2008,** *3* (1), 38-50.

6. Conn, P. M., *Progress in Molecular Biology and Translational Science*. Elsevier Inc.: London, 2008; Vol. 83, Part 1.

7. Harada, A.; Cammas, S.; Kataoka, K., Stabilized alpha-helix structure of poly(L-lysine)-block-poly(ethylene glycol) in aqueous medium through supramolecular assembly. *Macromolecules* **1996,** *29* (19), 6183-6188.

8. Appel, P.; Yang, J. T., Helix-Coil Transition of Poly-L-Glutamic Acid and Poly-L-Lysine in D_2O. *Biochemistry* **1965,** *4* (7), 1244-1249.

9. Ciferri, A.; Puett, D.; Rajagh, L., Potentiometric Titrations and Helix-Coil Transition of Poly(L-Glutamic Acid) and Poly-L-Lysine in Aqueous Salt Solutions. *Biopolymers* **1968,** *6* (8), 1019-1036.

10. Zimm, B. H.; Bragg, J. K., Theory of the Phase Transition between Helix and Random Coil in Polypeptide Chains. *Journal of Chemical Physics* **1959,** *31* (2), 526-535.

11. Reshetnyak, Y. K.; Andreev, O. A.; Segala, M.; Markin, V. S.; Engelman, D. M., Energetics of peptide (pHLIP) binding to and folding across a lipid bilayer membrane. *Proceedings of the National Academy of Sciences of the United States of America* **2008,** *105* (40), 15340-15345.

12. Zoonens, M.; Reshetnyak, Y. K.; Engelman, D. M., Bilayer interactions of pHLIP, a peptide that can deliver drugs and target tumors. *Biophysical Journal* **2008,** *95* (1), 225-235.

13. Reshetnyak, Y. K.; Andreev, O. A.; Lehnert, U.; Engelman, D. M., Translocation of molecules into cells by pH-dependent insertion of a transmembrane helix. *Proceedings of the National Academy of Sciences of the United States of America* **2006,** *103* (17), 6460-6465.

14. Yokoyama, M.; Kwon, G. S.; Okano, T.; Sakurai, Y.; Seto, T.; Kataoka, K., Preparation of micelle-forming polymer-drug conjugates. *Bioconjugate Chem.* **1992,** *3* (4), 295-301.

15. Kwon, G.; Naito, M.; Yokoyama, M.; Okano, T.; Sakurai, Y.; Kataoka, K., Micelles Based on Ab Block Copolymers of Poly(Ethylene Oxide) and Poly(Beta-Benzyl L-Aspartate). *Langmuir* **1993,** *9* (4), 945-949.

16. Katayose, S.; Kataoka, K., PEG-poly(lysine) block copolymer as a novel type of synthetic gene vector with supramolecular structure. *Advanced Biomaterials in Biomedical Engineering and Drug Delivery Systems* **1996**, 319-320.

17. Takae, S.; Miyata, K.; Oba, M.; Ishii, T.; Nishiyama, N.; Itaka, K.; Yamasaki, Y.; Koyama, H.; Kataoka, K., PEG-detachable polyplex micelles based on disulfide-linked block catiomers as bioresponsive nonviral gene vectors. *J. Am. Chem. Soc.* **2008,** *130* (18), 6001-6009.

18. Miyata, K.; Fukushima, S.; Nishiyama, N.; Yamasaki, Y.; Kataoka, K., PEG-based block catiomers possessing DNA anchoring and endosomal escaping functions to form polyplex micelles with improved stability and high transfection efficacy. *J. Control. Release* **2007,** *122* (3), 252-260.

19. Masago, K.; Itaka, K.; Nishiyama, N.; Chung, U. I.; Kataoka, K., Gene delivery with biocompatible cationic polymer: Pharmacogenomic analysis on cell bioactivity. *Biomaterials* **2007,** *28* (34), 5169-5175.

20. Opanasopit, P.; Yokoyama, M.; Watanabe, M.; Kawano, K.; Maitani, Y.; Okano, T., Block copolymer design for camptothecin incorporation into polymeric micelles for passive tumor targeting. *Pharmaceutical Research* **2004,** *21* (11), 2001-2008.

21. Itaka, K.; Ishii, T.; Hasegawa, Y.; Kataoka, K., Biodegradable polyamino acid-based polycations as safe and effective gene carrier minimizing cumulative toxicity. *Biomaterials* **2010,** *31* (13), 3707-3714.

22. Chen, S. F.; Cao, Z. Q.; Jiang, S. Y., Ultra-low fouling peptide surfaces derived from natural amino acids. *Biomaterials* **2009,** *30* (29), 5892-5896.

23. Wan, Q.; Chen, J.; Chen, G.; Danishefsky, S. J., A Potentially Valuable Advance in the Synthesis of Carbohydrate-Based Anticancer Vaccines through Extended Cycloaddition Chemistry. *The Journal of Organic Chemistry* **2006,** *71* (21), 8244-8249.

24. Yang, C. Y.; Song, B. B.; Ao, Y.; Nowak, A. P.; Abelowitz, R. B.; Korsak, R. A.; Havton, L. A.; Deming, T. J.; Sofroniew, M. V., Biocompatibility of amphiphilic diblock copolypeptide hydrogels in the central nervous system. *Biomaterials* **2009,** *30* (15), 2881-2898.

25. Pochan, D. J.; Pakstis, L.; Ozbas, B.; Nowak, A. P.; Deming, T. J., SANS and Cryo-TEM study of self-assembled diblock copolypeptide hydrogels with rich nano- through microscale morphology. *Macromolecules* **2002,** *35* (14), 5358-5360.

26. Nowak, A. P.; Breedveld, V.; Pakstis, L.; Ozbas, B.; Pine, D. J.; Pochan, D.; Deming, T. J., Rapidly recovering hydrogel scaffolds from self-assembling diblock copolypeptide amphiphiles. *Nature* **2002,** *417* (6887), 424-428.

27. Vaupel, P.; Kallinowski, F.; Okunieff, P., Blood-Flow, Oxygen and Nutrient Supply, and Metabolic Microenvironment of Human-Tumors - a Review. *Cancer Research* **1989,** *49* (23), 6449-6465.

28. Mellman, I., The Importance of Being Acid-The Role of Acidification in Intracellular Membrane Traffic. *J. Exp. Biol.* **1992,** *172*, 39-45.

29. Sonawane, N. D.; Szoka, F. C.; Verkman, A. S., Chloride accumulation and swelling in endosomes enhances DNA transfer by polyamine-DNA polyplexes. *Journal of Biological Chemistry* **2003,** *278* (45), 44826-44831.

30. Whitehead, K. A.; Langer, R.; Anderson, D. G., Knocking down barriers: advances in siRNA delivery. *Nat Rev Drug Discov* **2009,** *8* (2), 129-138.

31. Boeckle, S.; von Gersdorff, K.; van der Piepen, S.; Culmsee, C.; Wagner, E.; Ogris, M., Purification of polyethylenimine polyplexes highlights the role of free polycations in gene transfer. *Journal of Gene Medicine* **2004,** *6* (10), 1102-1111.

32. Adams, M. L.; Lavasanifar, A.; Kwon, G. S., Amphiphilic block copolymers for drug delivery. *Journal of Pharmaceutical Sciences* **2003,** *92* (7), 1343-1355.

33. Lynn, D. M.; Langer, R., Degradable poly(beta-amino esters): Synthesis, characterization, and self-assembly with plasmid DNA. *J. Am. Chem. Soc.* **2000,** *122* (44), 10761-10768.

34. Veron, L.; Ganee, A.; Charreyre, M. T.; Pichot, C.; Delair, T., New hydrolyzable pH-responsive cationic polymers for gene delivery: A preliminary study. *Macromolecular Bioscience* **2004,** *4* (4), 431-444.

35. Engler, A. C.; Lee, H. I.; Hammond, P. T., Highly Efficient "Grafting onto" a Polypeptide Backbone Using Click Chemistry. *Angewandte Chemie-International Edition* **2009,** *48* (49), 9334-9338.

36. Poche, D. S.; Moore, M. J.; Bowles, J. L., An unconventional method for purifying the N-carboxyanhydride derivatives of gamma-alkyl-L-glutamates. *Synth. Commun.* **1999,** *29* (5), 843-854.

37. Clayden, J.; Greeves, N.; Warren, S.; Wothers, P., *Organic Chemistry*. Oxford University Press: Oxford, 2001; p 1508.

38. Bhatia, S. R.; Khattak, S. F.; Roberts, S. C., Polyelectrolytes for cell encapsulation. *Current Opinion in Colloid & Interface Science* **2005,** *10* (1-2), 45-51.

39. Eicher, T.; Hauptmann, S.; Speicher, A., *The Chemistry of Heterocycles*. 2nd ed.; Wiley-VCH: Weinheim, 2003; p 221.

40. Alexandridis, P.; Holzwarth, J. F.; Hatton, T. A., Micellization of Poly(Ethylene Oxide)-Poly(Propylene Oxide)-Poly(Ethylene Oxide) Triblock Copolymers in Aqueous-Solutions - Thermodynamics of Copolymer Association. *Macromolecules* **1994,** *27* (9), 2414-2425.

41. Johnson, W. C., Protein Secondary Structure and Circular-Dichroism - a Practical Guide. *Proteins-Structure Function and Genetics* **1990,** *7* (3), 205-214.

42. Liu, X. H.; Zhang, J. T.; Lynn, D. M., Ultrathin Multilayered Films that Promote the Release of Two DNA Constructs with Separate and Distinct Release Profiles. *Advanced Materials* **2008,** *20* (21), 4148-4153.

43. Zhang, J. T.; Lynn, D. M., Ultrathin multilayered films assembled from "Charge-Shifting" cationic polymers: Extended, long-term release of plasmid DNA from surfaces. *Advanced Materials* **2007,** *19* (23), 4218-4223.

44. Myer, Y. P., The pH-Induced Helix-Coil Transition of Poly-L-lysine and Poly-L-glutamic Acid and the 238-mu Dichroic Band. *Macromolecules* **1969,** *2* (6), 624-628.

5 A Library of Synthetic Antimicrobial Polypeptides for Various Biomedical Applications

5.1 Introduction

Infectious disease is a potentially debilitating cause for concern in a variety of medical conditions and procedures. The severity of these infections is augmented by two primary factors: (1) biofilm formation and (2) drug-resistant bacteria.[1] Several methods for controlling the formation and growth of biofilms have been proposed; however the use of appropriately functionalized surfaces that prevent the critical step of bacteria attachment on an implant may be the most effective method for preventing biofilm formation entirely. Along with chronic infection due to biofilm formation, drug resistance in planktonic bacteria is a prominent factor that is making treatment of infections increasingly more difficult.[2] The systemic overuse of broad-spectrum antibiotics has led to a severe rise in multi-drug resistant bacteria over the last several decades. Compounded by a lack of discovery and approval of new classes of antibiotics, there is a pressing need for the development of novel antimicrobial agents.[1, 2]

The use of naturally occurring antimicrobial peptides (AmPs) for infection treatment is starting to be explored as a new class of therapeutics.[3, 4] These cationic peptides are part of the eukaryote immune system and are highly broad-spectrum, active against gram-positive, gram-negative, and drug-resistant bacteria, as well as fungi and viruses. Several modes of AmP activity have been proposed, all suggesting a low propensity for the development of resistance.[5, 6] Additionally, AmPs have been shown to act rapidly [7] and prevent biofilm formation.[4, 8] Despite the therapeutic potential for infection control, the practical applicability of AmPs is thus far limited. AmP production methods are traditionally expensive and are implicated as the principal

obstacle in preventing widespread AmP use.[7] Additionally, significantly larger doses of AmPs are required for activity comparable to conventional antibiotics; however at these large concentrations, AmPs have been shown to induce toxicity in mammalian cells.[4, 7, 9, 10] The cost-effective and efficient development of novel AmPs which yield comparable activity to natural AmPs and have a high degree of biocompatibility, will ultimately allow for clinical translation of these promising therapeutics.

Cationic polymers can be selectively designed to exhibit high levels of antimicrobial activity, are relatively inexpensive to synthesize, and can be produced on a large scale.[1] To design these antimicrobial polymers, typically a combination of cationic and hydrophobic groups are dispersed along a polymer backbone,[11-15] or hydrophobic long chain N-alkylated quaternary ammonium groups are utilized.[16-20] It is hypothesized that the quaternary amine polymers function by interacting with the bacterial membrane, leading to loss in membrane integrity and cell death. Several polymers synthesized utilizing these strategies, including polyethylenimines,[16, 18, 19, 21] polymethacrylates,[11, 20] polydiallyammonium salts, [17, 22] polyarylamides,[12, 13] protonated polystyrenes,[23] and polynorbornenes,[24] have shown a high degree of antimicrobial activity; however these polymers are non-biodegradable and not particularly biologically compatible, rendering them unsuitable for many biomedical applications. Alternatively, it was recently demonstrated that synthetic antimicrobial polypeptides can be synthesized by the ring opening polymerization (ROP) of the N-carboxyanhydrides (NCA) of cationic (lysine) and hydrophobic (alanine, phenylalanine, or leucine) amino acid residues, creating a biodegradable synthetic AmP mimic. These polymers showed antimicrobial activity comparable to naturally occurring AmPs but have a high degree of hemolytic activity,[14] making them unsuitable for systemic administration.

As a promising alternative to currently existing antimicrobial polymers, we have synthesized and characterized a library of synthetic cationic homopolypeptides, utilizing the synthetic approach described in Chapters 3 and 4 that mimic naturally occurring AmPs, shown in Scheme 5-1. The new antimicrobial polypeptides range in length from 30 to 140 repeat units and they have varied side group functionality, including primary, secondary, tertiary, and quaternary amines with hydrocarbon side chains ranging from 1 to 12 carbons long. Table 5-1 summarizes the polymers investigated and indicates whether they were tested for coating applications and/or solution antimicrobial activity. We have denoted the quaternary amine polypeptides as QCn, where Q indicates that the amine is quaternary and Cn indicates a carbon side chain of length n. The effect of the side chain functionality and the polypeptide length was evaluated using a modified microdilution assay to determine the minimum inhibitory concentration (MIC), or the lowest point at which visible bacteria growth is inhibited,[25] against both gram-negative and gram-positive bacteria. A bacteria attachment assay was also carried out on polypeptide coatings to evaluate their potential efficacy for use as antimicrobial surface coatings. To determine their level of biocompatibility, red blood cell (RBC) lysis was monitored in the presence of these polypeptides.

Scheme 5-1. Click functionalization of PPLG and various amine side groups. For the quaternary amines abbreviation, the abbreviation Q indicates that the amine is quaternary and Cn indicates a carbon chain length with n repeat units. For example, QC4 is a quaternary amine with a hydrocarbon tail that is 4 carbons long.

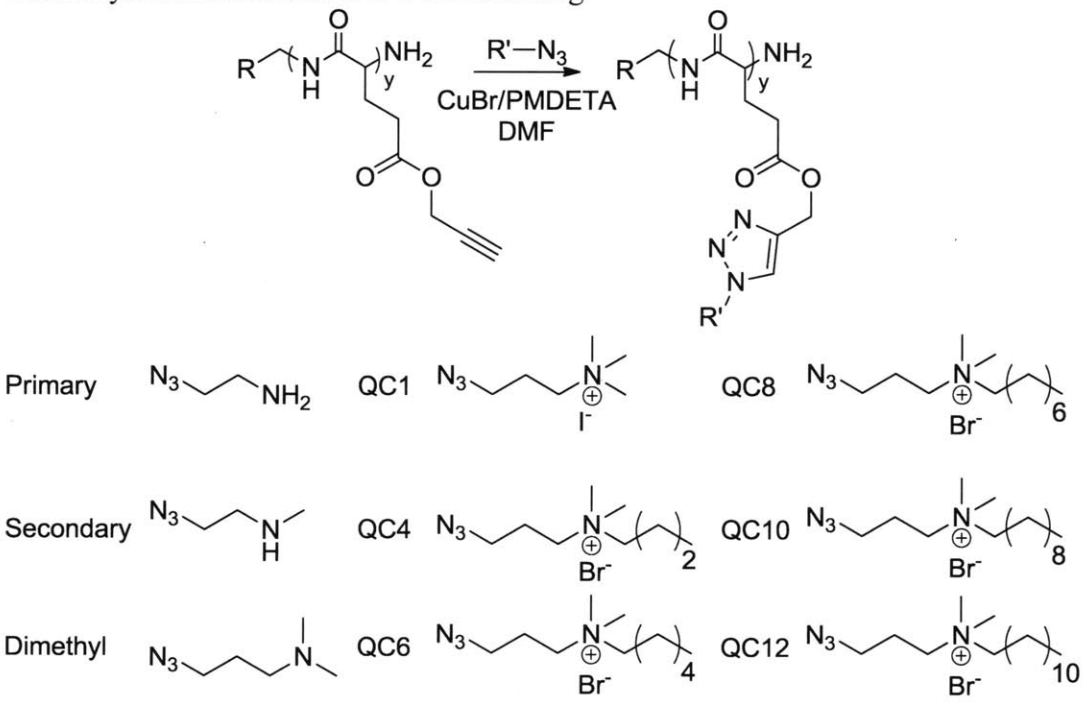

Table 5-1. Summary of polypeptides tested.[a]

DP	Primary	Secondary	Tertiary	Quaternary					
				QC1	QC4	QC6	QC8	QC10	QC12
30									
56									
75									
137									

Tested for MIC

Tested for MIC and coatings

Not tested

[a] Here DP is the degree of polymerization of the polypeptide. Primary, secondary, tertiary, and quaternary represent the degree of the amine functionalized side chains. In polypeptides defined as QCn, Q = quaternary and Cn = carbon side chain length of n.

5.2 Results and discussion

5.2.1 Antimicrobial polypeptide synthesis

To design and synthesize a family of antimicrobial synthetic polypeptides that mimic naturally occurring AmPs, we systematically varied the amino side chain functionality and polymer chain length of PPLG to determine the optimal polymer composition for the growth inhibition of both gram-negative and gram-positive bacteria as well as the prevention of biofilm formation by these bacteria. PPLG at four different degrees of polymerization (DP) from 30 to 140 repeat units was synthesized as previously described.[26] GPC traces of the PPLG backbone indicate that these polymers have a narrow molecular weight distribution with polydispersities (PDI) between 1.09 and 1.25, as shown in Figure 5-1. Figure 5-2A shows a representative ^{1}H-NMR spectrum of PPLG (DP = 140) which confirms the polymer structure. Various amine functional groups were coupled to the PPLG using the copper catalyzed Huisgen click reaction, shown in Scheme 5-1. ^{1}H-NMR was used to confirm the coupling efficiency of the click reaction. Representative ^{1}H-NMR of QC1 and QC6 substituted PPLG (DP = 140) compared to the ^{1}H-NMR of PPLG (DP = 140) are shown in Figure 5-2. In all cases, the coupling efficiency of the click reaction was near quantitative, as indicated by the disappearance of the PPLG alkyne peak (a, 3.4 ppm) and ester peak (b, 4.7 ppm) in Figure 5-2A and the appearance of a new ester peak (k, 5.2 ppm) in Figures 1B and 1C. Furthermore, the peak integration for all samples tested was as expected for near quantitative substitution. For polymers analyzed in D_2O, the original backbone peak (d, 2.0 ppm) did not overlap with the newly added side chains. This peak was used to determine the percent conversion of alkyne to triazole ring. For example, in Figure 5-2B, the integration of the backbone peak (d, 2.0 ppm) was compared to the integration of the triazole peak (m, 8.1 ppm) giving a substitution of 99.3%. When comparing the integration to other

peaks, the substitution rate ranged from 94.4-99.7%. For polymers analyzed in MeOD (QC6-QC12), where the backbone peak (d, 2.0 ppm) did overlap with the newly added side chains, the broader backbone peak (e, 4.0 ppm) was used to determine the conversion. For all polymers analyzed in MeOD, the substitution rate was above 98% when comparing the original backbone peak (e, 4.0 ppm) integration to the ester peak (k, 5.1 ppm) integration.

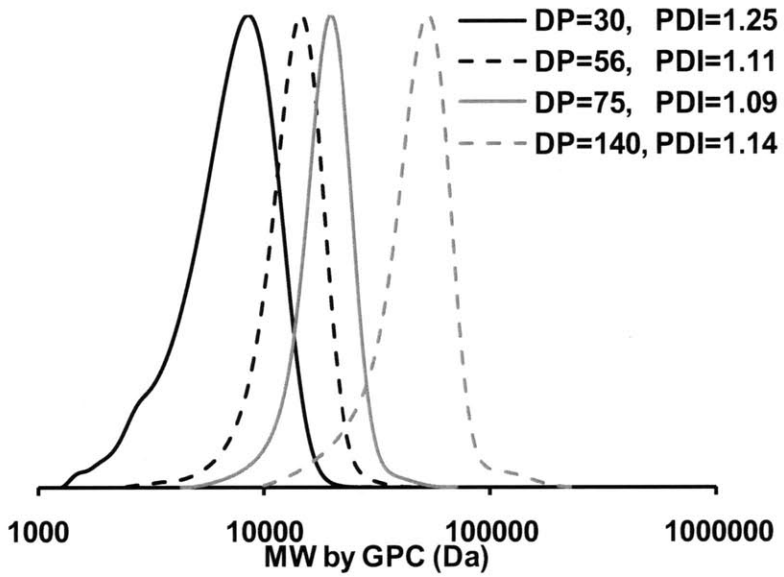

Figure 5-1. Molecular weight distribution of PPLG obtained using a DMF GPC and calculated using PMMA standards. The degree of polymerization was determined by ^{1}H-NMR.

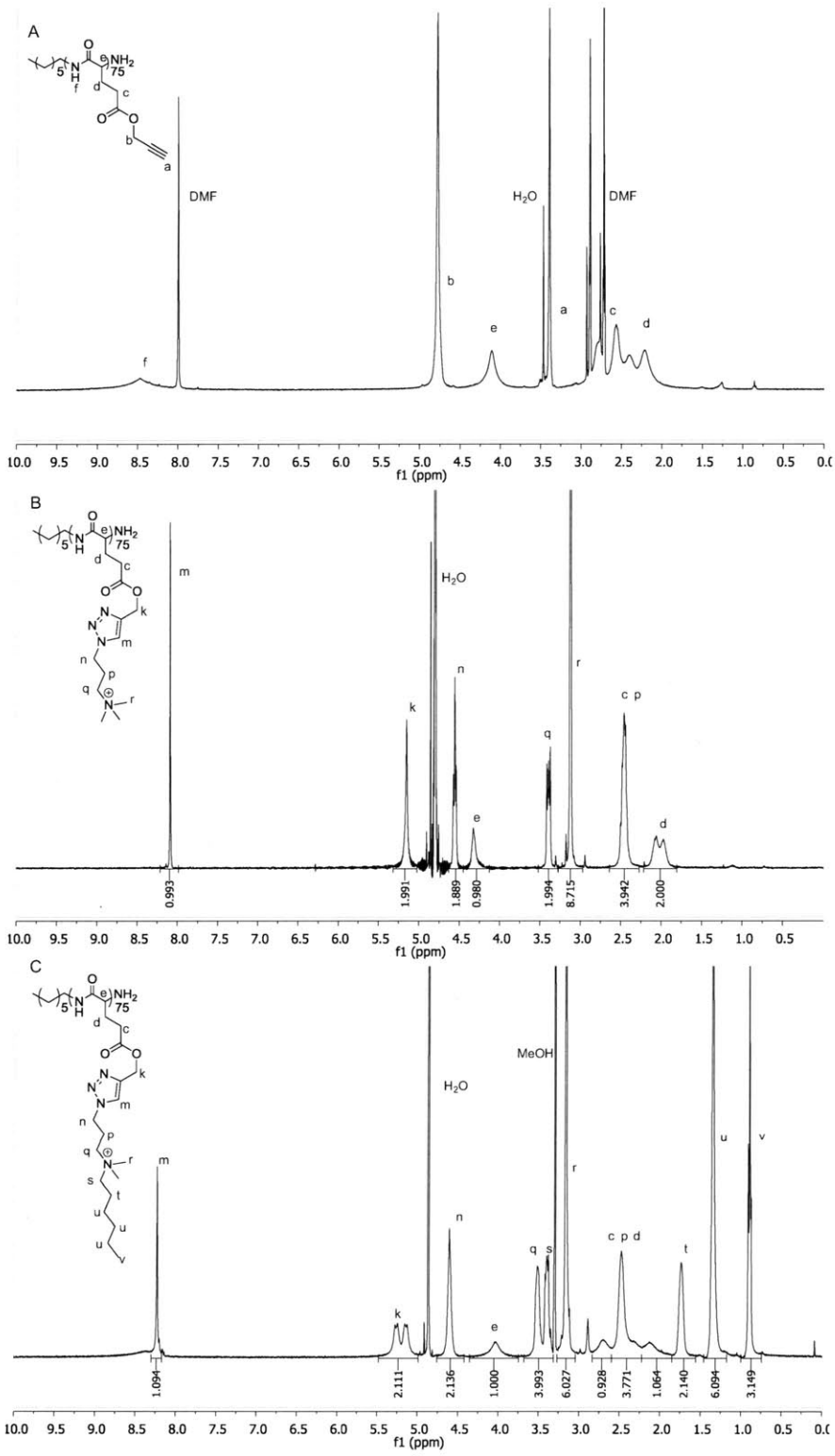

Figure 5-2. A) ^{1}H-NMR spectrum of PPLG (DP = 140) in d_7 DMF, B) ^{1}H-NMR spectrum of PPLG (DP = 140) functionalized with QC1 in D_2O, and C) ^{1}H-NMR spectrum of PPLG (DP = 140) functionalized with QC6 in CD_3OD.

Table 5-1 summarizes the polymers synthesized and how they were tested. To determine how to best test these polymers, water solubility and substrate coating experiments were performed. The water solubility of all polypeptides (except QC12 which is completely water insoluble) was determined to be greater than 50 mg/mL which was assumed to exceed what is necessary for MIC testing. Substrate coating experiments were performed to determine if these polymers are candidates for anti-biofilm coatings. Although, they have high water solubility, the QCn ($n \geq 4$) polymers also have surfactant like properties, causing them to readily adhere to surfaces. Glass substrates were coated by solvent casting these polymers from a methanol solution at a set concentration and dry film thicknesses were measured. Following exposure to bacteria culture media, film thicknesses were measured again. A significant amount of smooth polymer film remained on the substrate, which was estimated to be equivalent to at least 30 monolayers of packed polypeptide. A detailed discussion of this calculation as well as the thickness measurements can be found in the supplementary information. Based on the solubility and surface adsorption characteristics, the primary, secondary, tertiary, and QC1 polymers were tested for bacteria growth inhibition using the microdilution assay, and QCn ($n \geq 4$) polymers were tested for both bacteria growth inhibition and activity against bacteria attachment. Several of these polymers have potential for use in systemic or localized antimicrobial delivery applications; the QCn ($n \geq 4$) polymers may be suitable for semi-permanent antimicrobial coatings on medical devices.

5.2.2 Bacterial growth inhibition

We quantified the activity of all polypeptides synthesized in this work against two classes of bacteria that are commonly associated with infection. *S. aureus* and *E. coli* were chosen as gram-positive and gram-negative bacteria, respectively. The effect of the polypeptides on the

inhibition of bacterial growth was examined using a modified liquid microdilution assay for the primary, secondary, tertiary, and QC1 polypeptides as highlighted in Table 5-1. For the purposes of this work, we have expressed MIC as a polypeptide concentration range over which bacteria density normalized to a positive control of untreated bacteria and a negative control of growth media is found to decrease from greater than or equal to 0.1 to less than or equal to 0.02 (where 1.0 indicates the positive control). Samples that did not exhibit a significant decrease over the polypeptide concentration range of 70 – 4500 μg/mL and maintained a normalized bacteria density ≥ 1.0 at the highest tested concentration were defined as inactive. Figures 3A and 3B show the results of this assay for the primary amine functionalized polypeptides of varying molecular weight for *S. aureus* and *E. coli*, respectively. As seen in Figure 5-3A, there is a clear molecular weight dependence on *S. aureus* growth inhibition, for which the lowest molecular weight primary amine polypeptide (DP = 30) shows no *S. aureus* inhibition and the highest molecular weight (DP = 140) is the most active, with a MIC between 70.3 – 140.6 μg/mL. This MIC for *S. aureus* is comparable and in some cases lower than many highly effective naturally occurring antimicrobial peptides, including cecropin A and B, magainin 1 and 2, and defensin.[13, 14]

Table 5-2 summarizes the MIC for the primary, secondary, tertiary, and QC1 polypeptides tested against *S. aureus* as well as the normalized bacteria inhibition at the highest polypeptide concentration tested, 4500 μg/mL. Along with the highest molecular weight primary amine, the highest molecular weight secondary amine polypeptide also exhibits an MIC for *S. aureus* that is comparable to natural AmPs, between 140.6 – 281.3 μg/mL. The tertiary and quaternary (QC1) amine samples do not show any significant *S. aureus* growth inhibition.

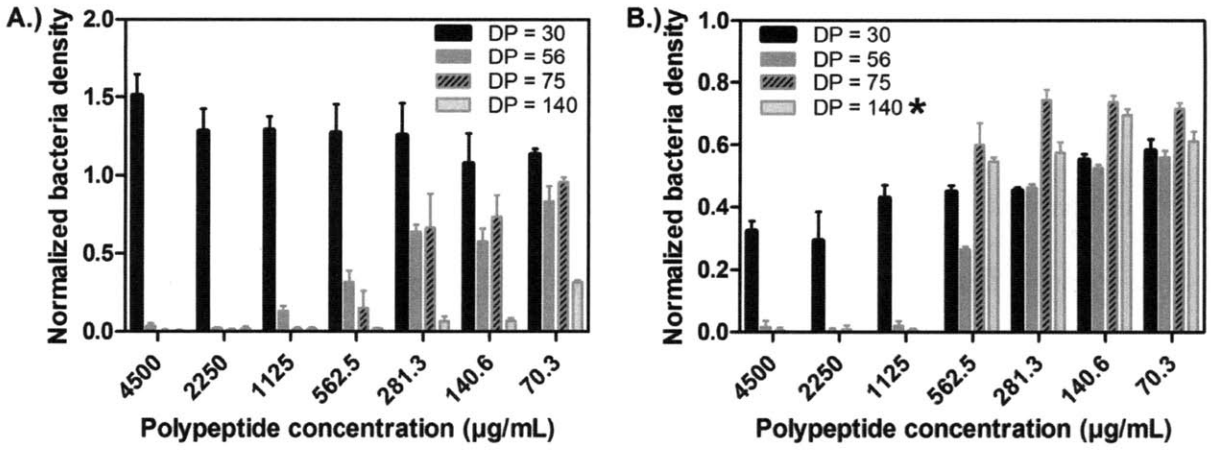

Figure 5-3. Bacteria growth inhibition for primary amine functionalized polymers based on normalized turbidity measurements. A.) *S. aureus* normalized bacteria density at varying polymer concentrations. B.) *E. coli* normalized bacteria density at varying polymer concentrations (*high turbidity was observed for DP = 140 polypeptides at concentrations of 4500 – 1125 µg/mL due to polypeptide precipitate forming; in these cases, however, complete bacteria growth inhibition was observed based on clear solution surrounding the polypeptide precipitate).

Table 5-2. *Staphylococcus aureus* growth inhibition properties

	Primary		Secondary		Tertiary		Quaternary (QC1)	
DP	MIC[a]	Normalized density[b]	MIC[a]	Normalized density[b]	MIC[a]	Normalized density[b]	MIC[a]	Normalized density[b]
30	NA	1.4 ± 0.1	NA	1.6 ± 0.2	NA	1.5 ± 0.4	NA	1.1 ± 0.2
56	1125-2250	< 0.05	NA	1.2 ± 0.1	NA	0.9 ± 0.1	NA	1.3 ± 0.05
75	562.5-1125	< 0.05	>4500	0.8 ± 0.2	NA	1.2 ± 0.3	NA	1.1 ± 0.2
140	70.3-140.6	< 0.05	140.6-281.3	< 0.05	NA	1.0 ± 0.2	>4500	0.6 ± 0.1

[a] MIC is in µg/mL. No activity (NA) was defined as normalized density ≥ 1.0 at polypeptide concentration of 4500 µg/mL.

[b] Normalized density is shown for bacteria exposed to 4500 µg/mL polypeptide.

Examining the polypeptides against *E. coli* growth, the primary amine samples were again found to be highly active against growth of this gram-negative bacteria. Figure 5-3B shows the results of *E. coli* growth inhibition for the four primary amine functionalized polypeptides. The molecular weight dependence is not as strongly visible with *E. coli* as with *S. aureus*; here the MIC against *E. coli* is found to lie between 562.5 – 1125 μg/mL for the three highest molecular weight primary amine polypeptides (DP = 56, 75, and 140). What appears as a bacteria density ≥ 1.0 in Figure 5-3B (for DP = 140) was optically visible polypeptide precipitate due to the test media conditions in a clear bacteria solution (signifying no bacteria present). Even the lowest molecular weight primary amine (DP = 30) exhibited approximately 70% inhibition of *E. coli* bacteria growth upon exposure to the 4500 μg/mL polypeptide concentration, although the same polymer was inactive at all concentrations for *S. aureus*. This was an unexpected finding, as traditionally, treatment of gram-negative bacteria has been more difficult than gram-positive strains due to the more complex membrane structure of these bacteria.[2] Table 5-3 summarizes the MIC of the tested polypeptides against *E. coli* along with the normalized bacteria density at the highest tested concentration of 4500 μg/mL. The highest molecular weight secondary amine shows activity against *E. coli*, although the MIC is above 4500 μg/mL. Interestingly, unlike *S. aureus* the mid-range molecular weight secondary amines show *E. coli* inhibition at the highest tested concentration (approximately 50% and 20% for DP = 56 and 75, respectively). Additionally, the DP = 140 tertiary amine and DP ≥ 56 QC1 polypeptides exhibited *E. coli* growth inhibition as shown in Table 5-3 at the highest tested concentration, which was not observed for *S. aureus*. Many of the polymers developed in this work appear to be excellent candidates for infection prevention by delivery from drug-eluting coatings, as has been previously examined for naturally occurring AmPs.[4, 27]

Table 5-3. *Escherichia coli* growth inhibition properties

	Primary		Secondary		Tertiary		Quaternary (QC1)	
DP	MIC[a]	Normalized density[b]	MIC[a]	Normalized density[b]	MIC[a]	Normalized density[b]	MIC[a]	Normalized density[b]
30	>4500	0.3 ± 0.03	NA	1.0 ± 0.2	NA	1.0 ± 0.02	NA	0.8 ± 0.2
56	562.5-1125	<0.05	>4500	0.5 ± 0.04	NA	1.0 0.06	>4500	0.6 ± 0.06
75	562.5-1125	<0.05	>4500	0.2 ± 0.006	NA	0.9 ± 0.2	>4500	0.2 ± 0.006
140	562.5-1125	1.6 ± 0.2[c]	>4500	0.3 ± 0.02	>4500	0.4 ± 0.04	>4500	0.3 ± 0.01

[a] MIC is in μg/mL. No activity (NA) was defined as normalized density ≥ 1.0 at polypeptide concentration of 4500 μg/mL.
[b] Normalized bacteria density is shown for bacteria exposed to 4500 μg/mL polypeptide.
[c] Polypeptide precipitate was optically visible in the clear bacteria solution, indicating growth inhibition, but leading to a large optical density reading resulting in large normalized bacteria density.

The quaternary amine functionalized polypeptides containing hydrophobic side chains (QCn, n ≥ 4), as highlighted in Table 5-1, were examined for bacterial growth inhibition from surface coatings. Polypeptides dissolved in methanol were allowed to coat a well plate via solvent evaporation to yield a polymer film, and these surfaces were subsequently exposed to bacteria solution. Table 5-4 summarizes the MIC for each of the tested polypeptides for both *S. aureus* and *E. coli*. Here, MIC again represents the polypeptide concentration range over which the normalized bacteria density transitions from greater than or equal to 0.1 to less than or equal to 0.02. Any polypeptides which exhibited a normalized bacteria density ≥ 1.0 at the highest tested surface concentration were defined as inactive. For *S. aureus*, bacteria growth inhibition activity was not seen for the QC4 and QC6 polypeptides. At an increased polymer hydrophobicity, QC8 was found to have a MIC between 156.3-312.5 μg/mL and 78.1-156.3

μg/mL for the DP = 75 and 140 polymers, respectively. The QC12 had the lowest MIC observed for *S. aureus* between 39.1-78.1 μg/mL (corresponding to a surface coverage of 12.2-24.4 $\mu g/cm^2$ for this water insoluble polypeptide). QC10 also exhibited a low MIC between 312.5-625 μg/mL against *S. aureus*. These results are consistent with what has been observed for antimicrobial activity against *S. aureus* of similar alkylated quaternary polyethylenimines [16]. We found that the quaternary amine polypeptides were more active against *E. coli* than *S. aureus* for QC6, had comparable activity for QC8, and were less active for QC10 and QC12 against *E. coli* than *S. aureus*. Figure 4 shows the results of this polypeptide coating dose response assay for the QC8 samples (DP = 75) for both *S. aureus* and *E. coli*. For *E. coli*, bacteria growth inhibition increased with increasing hydrophobicity up to an alkyl chain length of 8 and decreased with alkyl chain lengths of 10 and 12. The lowest MIC was observed for the QC8 samples with a range of 156.3-312.5 μg/mL. This trend is similar to what has been observed with pendant quaternary amine containing methacrylate polymers, where the carbon side chain lengths tested were 12, 14, and 16. As the length of the carbon side chain increased, the methacrylate polymer antimicrobial activity increased for *S. aureus* but decreased for *E. coli*.[20] We hypothesize that the difference in MIC trends observed for *S. aureus* and *E. coli* is a result of the different membrane structure of these bacteria.

Table 5-4. Bacteria response to QCn ($n \geq 4$) polypeptides.[a]

Bacteria	DP	Quaternary (QC4) MIC	Quaternary (QC6) MIC	Quaternary (QC8) MIC	Quaternary (QC10) MIC	Quaternary (QC12) MIC[b]
S. aureus	75	NA	NA	156.3-312.5	312.5-625	39.1-78.1
	140	NA	NA	78.1-156.3	312.5-625	39.1-78.1
E. coli	75	NA	312.5-625	156.3-312.5	1250-2500	1250-2500
	140	NA	312.5-625	156.3-312.5	1250-2500	1250-2500

[a] MIC is in μg/mL. No activity (NA) was defined as normalized density ≥ 1.0 at polypeptide concentration of 2500 μg/mL.

[b] QC12 is completely water insoluble; the MIC values for DP = 75 and 140 correspond to a surface coverage of 12.2-24.4 μg/cm^2 and 390-780 μg/cm^2, for *S. aureus* and *E. coli*, respectively.

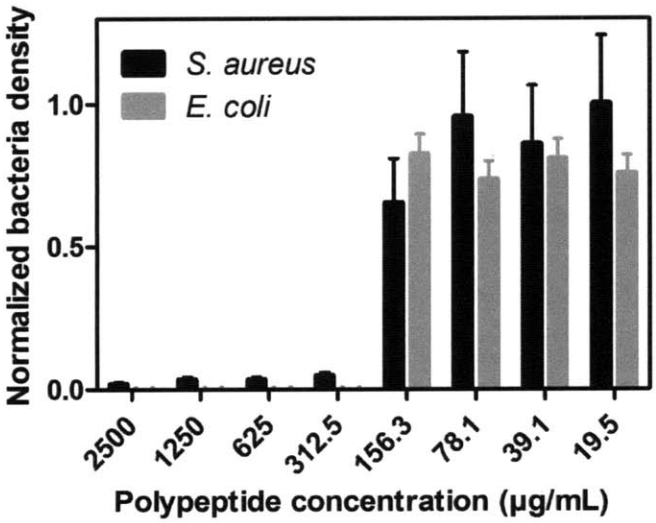

Figure 5-4. Bacteria growth inhibition by QC8 (DP = 75) coating for both S. aureus and E. coli.

The exact mechanism of action of the QCn ($n \geq 4$) polypeptides is currently under investigation. CD studies performed when the molecules were dissolved in methanol indicate that the QCn ($n \geq 4$) polymers adopt an α-helical conformation in solution before they are solvent cast, as indicated by the strong minimums at 208 nm and 222 nm (Figure 5-5).[28] After

solvent casting, FTIR was used to determine if the polymer backbone maintained a helical structure. The strong amide I peak at 1653 nm is characteristic of an α-helical structure (Figure 5-6).[29] As with other antimicrobial polycations, it is believed that these polymers function by electrostatic association with the negatively charged bacteria cell surface and subsequent disruption of the plasma membrane.[30] Due to the rigidity of the polypeptide backbone, these polymers act by complexing with the exterior surface of the bacterial cell membrane, rather than inserting fully across the membrane, as with more flexible polymers.[31] One of the advantages of applying a systematic approach to design synthetic antimicrobial polypeptides is that different properties can be decoupled and explored. For the current system, we are using a rigid α-helical backbone, but in the future, utilizing a mixture of D-L monomers, it is also possible to explore the effect of polymer backbone rigidity on the antimicrobial activity and mechanism of membrane disruption.

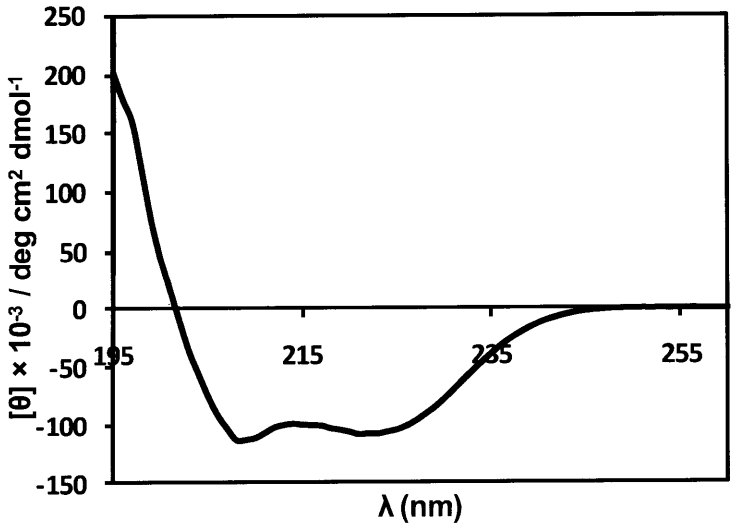

Figure 5-5. Circular dichroism of QC8 functionalized polypeptide in methanol at 1.67 mg/mL

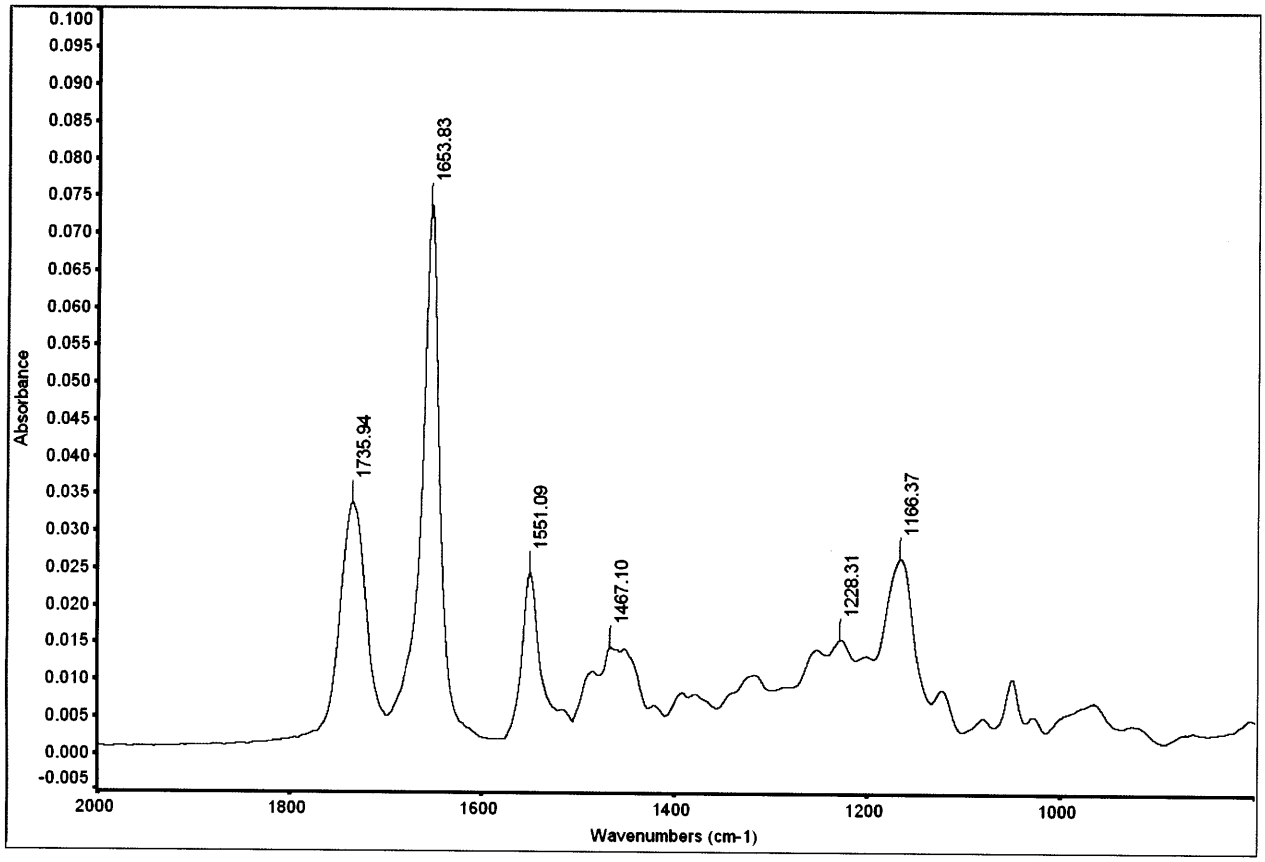

Figure 5-6. FTIR or QC8 DP = 75 polypeptide solvent cast from methanol

5.2.3 Bacterial attachment inhibition

An increasingly common cause of medical device failure and the spread of infection is the formation of biofilms on implants and dead tissue.[32] The first critical step necessary for biofilm formation is the attachment of bacteria on a surface. Preventing this attachment step will ultimately prevent biofilm formation and is a desirable characteristic of functionalized surfaces. To examine whether the QCn ($n \geq 4$) polypeptides have the potential to make anti-biofilm device coatings for orthopedic implants or intraocular lenses for example, the ability of substrates coated with these polypeptides to inhibit bacteria attachment was examined. Round glass substrates were coated with quaternary amine functionalized polypeptide samples with varying degrees of hydrophobicity at two different molecular weights (DP = 75 and 140) and allowed to

evaporate to evenly coat these substrates, yielding a final coating of 330 $\mu g/cm^2$. These substrates were then tested for prevention of bacterial attachment for both *S. aureus* and *E. coli*. Figure 5-7 and Figure 5-8 show the results for attachment inhibition of *S. aureus* and *E. coli*, respectively, by these coated substrates. It was found that increasing hydrophobicity of polypeptide functional groups leads to increased inhibition of bacterial attachment for *S. aureus* and *E. coli* up to an alkyl chain length of 10. Beyond this point, increasing hydrophobicity (alkyl chain length of 12) seems to decrease inhibition capability. Although the QC12 sample did have a comparable MIC to the QC10 in the polypeptide dose response liquid assay testing for bacteria growth inhibition, its attachment inhibition activity is not comparable to QC10. Increased hydrophobicity may assist penetration of the bacteria cell based on hydrophobic interactions with the lipid bilayer membranes; however it is also possible that this behavior is no longer sustained at greater alkyl chain lengths (i.e. QC12) in the case of *E. coli* due to changes in the compatibility between the cationic hydrophobic side chain and the amphiphilic lipid membrane of the cell. These changes may more significantly affect *E. coli* than *S. aureus* due to the more complex membrane structure of gram-negative bacteria, which may explain why there is no significant decrease in *S. aureus* attachment inhibition by the QC12 polypeptide compared to the QC8 and QC10 polymers. These results agree with the results of bacteria growth inhibition, where the QC12 has the lowest MIC for *S. aureus* and the QC8 and QC10 are also quite active against *S. aureus* growth. Additionally, both molecular weights tested displayed the same trends in activity.

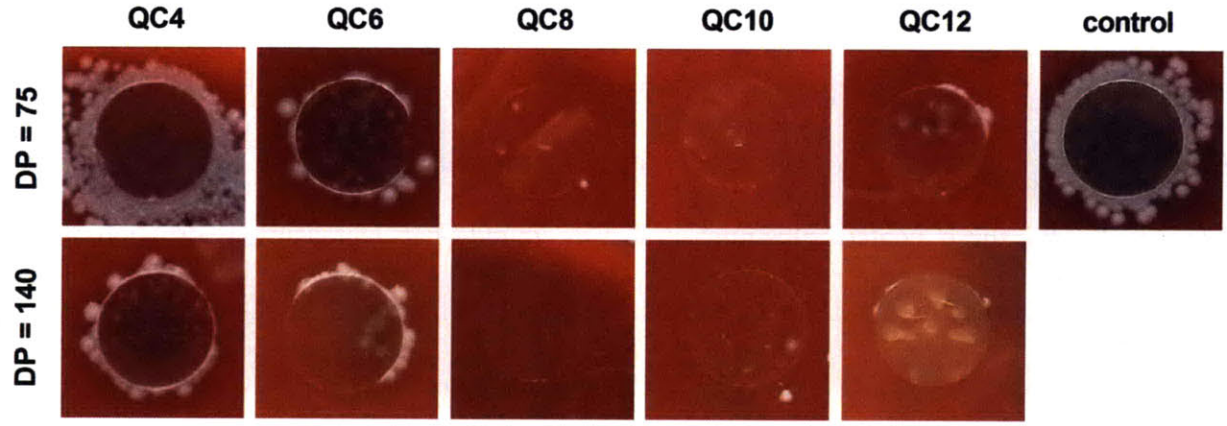

Figure 5-7. *S. aureus* attachment inhibition by quaternary amine functionalized polypeptides with varying hydrophobicity (QC4 – QC12; control = uncoated substrate).

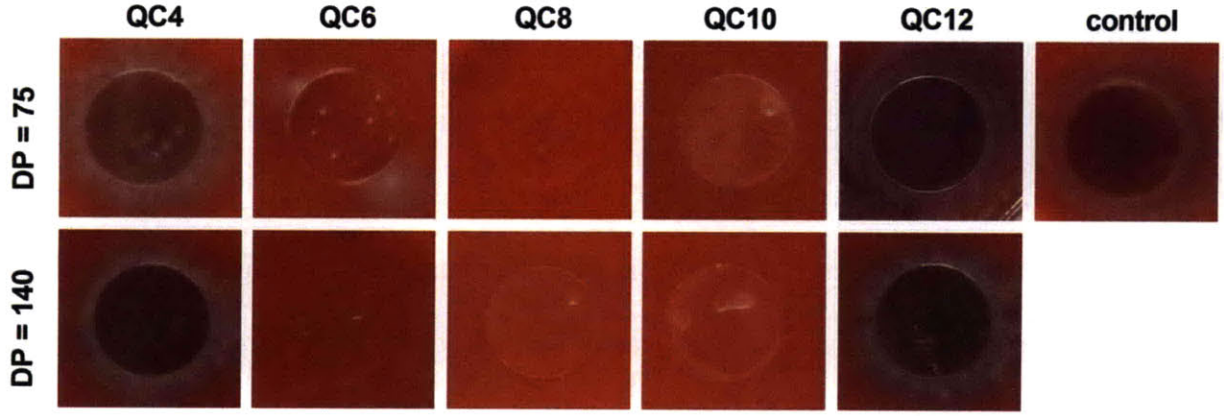

Figure 5-8. *E. coli* attachment inhibition by quaternary amine functionalized polypeptides with varying hydrophobicity (QC4 – QC12; control = uncoated substrate).

5.2.4 Polypeptide biocompatibility

The biocompatibility of these polypeptides was quantified using a hemolysis test in which RBC lysis in response to these polymers was examined by monitoring free hemoglobin absorbance. Table 5-5 shows results for all polypeptides that displayed a normalized hemolysis greater than 0.005 at the highest tested polypeptide concentration of 5000 μg/mL. All polypeptides were found to be highly non-cytotoxic in comparison to many naturally occurring

AmPs as well as several antimicrobial polymers that have recently been developed.[13, 14] In all cases in which hemolysis above 0.5% was observed, the concentration at which this occurred far exceeded the polypeptide MIC against *S. aureus* and *E. coli*. This is a necessary requirement for antimicrobial polymers to attain utility in clinical applications. The largest level of hemolysis was observed for the QC8 polypeptide, with a maximum of approximately 23% for the DP = 75 polypeptide at a 5000 μg/mL concentration. Figure 5-9 shows hemolysis in response to varying QC8 polypeptide concentrations. This polymer was also found to exhibit high activity against both gram-positive and gram-negative bacteria, and therefore was expected to have some degree of hemolysis. However, the concentrations at which the QC8 polymer exhibits complete bacteria growth inhibition were 78.1-156.3 μg/mL and 156.3-312.5 μg/mL for *S. aureus E. coli* respectively, which are far lower than the concentration at which significant hemolysis is observed (approximately less than 8%).

Table 5-5. Normalized red blood cell lysis.[a]

DP	Primary	Quaternary (QC8)	Quaternary (QC10)	Quaternary (QC12)
75	<0.005	0.23 ± 0.013	0.20 ± 0.024	0.085 ± 0.029
140	0.032 ± 0.003	0.11 ± 0.007	0.15 ± 0.008	0.052 ± 0.008

[a] Secondary, tertiary, and quaternary (QC1, QC4, QC6) amine samples showed less than 0.005 normalized red blood cell hemolysis at the highest tested concentration.

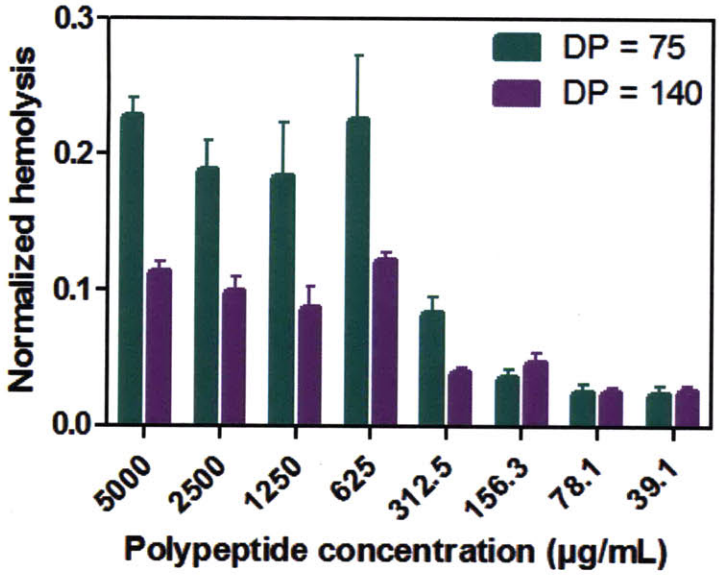

Figure 5-9. Normalized hemolysis for QC8 polypeptide.

5.3 Conclusions

In this work, we created a library of synthetic antimicrobial polypeptides that mimic naturally occurring AmPs. These polypeptides were designed by systematically varying the side chain functionality (primary to quaternary amine) and alkyl side chain length of a PPLG backbone of varying molecular weights. To assess the antimicrobial potential of these polypeptides, they were tested based on the criteria of bacteria growth and attachment inhibition for both gram-negative and gram-positive bacteria, as well as biocompatibility. With respect to bacteria growth inhibition, several polymers were found to exhibit MIC values that rival naturally existing AmPs. For the quaternary amine series, increasing side chain hydrophobicity led to increased bacteria growth inhibition within a certain limit. In particular, QC12 was the most potent polypeptide against *S. aureus*, while both QC6 and QC8 were most effective in inhibiting *E. coli* growth. The QC8 and QC10 polypeptides were optimal in completely

preventing bacteria attachment, and consequently biofilm formation, for both *S. aureus* and *E. coli*. Finally, with regards to biocompatibility, all of the antimicrobial polypeptides were found to be highly non-cytotoxic in comparison to many naturally occurring AmPs with extremely low hemolytic activity. Overall, these polymers possess many of the positive qualities of naturally occurring AmPs, including effective MIC values, broad-spectrum activity, and biofilm prevention capabilities. At the same time, these synthetic polypeptides are efficiently produced, cost-effective, and biocompatible. The antimicrobial polypeptides developed in this work are an important step forward in the production of a new class of antimicrobial therapeutics which have the potential for clinical translation in both systemic and local delivery applications as well as for use in semi-permanent medical device coatings. The flexibility of this system allows for the systematic variation of polymer properties, ranging from side chain functionality to backbone rigidity, which will provide insight into the mechanism of action of antimicrobial agents and aid in the rational design of future antimicrobial therapeutics.

5.4 Supporting Information

5.4.1 Calculation of Thickness Measurements

Thickness of solvent cast polymers was estimated by assuming that the polymer is a rigid rod α-helical peptide,[33] as shown below (Equations 1-6). The following schematic gives the polypeptide dimensions.

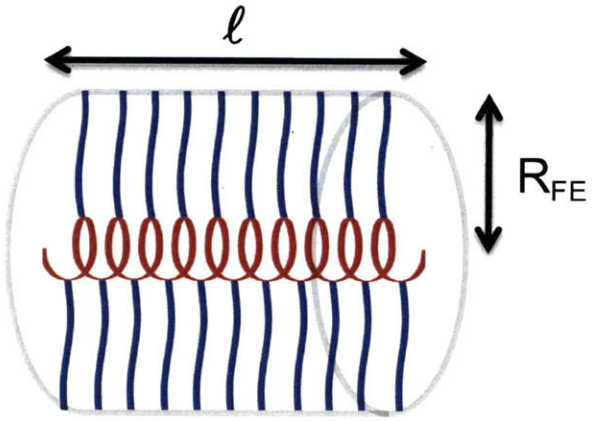

Figure 5-10. Schematic of the polypeptide dimensions

The length of the polypeptide, ℓ, was estimated by calculating how many turns each polymer has (3.62 repeat units per turn) and multiplying it by the distance between turns on an α-helical backbone (1.5 Å per turn). The polymer radius, R_{FE}, was estimated by assuming the polypeptide side chains protruded out from the α-helical backbone in a fully extended chain conformation. The surface area, A_{PP}, covered by a single polypeptide was estimated by multiplying ℓ by $2R_{FE}$ (the polymer diameter). The total area covered by polypeptides if they were packed as cylinders in a single monolayer, A_{SC}, was calculated by multiplying A_{PP} by the concentration of polymer solution, C_{PS}, and the volume casted, V_{PS}, as well as Avogadro's number, and dividing this by the molecular weight of the polypeptide, MW_{PP}. The number of polypeptide monolayers, L, was estimated by dividing the disc area, A_D, by A_{SC}. The thickness, h, was estimated by multiplying the number of polypeptide layers by $2R_{FE}$.

$$n_{turns} = \frac{DP}{3.62} \quad (1)$$

$$l = 1.5\text{Å} \times n_T \quad (2)$$

$$A_{PP} = l \times 2R_{FE} \quad (3)$$

$$A_{SC} = \frac{A_{PP} \times C_{PS} \times V_{PS} \times N_A}{MW_{PP}} \quad (4)$$

$$L = \frac{A_D}{A_{SC}} \quad (5)$$

$$h = L \times 2R_{FE} \quad (6)$$

5.4.2 Substrate Coating Experiments

The following graph shows thicknesses following solvent casting of QC6, QC8, and QC10 polypeptide films before and after bacteria culture media treatment (data shown here corresponds to incubation in CaMHB). The predicted thickness values before treatment based on the above model are also shown. The estimated polypeptide thickness was within 30% of the measured film thickness.

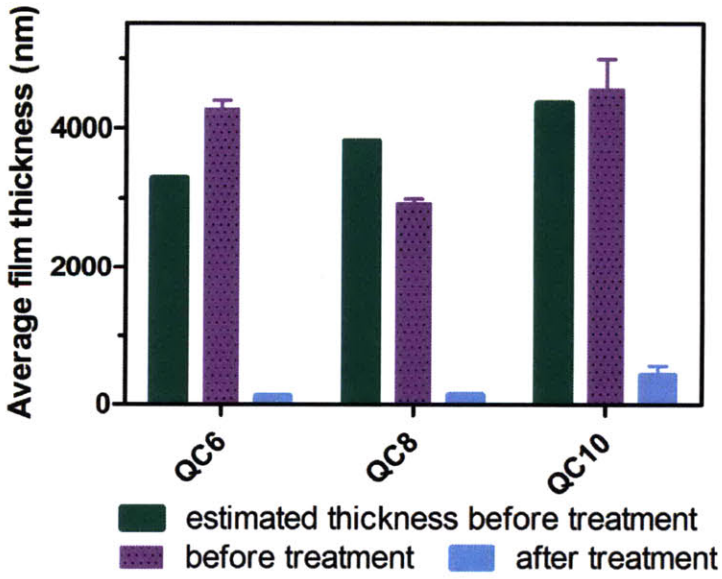

Figure 5-11. Morphology of films before and after treatment is shown for the QC10 polypeptide solvent cast substrates in the following atomic force microscopy images.

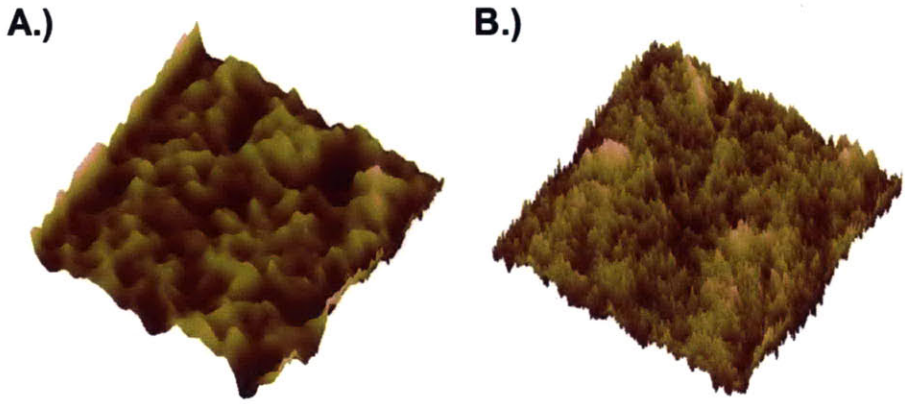

Figure 5-12. QC10 solvent cast substrate morphology (10 μm x 10 μm). (A) Before media treatment (maximum z-scale = 22.1 nm). (B) After media treatment (maximum z-scale = 1.7 nm).

5.5 References

1. Gabriel, G. J.; Som, A.; Madkour, A. E.; Eren, T.; Tew, G. N., Infectious disease: Connecting innate immunity to biocidal polymers. *Materials Science and Engineering: R: Reports* **2007,** *57* (1-6), 28-64.

2. Taubes, G., The Bacteria Fight Back. *Science* **2008,** *321* (5887), 356-361.

3. Gordon, Y. J.; Romanowski, E. G.; McDermott, A. M., A Review of Antimicrobial Peptides and Their Therapeutic Potential as Anti-Infective Drugs. *Current Eye Research* **2005,** *30* (7), 505-515.

4. Shukla, A.; Fleming, K. E.; Chuang, H. F.; Chau, T. M.; Loose, C. R.; Stephanopoulos, G. N.; Hammond, P. T., Controlling the release of peptide antimicrobial agents from surfaces. *Biomaterials* **2010,** *31* (8), 2348-2357.

5. Hancock, R. E. W.; Diamond, G., The role of cationic antimicrobial peptides in innate host defences. *Trends in Microbiology* **2000,** *8* (9), 402-410.

6. Ganz, T., The Role of Antimicrobial Peptides in Innate Immunity. *Integr. Comp. Biol.* **2003,** *43* (2), 300-304.

7. Marr, A. K.; Gooderham, W. J.; Hancock, R. E. W., Antibacterial peptides for therapeutic use: obstacles and realistic outlook. *Current Opinion in Pharmacology* **2006,** *6* (5), 468-472.

8. Singh, P. K.; Parsek, M. R.; Greenberg, E. P.; Welsh, M. J., A component of innate immunity prevents bacterial biofilm development. *Nature* **2002,** *417* (6888), 552-555.

9. Etienne, O.; Gasnier, C.; Taddei, C.; Voegel, J.-C.; Aunis, D.; Schaaf, P.; Metz-Boutigue, M.-H.; Bolcato-Bellemin, A.-L.; Egles, C., Antifungal coating by biofunctionalized polyelectrolyte multilayered films. *Biomaterials* **2005,** *26* (33), 6704-6712.

10. Pacor, S.; Giangaspero, A.; Bacac, M.; Sava, G.; Tossi, A., Analysis of the cytotoxicity of synthetic antimicrobial peptides on mouse leucocytes: implications for systemic use. *J. Antimicrob. Chemother.* **2002,** *50* (3), 339-348.

11. Kuroda, K.; Caputo, G. A.; DeGrado, W. F., The Role of Hydrophobicity in the Antimicrobial and Hemolytic Activities of Polymethacrylate Derivatives. *Chemistry-a European Journal* **2009,** *15* (5), 1123-1133.

12. Epand, R. F.; Mowery, B. P.; Lee, S. E.; Stahl, S. S.; Lehrer, R. I.; Gellman, S. H.; Epand, R. M., Dual mechanism of bacterial lethality for a cationic sequence-random copolymer that mimics host-defense antimicrobial peptides. *Journal of Molecular Biology* **2008,** *379* (1), 38-50.

13. Mowery, B. P.; Lee, S. E.; Kissounko, D. A.; Epand, R. F.; Epand, R. M.; Weisblum, B.; Stahl, S. S.; Gellman, S. H., Mimicry of antimicrobial host-defense peptides by random copolymers. *Journal of the American Chemical Society* **2007,** *129* (50), 15474-15476.

14. Zhou, C. C.; Qi, X. B.; Li, P.; Chen, W. N.; Mouad, L.; Chang, M. W.; Leong, S. S. J.; Chan-Park, M. B., High Potency and Broad-Spectrum Antimicrobial Peptides Synthesized via Ring-Opening Polymerization of alpha-Aminoacid-N-carboxyanhydrides. *Biomacromolecules* **2010,** *11* (1), 60-67.

15. Tew, G. N.; Liu, D. H.; Chen, B.; Doerksen, R. J.; Kaplan, J.; Carroll, P. J.; Klein, M. L.; DeGrado, W. F., De novo design of biomimetic antimicrobial polymers. *Proceedings of the National Academy of Sciences of the United States of America* **2002,** *99* (8), 5110-5114.

16. Lin, J.; Qiu, S. Y.; Lewis, K.; Klibanov, A. M., Bactericidal properties of flat surfaces and nanoparticles derivatized with alkylated polyethylenimines. *Biotechnology Progress* **2002,** *18* (5), 1082-1086.

17. Tiller, J. C.; Liao, C. J.; Lewis, K.; Klibanov, A. M., Designing surfaces that kill bacteria on contact. *Proceedings of the National Academy of Sciences of the United States of America* **2001,** *98* (11), 5981-5985.

18. Mukherjee, K.; Rivera, J. J.; Klibanov, A. M., Practical aspects of hydrophobic polycationic bactericidal "paints". *Applied Biochemistry and Biotechnology* **2008,** *151* (1), 61-70.

19. Park, D.; Wang, J.; Klibanov, A. M., One-step, painting-like coating procedures to make surfaces highly and permanently bactericidal. *Biotechnology Progress* **2006,** *22* (2), 584-589.

20. Dizman, B.; Elasri, M. O.; Mathias, L. J., Synthesis and antibacterial activities of water-soluble methacrylate polymers containing quaternary ammonium compounds. *Journal of Polymer Science Part a-Polymer Chemistry* **2006,** *44* (20), 5965-5973.

21. Wong, S. Y.; Li, Q.; Veselinovic, J.; Kim, B. S.; Klibanov, A. M.; Hammond, P. T., Bactericidal and virucidal ultrathin films assembled layer by layer from polycationic N-alkylated polyethylenimines and polyanions. *Biomaterials* **2010,** *31* (14), 4079-4087.

22. Timofeeva, L. M.; Kleshcheva, N. A.; Moroz, A. F.; Didenko, L. V., Secondary and Tertiary Polydiallylammonium Salts: Novel Polymers with High Antimicrobial Activity. *Biomacromolecules* **2009,** *10* (11), 2976-2986.

23. Gelman, M. A.; Weisblum, B.; Lynn, D. M.; Gellman, S. H., Biocidal activity of polystyrenes that are cationic by virtue of protonation. *Organic Letters* **2004,** *6* (4), 557-560.

24. Ilker, M. F.; Nusslein, K.; Tew, G. N.; Coughlin, E. B., Tuning the hemolytic and antibacterial activities of amphiphilic polynorbornene derivatives. *Journal of the American Chemical Society* **2004,** *126* (48), 15870-15875.

25. Andrews, J. M., Determination of minimum inhibitory concentrations. *J. Antimicrob. Chemother.* **2001,** *48* (suppl_1), 5-16.

26. Engler, A. C.; Lee, H. I.; Hammond, P. T., Highly Efficient "Grafting onto" a Polypeptide Backbone Using Click Chemistry. *Angewandte Chemie-International Edition* **2009,** *48* (49), 9334-9338.

27. Guyomard, A.; Dé, E.; Jouenne, T.; Malandain, J.-J.; Muller, G.; Glinel, K., Incorporation of a Hydrophobic Antibacterial Peptide into Amphiphilic Polyelectrolyte Multilayers: A Bioinspired Approach to Prepare Biocidal Thin Coatings. *Advanced Functional Materials* **2008,** *18* (5), 758-765.

28. Johnson, W. C., Protein Secondary Structure and Circular-Dichroism - a Practical Guide. *Proteins-Structure Function and Genetics* **1990,** *7* (3), 205-214.

29. Haris, P. I.; Chapman, D., The Conformational-Analysis of Peptides Using Fourier-Transform IR Spectroscopy. *Biopolymers* **1995,** *37* (4), 251-263.

30. Ikeda, T.; Hirayama, H.; Yamaguchi, H.; Tazuke, S.; Watanabe, M., Polycationic biocides with pendant active groups: molecular weight dependence of antibacterial activity. *Antimicrob. Agents Chemother.* **1986,** *30* (1), 132-136.

31. Ivankin, A.; Livne, L.; Mor, A.; Caputo, G. A.; DeGrado, W. F.; Meron, M.; Lin, B.; Gidalevitz, D., Role of the Conformational Rigidity in the Design of Biomimetic Antimicrobial Compounds. *Angewandte Chemie International Edition* **2010,** *online*, n/a-n/a.

32. Costerton, J. W.; Stewart, P. S.; Greenberg, E. P., Bacterial Biofilms: A Common Cause of Persistent Infections. *Science* **1999,** *284* (5418), 1318-1322.

33. Feuz, L.; Strunz, P.; Geue, T.; Textor, M.; Borisov, O., Conformation of poly(L-lysine)-graft-poly(ethylene glycol) molecular brushes in aqueous solution studied by small-angle neutron scattering. *Eur. Phys. J. E* **2007,** *23* (3), 237-245.

6 Thesis summary and future work

6.1 Summary

The main objective of the work in this thesis was to develop new synthetic polypeptide systems that mimic naturally occurring proteins. An emphasis was placed on the initial design and demonstration of the utility of the PPLG system. The PPLG system allows for control over the polypeptide functionality as well as secondary structure giving it an advantage over traditional random coiled polymer systems. Within this thesis, the utility of this system is demonstrated in the areas of biomimetic materials, drug delivery, gene delivery, and antimicrobial polymers. In Chapter 2, a summary of detailed experimental methods was presented to aid future researchers working with this system. In Chapter 3, the synthesis is first introduced and graft copolymers inspired by proteoglycans and glycoproteins were synthesized. PEG chains with varying molecular weight from 750 g mol^{-1} to 5000 g mol^{-1} were grafted onto a PPLG backbone at nearly perfect grafting densities. In Chapter 4, the PPLG system was utilized to create an entire library of pH responsive polypeptides. We demonstrated that we can tune for specific interactions and responsive behaviors. These polymers can adopt an α-helical structure at biologically relevant pHs and change solubility over these pHs. These properties are of interest for a number of applications; here we have performed preliminary experiments that demonstrate that these polymers are strong candidates for drug and gene delivery. In Chapter 5, the PPLG system was utilized to synthesize an entire library of antimicrobial polypeptides that mimic naturally occurring AmPs. The flexibility of this system allows for the systematic variation of polymer properties, ranging from side chain functionality to backbone rigidity,

which will provide insight into the mechanism of action of antimicrobial agents and aid in the rational design of future antimicrobial therapeutics.

6.2 Summary of clickable polypeptide systems published after PPLG

Since our initial report of PPLG in 2009[1], other research groups have extended this platform methodology of combining NCA polymerization and click chemistry side chain modification. Chen et al. used PPLG to click on several different azide functionalized monosaccharides to form glycopolypeptides.[2] Tang and Zhang reported the synthesis of poly(γ-azidopropyl-L-glutamate), which was functionalized with alkyne containing mannose moieties via the Huisgen click reaction.[3] Sun and Schlaad developed thiol-ene clickable polypeptides, where they synthesized poly(D,L-allylglycine) and clicked on thiol functionalized sugars.[4] Huang et al. synthesized poly(D,L-propargylglycine) and clicked on azide containing protected galactose, using Huisgen click chemistry.[5] Currently, the Hammond group is exploring new clickable polypeptide systems that utilize the Huisgen click reaction and the thiol-ene reaction.

6.3 Future work

The materials and methodologies developed in thesis provide the foundation for the development of a vast library of materials that have applications in many different aspects of biomaterials. In this section, future research directions related to the study and improvement of the brush polymer system, responsive polymers, and the antimicrobial system are discussed.

6.3.1 Extension of the polymer grafting system

The ultimate goal of the PPLG polymer grafting system is to develop molecules that closely mimic natural brush like macromolecules. There are several relevant brush polymer systems that should be explored. Through the use of living polymerization methods, well

defined polymeric side chains with a wide variety of functionality can be synthesized and attached to PPLG. Furthermore, the incorporation of naturally occurring polymer side chains will more closely mimic natural brush like macromolecules.

- **Introduction of nondegradable side groups.** An ATRP initiator containing an azide group has been synthesized. This initiator can be used to broaden the scope of polymeric materials that can be clicked onto the PPLG backbone.[6] Scheme 6-1, shows the synthesis of an acrylate polymer bearing oligo(ethylene oxide) $(EO)_n$ side chains prepared by ATRP using an azide containing initiator. The introduction of these side groups will increase the bulk of the side groups and will also introduce thermal responsiveness.[7, 8] A similar approach could be used to incorporate polymers synthesized by RAFT polymerization. These large macromolecules can act as 'crowder' molecules that represent the crowded protein microenvironment of the cell or sensing macromolecules.

Scheme 6-1. Synthesis of polymeric clickable side groups using an ATRP initiator

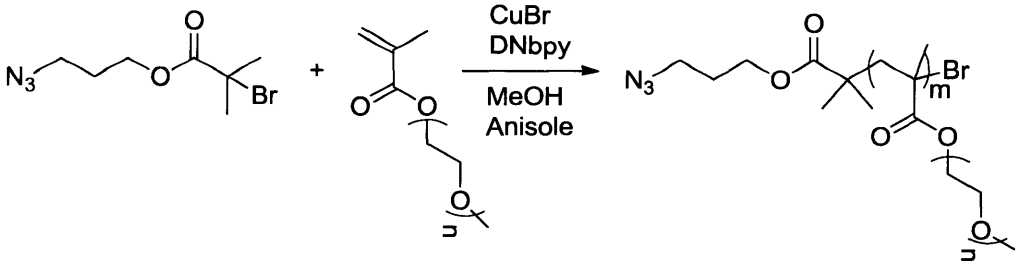

Introduction of degradable side groups. ATRP and RAFT are convenient methods to introduce side chains with a carbon backbone. The ring opening polymerization of functionalized cyclic carbonates (Scheme 6-2) is one method for introducing degradable polyester side chains. These monomers can be produced with a wide

variety of monomer functionality.[9] Biodegradable NCA polymers can also be synthesized using an azido amine initiator.[10]

Scheme 6-2. Ring opening polymerization of carbonates initiated by an azido alcohol

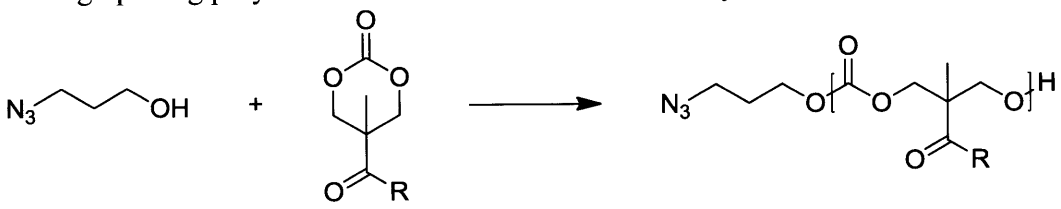

- **Introduction of biologically occurring molecules.** The incorporation of biologically occurring molecules is somewhat more challenging but will provide a means of more closely mimicking proteoglycans and glycoproteins. Single sugars have already been clicked onto the PPLG system.[2] There are commercially available disaccharide molecules that can be clicked onto the PPLG backbone. The direct attachment of polysaccharides to the PPLG may be accomplished by functionalizing the reducing end of the sugar molecule.

6.3.2 Extension of the responsive colloidal system for drug and gene delivery

An entire library of pH responsive polypeptides has been synthesized and the utility of these molecules for drug and gene delivery has been demonstrated. From this system, we have gained a considerable amount of information on how to better design colloidal responsive systems.

6.3.2.1 Gene delivery

For gene delivery, one of the limiting factors is endosomal escape. Increasing the charge density of these molecules will increase endosomal buffering and this increased buffering will improve endosomal escape. There are protocols available for the synthesis of linear short azide terminated polyamines,[11] and other buffering groups such as arginine or pyridyl groups can be

modified with an azide. The incorporation of these molecules will increase the side chain charge density by as much as a factor of 3 and will significantly enhance endosomal buffering. An alternative to increasing charge density could be the incorporation of endosomal escape peptides. These peptides change conformation when taken up into the endosome causing the endosome to rupture.[12, 13]

Another challenge associated with siRNA delivery is the release of the cargo once delivery vehicle has escaped the endosome. One strategy that could be employed is the addition of a disulfide bond between the triazole ring and the primary amine used to complex the siRNA. When this linkage is broken apart in the presence of glutathione in the cell or other reducing agents, the siRNA will be released from the polymer/siRNA complex.[14-17] The incorporation of asymmetric disulfides is challenging but there are multiple strategies in the literature for synthesizing these molecules.[18-21]

6.3.2.2 Drug delivery

The PEG-b-PPLG system substituted with diethyl and diisopropyl amine can assemble and disassemble as a function of pH for pH responsive drug delivery. Several improvements can be made to this system to successfully delivery drug cargo to desired cells. Although these groups accomplish reversible micellization, they may not be the best groups for solubilizing hydrophobic drugs. Incorporating groups that enhance hydrogen bonding will enhance drug loading and reduce cargo leaking into the blood stream before it had reached its intended target.[9] Mixing different hydrophobic groups has also been shown to increase the loading of drugs inside the micelle core.[22] For releasing cargo, a different strategy could be introducing acid labile groups that when the acid labile bonds are degraded, the interior block of the micelle goes from hydrophobic to hydrophilic.[23] An alternative to solubilizing the drugs into the hydrophobic core,

drugs can be covalently attached to the polymer backbone utilizing labile linkers that break once the cargo has reached its final destination.[24, 25]

6.3.2.3 Incorporation of other responsive groups

The incorporation of other responsive groups (e.g. thermal or UV responsive) could be useful for modulating molecule secondary structure, self-assembly, and overall function of these materials. The incorporation of short oligo(ethylene oxide) side chains can induce lower critical solution temperature (LCST) behavior in polymers.[8] Preliminary studies have shown that these short side chains, when attached to PPLG can induce an LCST. Furthermore, when short oligo(ethylene oxides) have been attached to similar poly(lysine), a high LCST was observed.[26] The Hammond group has shown that temperature can be used to reversibly assemble micelles, by using an LCST polymer as the interior block.[27] UV responsive groups have also been incorporated into polymers to make photoresponsive materials, for optical and electrical switching, data recording, reversible solubility control of enzymes, light-actuated nanovalves, and light responsive reversible micelle assembly.[28-30] In nature, photochromic molecules represent the basic molecular trigger for photoreceptors for molecular signaling.[31] For polypeptides, the introduction of both spiropyran and azobenzene, have been shown to control the secondary structure of polypeptides as well as the hydrophobicity of the polymers.[31]

6.3.3 Extension of antimicrobial polymer work and the development of membrane insertion peptides

The exact mechanism of the antimicrobial polypeptides is currently unknown. There are several possible modes of action of these polypeptides and exploration of the mechanism of action will provide insight into the design of more potent antimicrobial polymers. The review article by Gabriel et al. provides an overview of experimental protocols for exploring the mode

of action of antimicrobial polymers.[32] Once protocols are established for determining the mechanism of action, new polymers should be synthesized that have different side chain functionality as well as backbone rigidity. Ivankin et al. showed that backbone rigidity plays an important role in the method of action of naturally occurring AmPs.[33] With the clickable polypeptides, we are able to explore this complex aspect of AmPs which is not possible with other polymeric systems that can only adopt a flexible backbone conformation.

The antimicrobial peptides synthesized in this work interact with the membrane of the bacteria. These polymers could also be used to mimic membrane interacting proteins that undergo reversible transmembrane insertion. Membrane proteins play an important role in many cellular processes, including cell signaling, active transport, ion flow, and cell-cell interactions. Short transmembrane peptide series are typically hydrophobic in nature, making them difficult to study because oftentimes if they are placed in water, they will self assemble with themselves rather than with a lipid bilayer.[34] A water soluble, short membrane insertion peptide, pHLIP, which undergoes membrane insertion at low pH (< 7.0), has been recently reported. This peptide is synthesized by solid-phase peptide synthesis using standard Fmoc chemistry.[34] A unique aspect of this peptides is that it is fully, monomerically water soluble at biological pH (7.4), making it convenient to study. It is typically present in one of three different states: (1) completely water soluble, (2) bond to the surface of a lipid bilayer in a monomeric, unstructured state, and (3) inserted into the membrane in a structured alpha helix (pH <7.0).[34, 35] Studies have been performed to determine the mechanism and energetics of insertion and to explore possible applications of these membrane peptides in drug therapy, diagnostic imaging, genetic control, or cell regulation.[34-40] The pHLIP peptide has been used to deliver cargo molecules such as polar molecules and cyclic peptides that are normally not permeable to cells across the cell membrane

via attachment with a labile linker to the C terminus of the protein.[38] The peptide has also been demonstrated as an imaging diagnostic agent for hypoxic tumors.[41, 42] Despite its great promise, the cost of generating this relatively long peptide using solid-phase approaches is high and yields only small quantities thus limiting the technology and the ability to utilize these systems for a range of biomaterial or biological, environmental, and other engineering applications. With the clickable PPLG system, we could use the various click groups to mimic the pH responsive behavior of the pHLIP peptide and other membrane interacting peptides.

6.4 Concluding remarks

This thesis introduces and demonstrates the utility of a clickable polypeptide system. The synthesis of PPLG and post functionalization with various molecules and macromolecules provide a unique opportunity to create vast libraries of biomimetic materials. Libraries of pH responsive polypeptides, antimicrobial polypeptides, and PEG brush polymers were synthesized and characterized in this body of work. It is hoped that these systems provide the foundation for better material systems and provide a unique opportunity to study complex macromolecule systems that mimic naturally occurring macromolecules. Ultimately, this synthetic platform could be used to develop new therapeutics, as well as develop a fundamental understanding of how complex biological systems work.

6.5 References

1. Engler, A. C.; Lee, H. I.; Hammond, P. T., Highly Efficient "Grafting onto" a Polypeptide Backbone Using Click Chemistry. *Angewandte Chemie-International Edition* **2009,** *48* (49), 9334-9338.

2. Xiao, C.; Zhao, C.; He, P.; Tang, Z.; Chen, X.; Jing, X., Facile Synthesis of Glycopolypeptides by Combination of Ring-Opening Polymerization of an Alkyne-Substituted

N-carboxyanhydride and Click "Glycosylation". *Macromol. Rapid Commun.* **2010,** *31* (11), 991-997.

3. Tang, H. Y.; Zhang, D. H., General Route toward Side-Chain-Functionalized alpha-Helical Polypeptides. *Biomacromolecules* **2010,** *11* (6), 1585-1592.

4. Sun, J.; Schlaad, H., Thiol-Ene Clickable Polypeptides. *Macromolecules* **2010,** *43* (10), 4445-4448.

5. Huang, J.; Habraken, G.; Audouin, F.; Heise, A., Hydrolytically Stable Bioactive Synthetic Glycopeptide Homo- and Copolymers by Combination of NCA Polymerization and Click Reaction. *Macromolecules* **2010,** *43* (14), 6050-6057.

6. Matyjaszewski, K., *Controlled/Living Radical Polymerization: Progress in ATRP.* American Chemical Society (distributed by Oxford University Press): Washington, DC, 2009.

7. Gao, H. F.; Matyjaszewski, K., Synthesis of molecular brushes by "grafting onto" method: Combination of ATRP and click reactions. *J. Am. Chem. Soc.* **2007,** *129* (20), 6633-6639.

8. Skrabania, K.; Kristen, J.; Laschewsky, A.; Akdemir, O.; Hoth, A.; Lutz, J. F., Design, synthesis, and aqueous aggregation behavior of nonionic single and multiple thermoresponsive polymers. *Langmuir* **2007,** *23* (1), 84-93.

9. Kim, S. H.; Tan, J. P. K.; Nederberg, F.; Fukushima, K.; Colson, J.; Yang, C. A.; Nelson, A.; Yang, Y. Y.; Hedrick, J. L., Hydrogen bonding-enhanced micelle assemblies for drug delivery. *Biomaterials* **2010,** *31* (31), 8063-8071.

10. Agut, W.; Agnaou, R.; Lecommandoux, S.; Taton, D., Synthesis of block copolypeptides by click chemistry. *Macromol. Rapid Commun.* **2008,** *29* (12-13), 1147-1155.

11. Carboni, B.; Benalil, A.; Vaultier, M., Aliphatic Amino Azides as Key Building-Blocks for Efficient Polyamine Syntheses. *J. Org. Chem.* **1993,** *58* (14), 3736-3741.

12. Funhoff, A. M.; Van Nostrum, C. F.; Lok, M. C.; Kruijtzer, J. A. W.; Crommelin, D. J. A.; Hennink, W. E., Cationic polymethacrylates with covalently linked membrane destabilizing peptides as gene delivery vectors. *Journal of Controlled Release* **2005,** *101* (1-3), 233-246.

13. Plank, C.; Zauner, W.; Wagner, E., Application of membrane-active peptides for drug and gene delivery across cellular membranes. *Advanced Drug Delivery Reviews* **1998,** *34* (1), 21-35.

14. Ambrogio, M. W.; Pecorelli, T. A.; Patel, K.; Khashab, N. M.; Trabolsi, A.; Khatib, H. A.; Botros, Y. Y.; Zink, J. I.; Stoddarrt, J. F., Snap-Top Nanocarriers. *Organic Letters* **2010,** *12* (15), 3304-3307.

15. El-Sayed, M. E. H.; Hoffman, A. S.; Stayton, P. S., Rational design of composition and activity correlations for pH-sensitive and glutathione-reactive polymer therapeutics. *Journal of Controlled Release* **2005,** *101* (1-3), 47-58.

16. Saito, G.; Swanson, J. A.; Lee, K. D., Drug delivery strategy utilizing conjugation via reversible disulfide linkages: role and site of cellular reducing activities. *Advanced Drug Delivery Reviews* **2003,** *55* (2), 199-215.

17. Tang, L. Y.; Wang, Y. C.; Li, Y.; Du, J. Z.; Wang, J., Shell-Detachable Micelles Based on Disulfide-Linked Block Copolymer As Potential Carrier for Intracellular Drug Delivery. *Bioconjugate Chemistry* **2009,** *20* (6), 1095-1099.

18. Tam-Chang, S. W.; Mason, J. C., Synthesis of symmetrical and unsymmetrical alkyl disulfides with attached flavin analog for formation of self-assemble monolayers on gold. *Tetrahedron* **1999,** *55* (47), 13333-13344.

19. Klayman, D. L.; White, J. D.; Sweeney, T. R., Unsymmetrical Disulfides from Amino Bunte Salt. *J. Org. Chem.* **1964,** *29* (12), 3737-&.

20. Kowalczyk, J.; Barski, P.; Witt, D.; Grzybowski, B. A., Versatile and efficient synthesis of omega-functionalized asymmetric disulfides via sulfenyl bromide adducts. *Langmuir* **2007,** *23* (5), 2318-2321.

21. Hunter, R.; Caira, M.; Stellenboom, N., Inexpensive, one-pot synthesis of unsymmetrical disulfides using 1-chlorobenzotriazole. *J. Org. Chem.* **2006,** *71* (21), 8268-8271.

22. Opanasopit, P.; Yokoyama, M.; Watanabe, M.; Kawano, K.; Maitani, Y.; Okano, T., Block copolymer design for camptothecin incorporation into polymeric micelles for passive tumor targeting. *Pharmaceutical Research* **2004,** *21* (11), 2001-2008.

23. Griset, A. P.; Walpole, J.; Liu, R.; Gaffey, A.; Colson, Y. L.; Grinstaff, M. W., Expansile Nanoparticles: Synthesis, Characterization, and in Vivo Efficacy of an Acid-Responsive Polymeric Drug Delivery System. *J. Am. Chem. Soc.* **2009,** *131* (7), 2469-+.

24. Oh, K. T.; Yin, H. Q.; Lee, E. S.; Bae, Y. H., Polymeric nanovehicles for anticancer drugs with triggering release mechanisms. *Journal of Materials Chemistry* **2007,** *17* (38), 3987-4001.

25. Khandare, J.; Minko, T., Polymer-drug conjugates: Progress in polymeric prodrugs. *Prog. Polym. Sci.* **2006,** *31* (4), 359-397.

26. Yu, M.; Nowak, A. P.; Deming, T. J.; Pochan, D. J., Methylated mono- and diethyleneglycol functionalized polylysines: Nonionic, alpha-helical, water-soluble polypeptides. *J. Am. Chem. Soc.* **1999,** *121* (51), 12210-12211.

27. Lee, H. I.; Lee, J. A.; Poon, Z. Y.; Hammond, P. T., Temperature-triggered reversible micellar self-assembly of linear-dendritic block copolymers. *Chem. Commun.* **2008,** (32), 3726-3728.

28. Parthenopoulos, D. A.; Rentzepis, P. M., 3-Dimensional Optical Storage Memory. *Science* **1989,** *245* (4920), 843-845.

29. Ito, Y.; Sugimura, N.; Kwon, O. H.; Imanishi, Y., Enzyme modification by polymers with solubilities that change in response to photoirradiation in organic media. *Nature Biotechnology* **1999,** *17* (1), 73-75.

30. Lee, H. I.; Wu, W.; Oh, J. K.; Mueller, L.; Sherwood, G.; Peteanu, L.; Kowalewski, T.; Matyjaszewski, K., Light-induced reversible formation of polymeric micelles. *Angewandte Chemie-International Edition* **2007,** *46* (14), 2453-2457.

31. Pieroni, O.; Fissi, A.; Angelini, N.; Lenci, F., Photoresponsive polypeptides. *Accounts of Chemical Research* **2001,** *34* (1), 9-17.

32. Gabriel, G. J.; Som, A.; Madkour, A. E.; Eren, T.; Tew, G. N., Infectious disease: Connecting innate immunity to biocidal polymers. *Materials Science and Engineering: R: Reports* **2007,** *57* (1-6), 28-64.

33. Ivankin, A.; Livne, L.; Mor, A.; Caputo, G. A.; DeGrado, W. F.; Meron, M.; Lin, B.; Gidalevitz, D., Role of the Conformational Rigidity in the Design of Biomimetic Antimicrobial Compounds. *Angewandte Chemie International Edition* **2010,** *online*, n/a-n/a.

34. Reshetnyak, Y. K.; Andreev, O. A.; Lehnert, U.; Engelman, D. M., Translocation of molecules into cells by pH-dependent insertion of a transmembrane helix. *Proceedings of the National Academy of Sciences of the United States of America* **2006,** *103* (17), 6460-6465.

35. Reshetnyak, Y. K.; Andreev, O. A.; Segala, M.; Markin, V. S.; Engelman, D. M., Energetics of peptide (pHLIP) binding to and folding across a lipid bilayer membrane. *Proceedings of the National Academy of Sciences of the United States of America* **2008,** *105* (40), 15340-15345.

36. Zoonens, M.; Reshetnyak, Y. K.; Engelman, D. M., Bilayer interactions of pHLIP, a peptide that can deliver drugs and target tumors. *Biophysical Journal* **2008,** *95* (1), 225-235.

37. Segala, J.; Engelman, D. M.; Reshetnyak, Y. K.; Andreev, O. A., Accurate Analysis of Tumor Margins Using a Fluorescent pH Low Insertion Peptide (pHLIP). *International Journal of Molecular Sciences* **2009,** *10* (8), 3478-3487.

38. Thevenin, D.; An, M.; Engelman, D. M., pHLIP-Mediated Translocation of Membrane-Impermeable Molecules into Cells. *Chemistry & Biology* **2009,** *16* (7), 754-762.

39. Andreev, O. A.; Engelman, D. M.; Reshetnyak, Y. K., pHLIP technology for imaging and drug delivery. *Amino Acids* **2009,** *37*, 40-40.

40. Andreev, O. A.; Engelman, D. M.; Reshetnyak, Y. K., Targeting acidic diseased tissue New technology based on use of the pH (Low) Insertion Peptide (pHLIP). *Chimica Oggi-Chemistry Today* **2009,** *27* (2), 34-37.

41. Andreev, O. A.; Dupuy, A. D.; Segala, M.; Sandugu, S.; Serra, D. A.; Chichester, C. O.; Engelman, D. M.; Reshetnyak, Y. K., Mechanism and uses of a membrane peptide that targets tumors and other acidic tissues in vivo. *Proceedings of the National Academy of Sciences of the United States of America* **2007,** *104* (19), 7893-7898.

42. Vavere, A. L.; Biddlecombe, G. B.; Spees, W. M.; Garbow, J. R.; Wijesinghe, D.; Andreev, O. A.; Engelman, D. M.; Reshetnyak, Y. K.; Lewis, J. S., A Novel Technology for the Imaging of Acidic Prostate Tumors by Positron Emission Tomography. *Cancer Research* **2009,** *69* (10), 4510-4516.